2 Water and Ice

David S. Reid and Owen R. Fennema

CONTENTS

2.1 INTRODUCTION

When we examine the composition of most foods, water is found to be a substantial component. Also, when we consider our own metabolic processes, water is the primary solvent in which these life processes occur. It is therefore appropriate to delve into the nature and properties of water and aqueous solutions, and to consider the many roles played by water in food systems in order to understand the central role of water in food chemistry.

2.2 THE PHYSICAL PROPERTIES OF WATER AND ICE

As a first step in becoming familiar with water, it is appropriate to consider its physical properties, as shown in Table 2.1. By comparing water's properties with those of molecules of similar molecular weight and atomic composition (Table 2.2), it is possible to determine whether water behaves in a normal fashion or whether its behavior is unusual. On the basis of these comparisons [1], water is seen to have unusually high melting and boiling point temperatures, to exhibit unusually large values for surface energy, permittivity, heat capacity, and heats of phase transformation (fusion, vaporization, and sublimation), to have a somewhat lower than expected density, to exhibit the unusual property of expansion upon solidification, and yet, despite these unusual properties, to have a viscosity that is quite normal. This apparent normality for a clearly anomalous liquid will be explained later.

Other properties of water are also remarkable. The thermal conductivity of water is large as compared with most other liquids, and the thermal conductivity of ice is larger than might be expected for a nonmetallic solid. It is noteworthy that the thermal conductivity of ice at 0°C is approximately quadruple that of liquid water at the same temperature, indicating that ice will conduct thermal energy at a much greater rate than will immobilized (e.g., tissue) water. Since the heat capacity of water is approximately twice that of ice, the thermal diffusivities of water and ice differ by about a factor of 9 [2]. Since thermal diffusivity is indicative of the rate at which a material will undergo a change in temperature, we would expect that ice, in a given thermal environment, will undergo temperature change at a rate 9 times greater than that for liquid water. These differences in thermal conductivity and diffusivity values for water and ice provide a good basis for understanding why tissues freeze more rapidly than they thaw under symmetrically applied temperature differentials [2].

2.3 THE WATER MOLECULE

The unusual properties of water suggest that strong attractive forces exist among water molecules and also suggest that the structures of water and ice might be unusual. To explain the features and

TABLE 2.1
Physical Properties of Water and Ice

Property	Value
Molecular weight	18.0153
Melting point (at 101.3 kPa)	0.00°C
Boiling point (at 101.3 kPa)	100.00°C
Critical temperature	373.99°C
Critical pressure	22.064 Mpa
Triple point temperature	0.01°C
Triple point pressure	611.73 Pa
ΔH_{vap} at 100°C	40.647 kJ/mol
ΔH_{sub} at 0°C	50.91 kJ/mol
ΔH_{fus} at 0°C	6.002 kJ/mol

	Temperature (°C)			
	Ice		Water	
Other Temperature-Dependent Properties	**−20**	**0**	**0**	**+20**
Density (g/cm^3)	0.9193	0.9168	0.99984	0.99821
Vapor pressure (kPa)	0.103	0.6113	0.6113	2.3388
Heat capacity (J/g/K)	1.9544	2.1009	4.2176	4.1818
Thermal conductivity (W/m/K)	2.433	2.240	0.561	0.5984
Thermal diffusivity (m^2/s)	11.8×10^{-7}	11.7×10^{-7}	1.3×10^{-7}	1.4×10^{-7}
Compressibility (Pa^{-1})		2	4.9	
Permittivity	98	90	87.9	80.2

Source: Lide, D.R. (Ed.) (1993/1994) *Handbook of Chemistry and Physics*, 74 edn. CRC Press: Boca Raton, FL.

TABLE 2.2
Properties of Related Small Molecules

	CH_4	NH_3	H_2O	H_2S	H_2Se	HF
MW	16.04	17.0	18.01	34.08	80.9	20.01
mp (°C)	−182.6	−77.7	0	−86	−60	−83.1
bp (°C)	−161.4	−33.3	100	−61	−41	19.5
ΔH_v (kJ/mol)	8.16	23.26	40.71	18.66		

Source: Lide, D.R. (Ed.) (1993/1994) *Handbook of Chemistry and Physics*, 74 edn. CRC Press: Boca Raton, FL.

unusual behavior of water and ice, it is best first to consider the nature of a single water molecule, and then to consider the characteristics of clusters of water molecules of increasing size, before finally considering the nature of the bulk system. The water molecule is often described as comprised of two hydrogen atoms interacting with the two sp^3 bonding orbitals of oxygen, forming two covalent sigma (σ) bonds of 40% ionic character, each of which has a dissociation energy of 4.6×10^2 kJ/mol. The localized molecular orbitals are assumed to remain symmetrically oriented about the original orbital axes, hence retaining an approximate tetrahedral structure. A schematic model is shown in

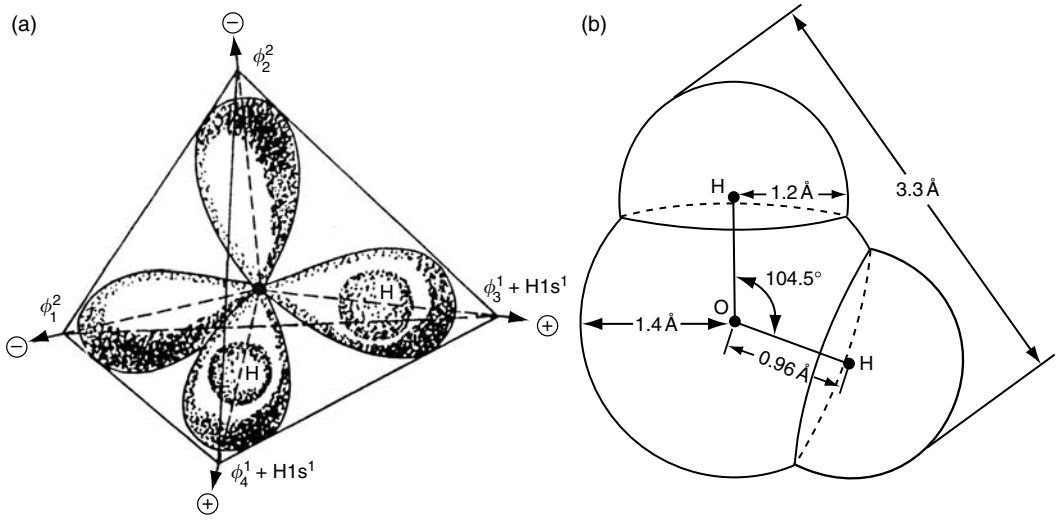

FIGURE 2.1 Schematic model of a single HOH molecule. (a) Possible sp^3 configuration and (b) van der Waals radii for a HOH molecule in vapor state.

Figure 2.1a and the van der Waals radii in Figure 2.1b. While the geometric behavior of water molecules associated through hydrogen bonding is consistent with this model, the assumption of extensive sp^3 hybridization of the lone pairs has been increasingly challenged [3].

In the vapor state, the bond angle of an isolated water molecule is 104.5° close to the perfect tetrahedral angle of 109.5° and the van der Waals radii for oxygen and hydrogen are, respectively, 1.40 and 1.2 Å [4].

At this point, it is important to note that the picture presented so far, describing only the HOH molecule, is oversimplified. The material we know as pure water is a mixture of HOH molecules and many other related constituents. In addition to the common isotopes of oxygen and hydrogen, ^{16}O and ^{1}H, also present are ^{17}O, ^{18}O, ^{2}H (D), and ^{3}H (T) with a resultant 18 isotopic variants of molecular HOH. Additionally, water contains ionic species such as hydrogen ions (existing in forms such as H_3O^+, $H_9O_4^+$) and hydroxyl ions, also with their isotopic variants. "Pure" water thus consists of more than 33 chemical variants of HOH, but since these variants are present in minute amounts, the properties are dominated by the HOH species.

2.4 ASSOCIATION OF WATER MOLECULES

The V-like shape of an HOH molecule and the polarized nature of the O—H bond result in an asymmetric charge distribution within the molecule and a dipole moment in the vapor state of 1.84 D for pure water. Polarity of this magnitude results in considerable intermolecular attractive forces, and hence water molecules associate with considerable tenacity. Note, however, that the unusually large intermolecular attractive force of water cannot be fully accounted for solely on the basis of the large molecular dipole moment. This is to be expected, since dipole moments are a property of the entire molecule, and give no indication of the degree to which individual charges are exposed or of the geometry of the molecule, aspects that have an important bearing on the intensity of the intermolecular association.

The large intermolecular attractive forces between water molecules can be explained satisfactorily in terms of their ability to engage in multiple hydrogen bonding associations in a three-dimensional manner. As compared with covalent bonds (average bond energy about 335 kJ/mol) hydrogen bonds are weak (typically 2–40 kJ/mol) and have greater and more variable lengths. The oxygen–hydrogen

bond has a dissociation energy of about 11–25 kJ/mol, and ranges in length from around 1.7 to 2.0 Å, as compared to the approximately 1.0 Å length of the oxygen–hydrogen covalent bond [1].

Since electrostatic forces provide a major contribution to the energy of the hydrogen bond, and since an electrostatic model of water is simple and leads to an essentially correct geometric picture of HOH molecules as they are known to exist in ice, further discussion of geometric patterns formed by associating HOH molecules will emphasize electrostatic effects. This simplified approach, while entirely satisfactory for this purpose, will prove to be inadequate, and must be modified if other behavioral characteristics of water, such as the influence of apolar solutes, are to be explained satisfactorily.

The highly electronegative oxygen of the water molecule can be visualized as partially drawing away the single electrons from the two covalently bonded hydrogen atoms, thereby leaving each hydrogen atom with a partial positive charge and a minimal electron shield; that is, each hydrogen atom assumes some of the characteristics of a bare proton. Since the hydrogen–oxygen bonding orbitals are located on two of the axes of an imaginary tetrahedron (Figure 2.1a), these two axes can be considered as representing lines of positive force (hydrogen bond donor sites). Oxygen's two lone pair orbitals can be considered as residing along the remaining two axes of the tetrahedron, representing lines of negative force (hydrogen bond acceptor sites). By virtue of these four lines of force in a tetrahedral orientation, each water molecule has the potential to hydrogen bond with a maximum of four others. The resulting tetrahedral arrangement is depicted in Figure 2.2.

Because each water molecule has an equal number of hydrogen bond donor and acceptor sites, arranged in such a way as to permit three-dimensional hydrogen bonding, it is found that the attractive

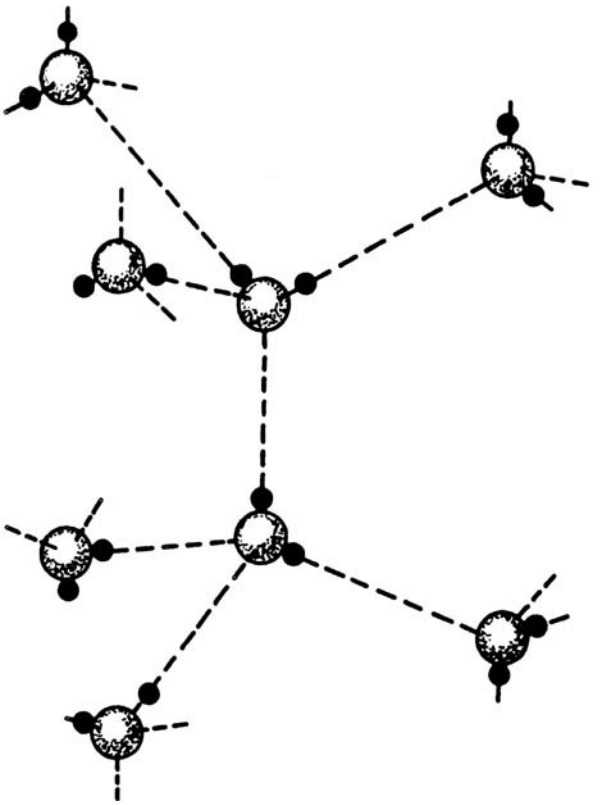

FIGURE 2.2 Hydrogen bonding of water molecules in a tetrahedral configuration. Open circles are oxygen atoms, closed circles are hydrogen atoms. Hydrogen bonds are represented by dashed lines.

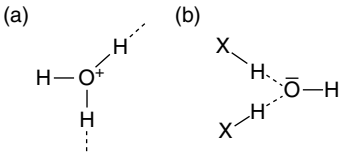

FIGURE 2.3 Structure and hydrogen bond possibilities: (a) for a hydronium ion and (b) for a hydroxyl ion. Dashed lines represent hydrogen bonds, X—H represents a solute or another water molecule.

forces among water molecules are unusually large, even when compared with those existing among other small molecules that also engage in hydrogen bonding associations (e.g., NH_3, HF). Since ammonia (with its tetrahedral arrangement of three donor and one acceptor site) and hydrogen fluoride (with its tetrahedral arrangement of one donor and three acceptor sites) do not have equal numbers of donor and acceptor sites, neither can form three-dimensional hydrogen bonded networks of the type found in water. Both are limited to forming extensive two-dimensional networks, involving fewer hydrogen bonds per molecule than found in water.

Conceptualizing the association of a few water molecules becomes much more complicated when isotopic variants and hydronium and hydroxyl ions are taken into account. The hydronium ion, as a result of its positive charge, would be expected to exhibit a greater hydrogen bond donating potential than nonionized water (Figure 2.3a) and the hydroxyl ion, because of its negative charge, would be expected to exhibit greater hydrogen bond acceptor potential than nonionized water (Figure 2.3b).

This ability of water to engage in extensive three-dimensional hydrogen bonding provides a logical explanation for many of its unusual properties, such as the observed large values of heat capacity, melting point, boiling point, surface tension, and enthalpies of phase transition. All of these can be related to the additional energy necessary to break large numbers of intermolecular hydrogen bonds.

The permittivity (dielectric constant) of water is also influenced by hydrogen bonding. Although water is a dipole, this alone does not account for its large permittivity. It appears that hydrogen-bonded molecular clusters give rise to multimolecular dipoles, effectively increasing the permittivity.

2.5 DISSOCIATION OF WATER MOLECULES

As has already been indicated, two of the species in pure water are the ions produced by the self-dissociation of the molecule, identified in their simplest form as the hydrogen ion, H^+ and the hydroxyl ion OH^-, though in reality these exist in a hydrated form. In pure water, these will exist in equimolar quantities, since they arise from the self-dissociation process.

$$H_2O \longleftrightarrow H^+ + OH^-$$

At 298 K, the equilibrium constant for this dissociation is $K_w = 10^{-14}$ and the pH is 7. It is important to realize that this dissociation is enhanced at higher temperatures, and in consequence, the pH of pure water is temperature dependent. K_w approaches 10^{-12} at 373 K, leading to a pH close to 6 at this temperature. Note that, while a pH of 6 at 298 K implies a concentration of OH^- of 10^{-8} M, at 373 K a pH of 6 implies a concentration of OH^- close to 10^{-6} M.

2.6 STRUCTURES IN PURE WATER SYSTEMS

2.6.1 The Structure of Ice

It is appropriate to discuss the structure of ice before that of liquid water, both because the structure of ice is better understood, and because it is a logical extension of the information presented previously.

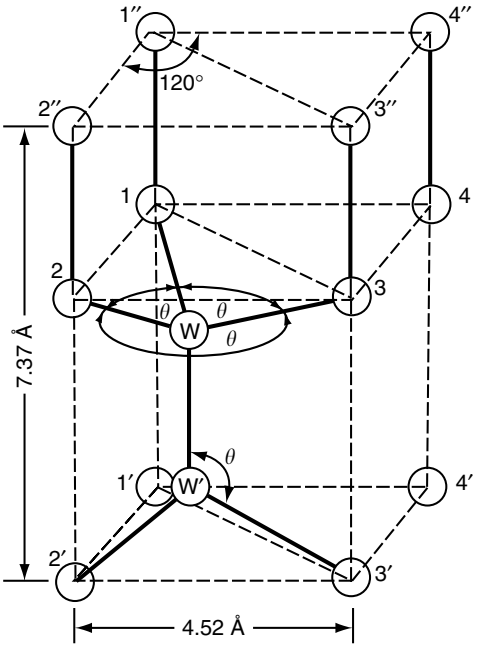

FIGURE 2.4 Unit cell of ordinary ice at 0°C. Circles represent oxygen atoms of water molecules. Nearest neighbor internuclear O—O distance is 2.76 Å. θ is 109°.

Water, with its tetrahedrally directed forces, crystallizes in an open, low density, structure that has been accurately determined. The O—O internuclear nearest neighbor distance, in ice, is 2.76 Å and the O—O—O bond angle is about 109°, very close to the perfect tetrahedral angle of 109.28° (Figure 2.4). The manner in which each HOH bond can associate with four others (coordination number of 4) is readily visualized in the unit cell of Figure 2.4 by considering molecule W and its four nearest neighbors, 1, 2, 3, and W′.

When several unit cells are combined and viewed from the top (down the *c*-axis) the hexagonal symmetry of ice is apparent (Figure 2.5). The tetrahedral substructure is evident from molecule W and its four nearest neighbors, with 1, 2, and 3 being visible and the fourth lying below the plane of the paper, directly under molecule W. When Figure 2.5a is viewed in three dimensions, as in Figure 2.5b, it is evident that two planes of molecules are involved (open and filled circles). These two planes are parallel, very close together, and they move as a unit during the "slip" or flow of ice under pressure, as in a glacier. Pairs of planes of this type comprise the basal planes of ice. By stacking several basal planes an extended structure of ice is obtained. Three basal planes have been combined to form the structure represented in Figure 2.6. Viewed down the *c*-axis, the appearance is exactly the same as that shown in Figure 2.5a indicating that the basal planes are perfectly aligned. Ice is monorefringent in this direction, whereas it is birefringent in all other directions. The *c*-axis is therefore the optical axis of ice. It is interesting to note that, in large sheets of ice, the *c*-axis is often found to be perpendicular to the main plane of the sheet [5]. A fully satisfactory explanation for this has not yet been advanced, though it may reflect the different propagation velocities of ice growth along the different symmetry axes.

With regard to the location of hydrogen atoms in ice, there is general agreement regarding the following:

1. Each line connecting two nearest neighbor oxygen atoms is occupied by one hydrogen atom centered 1 ± 0.01 Å from the oxygen to which it is covalently bonded, and

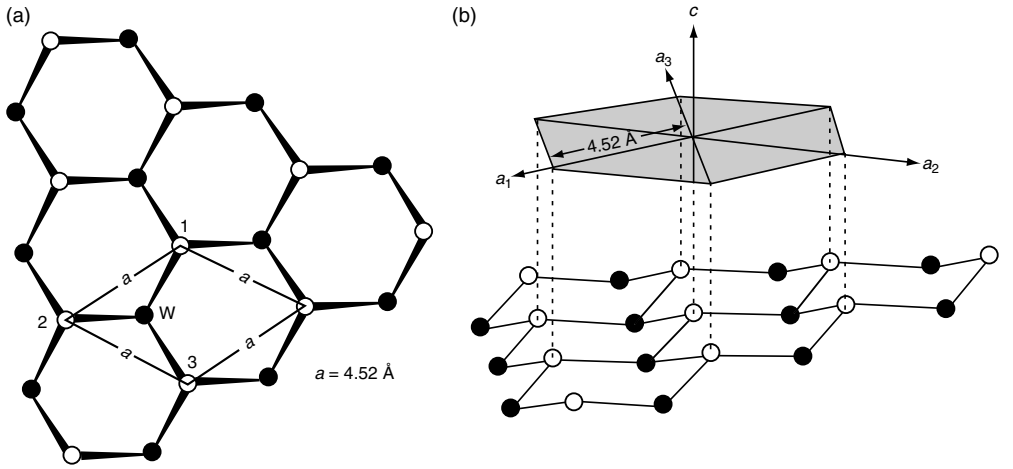

FIGURE 2.5 The basal plane of ice (a combination of two layers of slightly different elevation). Each circle represents the oxygen atom of a water molecule. Open and shaded circles represent, respectively, oxygen atoms in the upper and lower layers of the basal plane. (a) Hexagonal structure viewed down the *c*-axis. Numbered atoms refer to the unit cell of Figure 2.4. (b) Three-dimensional view of the basal plane. The front edge in this view corresponds to the bottom edge of view (a). The crystallographic axes are positioned in accordance with external point symmetry.

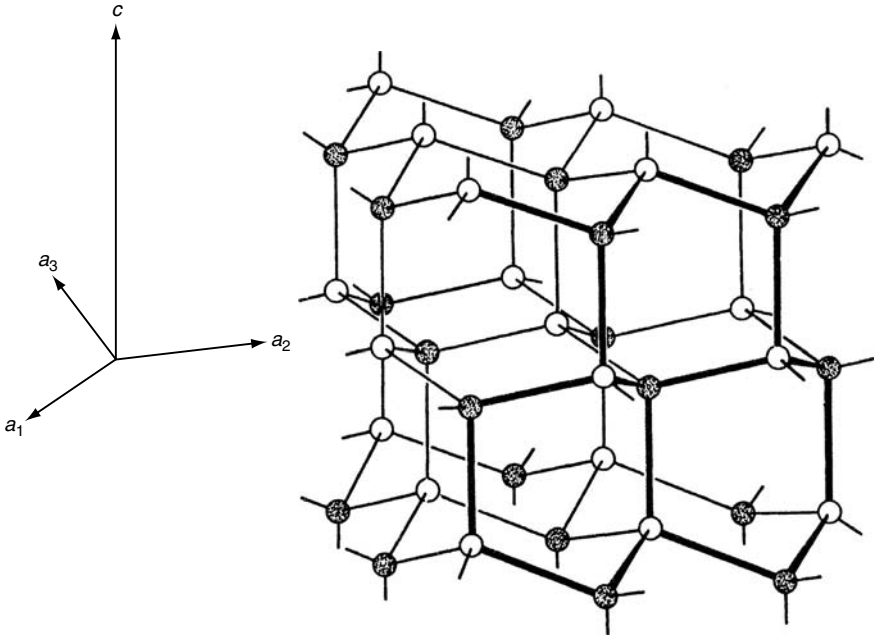

FIGURE 2.6 The extended structure of ordinary ice. Only oxygen atoms are shown. Open and shaded circles represent, respectively, oxygen atoms in upper and lower layers of a basal plane.

1.76 ± 0.01 Å from the oxygen to which it is hydrogen bonded. This configuration is shown in Figure 2.7a.

2. However, if the locations of hydrogen atoms are viewed over time, rather than as a snapshot in time, a somewhat different picture to that described above is obtained. A hydrogen atom

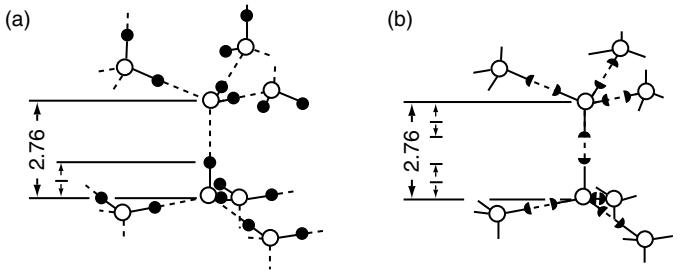

FIGURE 2.7 The location of hydrogen atoms (●) in the structure of ice: (a) instantaneous structure and (b) mean structure (also known as half hydrogen (◖), Pauling, or statistical structure). Open circles are oxygen atoms.

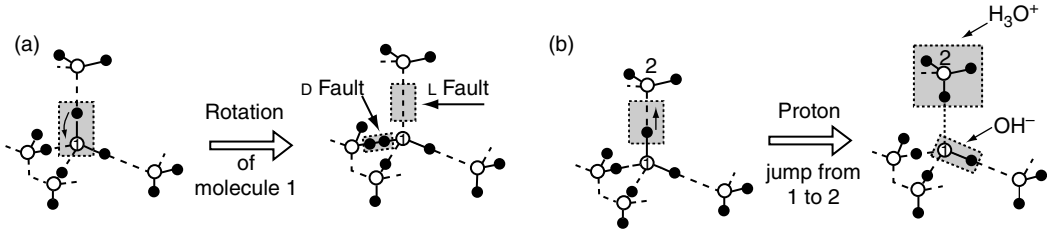

FIGURE 2.8 Schematic representation of proton defects in ice. (a) Formation of orientational defects and (b) formation of ionic defects. Open and filled circles represent, respectively, oxygen and hydrogen atoms. Solid and dashed lines represent, respectively, chemical bonds and hydrogen bonds.

on a line connecting two nearest neighbor oxygen atoms, X and Y, can situate itself in one of two possible positions, either 1 Å from X or 1 Å from Y. Since these two positions have equal probability of occupation, it is believed that each position is occupied on average half of the time. This is possible because, except at extremely low temperatures, HOH molecules can cooperatively rotate, and therefore allow hydrogen atoms to "jump" between adjacent oxygen atoms. A representation of the resulting mean structure, known variously as the half hydrogen, Pauling, or statistical structure, is shown in Figure 2.7b.

From the perspective of crystal symmetry, ordinary ice belongs to the dihexagonal bipyramidal class of the hexagonal system. Ice can also exist in nine other crystalline polymorphic structures and also in an amorphous or vitreous state of uncertain, but largely noncrystalline structure. Of the 11 total structures, only ordinary hexagonal ice is stable under normal pressure at 0°C.

The true structure of ice is not as simple as the foregoing discussion might indicate. First of all, pure ice contains not only ordinary HOH molecules, but also the isotopic and ionic variants of HOH that have been noted as minor constituents of water. Fortunately, we can in most instances ignore the structural influence of the isotopic variants, as they are present in such small amounts. Structurally, major consideration need only be given to the contributions from HOH, H^+ (H_3O^+), and OH^-.

Real ice crystals are never perfect, and the structural defects encountered are usually of the orientational type (caused by proton dislocation accompanied by neutralizing orientational adjustments) or ionic type (caused by proton dislocation with formation of H_3O^+ and OH^-) (see Figure 2.8). The presence of these structural defects provides a means for explaining the unexpectedly high mobility of protons in ice, and also the relatively small decrease in electrical conductivity that occurs when water is frozen, where intuitively one might expect a large loss in conductivity on solidification.

In addition to the atomic mobilities involved in crystal (lattice) defects, there are other types of motional activity in ice. Each HOH molecule in ice is believed to vibrate with a root mean amplitude

of vibration (assuming each molecule vibrates as a unit) of about 0.4 Å at −10°C [5]. Additionally, the individual HOH molecules that presumably occupy some of the interstitial spaces of ice can apparently diffuse slowly through the lattice rather than being trapped in a particular interstitial space.

Ice therefore is far from being a static or homogeneous molecular assembly, and its characteristics are dependent upon temperature. Although HOH molecules in ice are four coordinated at all temperatures, it is necessary to reduce the temperature to about −180°C or lower to constrain the hydrogen atoms to only one of the many possible configurations. Hence, only at temperatures near −180°C or lower will all hydrogen bonds be intact, and as the temperature is raised the mean number of intact (fixed) hydrogen bonds will gradually decrease.

2.6.2 The Structure of Water (Liquid)

At first sight, the concept of structure in a liquid may seem strange since fluidity is the essence of the liquid state, yet it is an old, and well-accepted idea [6] that liquid water possesses some level of structure, not sufficiently established to produce long-range rigidity, but yet far more organized than that of the vapor state, and sufficient in extent to cause the orientation and mobility of any given water molecule to be influenced by neighboring water molecules. One useful conceptual approach has been to think of the structure in the liquid as a series of short-term structured associations, always rapidly interconverting, but nevertheless maintaining an average degree of structure within the liquid at all times.

Evidence for this view of water as a structured liquid is extensive and compelling. For example, water is an "open" liquid, with a density only 60% of that to be expected of a liquid in which the molecules are close packed. Partial retention of the open, hydrogen-bonded tetrahedral arrangement of ice can easily account for the low density of liquid water. Furthermore, while the enthalpy of fusion of ice is unusually high for a solid, it corresponds to the energy that would be required to break only about 15% of the hydrogen bonds believed to exist in ice. Although this does not necessarily imply that 85% of the hydrogen bonds existing in ice are retained in liquid water (e.g., more bonds could be broken but the resulting change in energy could be masked by a simultaneous increase in van der Waals interactions), the results of many separate studies strongly support the concept that many water–water hydrogen bonds continue to exist in the liquid, with the extent of hydrogen bonding decreasing as the temperature of the liquid increases [1,7].

Elucidation of the structure(s) of pure liquid water is an extremely complex and challenging problem. Many theories have been proposed, but all are incomplete, oversimplified, and subject to weaknesses that are quickly cited by proponents of rival theories. This is a healthy situation, which should eventually result in an accurate structural description of liquid water. In recent years, the increased power of computers has rendered feasible computer simulations of the molecular dynamics of water, governed by the equations of motion, and molecular potential functions that seek to approximate the significant interactive modes of the water molecule [8–10]. These simulations, limited as they are by the errors and approximations of the chosen potential function, are found to display many of the characteristic properties of water, and are providing powerful new insights into the realities of liquid water. Visual displays of the movements of the molecules represented in the simulation are very instructive, but difficult to capture on paper. Notwithstanding the increasing sophistication of these simulations, and the valuable insights that they provide, it is a valuable exercise to consider models generated before access to such raw computational power as exists today became commonplace.

Three general types of model for liquid water have been proposed: mixture models, interstitial models, and continuum models (also termed homogeneous or uniformist models) [11,12]. Mixture models embody the concept of intermolecular hydrogen bonds being momentarily concentrated in bulky clusters of water molecules that exist in dynamic equilibrium with more dense species, with "momentarily" indicating a timescale of 10^{-11} s or thereabouts [12]. The molecular dynamic

computer simulations are often an embodiment of this type of approach, with the simulation providing a time sequence of snapshots of the location (and often orientation) of the constituent molecules represented in the model. The exact characteristics exhibited by the model depend upon the interaction potential function ascribed to water, and many different potential functions have been proposed and utilized, each with its particular strengths and weaknesses.

Continuum models involve the idea that intermolecular hydrogen bonds are distributed uniformly through the sample, and that many of the bonds existing in ice simply become distorted rather than broken when ice is melted. It has been suggested that this permits a continuous network of water molecules to exist that is, of course, dynamic in nature, with the distortions able to relocate in space by transfer across the network [13,14].

The interstitial model involves the concept of water retaining, with little distortion, either an ice-like or clathrate-type hydrogen-bonded network structure with unbonded individual water molecules filling the interstitial spaces of the network. In all three models, the dominant structural feature is the concept of a hydrogen-bonded association of liquid water in ephemeral, distorted tetrahedra. All models also permit individual water molecules to frequently alter their bonding arrangements by rapidly terminating one hydrogen bond in exchange for a new one, while still maintaining, at constant temperature, a constant degree of hydrogen bonding and structure for the system as a whole.

In many respects, the more recent computer models demonstrate facets of each of the more traditional models [10]. Evidence is found for changing orientations of hydrogen bonds and for relocation of water molecules in positions not supported by a traditional hydrogen-bonded network. A variety of modeling studies have successfully approximated the observed behaviors of water. In the computer models, which produce time-averaged pictures, while hydrogen bonding is clearly very important, the appearance of well-defined structures, as might be implied by the simpler models, does not occur.

It is now possible to discuss the seemingly anomalous low viscosity of water. This attribute is readily reconcilable with the types of structures that have been described, since the hydrogen-bonded arrangements of water molecules are highly dynamic, allowing individual molecules within a timeframe of nano- to picoseconds to alter their hydrogen-bonding relationships with neighboring molecules, thereby facilitating mobility and fluidity. The unusually high heat capacity of liquid water is seen to be in part a reflection of the energy required to break additional hydrogen bonds as the temperature is increased. The high enthalpy of vaporization reflects the breaking of most or all remaining hydrogen bonds as the liquid vaporizes, since most molecules in the vapor are believed to be monomers.

The degree of intermolecular hydrogen bonding among water molecules is, of course, temperature dependent. Ice at 0°C has a coordination number (number of nearest neighbors) of 4.0, with the nearest neighbor distance being 2.76 Å. With input of the enthalpy of fusion, melting occurs. The enthalpy of fusion reflects some hydrogen bonds being broken (the distance between nearest neighbors increases) and other hydrogen bonds becoming strained as water molecules assume a fluid state with associations that are, on average, more compact. As the temperature is raised, the coordination number increases from 4.0 in ice at 0°C to 4.4 in water at 1.50°C then to 4.9 at 83°C. Simultaneously, the distance between nearest neighbors increases from 2.76 Å in ice at 0°C to 2.9 Å in water at 1.50°C then to 3.05 Å at 83°C [15,16].

It is evident, therefore, that the ice to water transformation is accompanied by an increase in the distance between nearest neighbors (decreased density), and by an increase in the average number of nearest neighbors (increased density) with the latter predominating during the phase change to yield the familiar net increase in density associated with melting. Further warming above the melting point causes the density to pass through a maximum at 3.98°C, then gradually decline. It is apparent that the effect of an increase in coordination number is predominant at temperatures between 0°C and 3.98°C, and that an effect of increasing distance between nearest neighbors (thermal expansion) is predominant above 3.98°C.

2.7 PHASE RELATIONSHIPS OF PURE WATER

Up to this point, we have considered only molecular and structural aspects of water; in other words, interactions and interrelationships at the microscopic and submicroscopic level. It is appropriate now to discuss the observable phase behavior of water, as this will be relevant not just to our appreciation of the properties of pure water, but also to later discussions on the behavior of aqueous solutions under a wide range of conditions of temperature and pressure. When we study the phase relationships of pure water, the influences of both temperature and pressure must be considered.

Figure 2.9a shows the phase diagram for pure water. Of particular relevance to food science is the vapor–liquid equilibrium line, and also the pressure dependence of stable forms of ice. As mentioned earlier, several forms of ice have been identified, each stable in a particular region of the temperature–pressure diagram. Under the conditions of temperature and pressure utilized in food processing, the only ice phase of interest is ice I. It is noteworthy that, for ice I, with increasing pressure, the melting point of ice Ih decreases (Figure 2.9b). Particularly, note that at a pressure of 270 MPa the melting point of ice Ih is below −20°C. This fact finds application in techniques such as pressure shift freezing [17,18] where a food is cooled to −20°C while experiencing a high pressure. Under these conditions, the material is above the freezing point of ice and so water remains liquid, though enthalpy (heat content) is reduced. On release of the pressure, freezing is very rapid, as the stable form of water under the new conditions of temperature and pressure is ice, and the unchanged heat content of the sample is that of a sample containing a significant fraction of ice. A reverse thawing process has also been designed, in which a frozen material is subjected to a sufficiently high pressure to enable water to become the stable phase with no change in temperature. Since pressure can be applied almost instantaneously, thawing is immediate. After increasing the temperature to above 0°C, the applied pressure can be released without ice forming. Thus, a thawing process in which the phase change is uniform through the material can be achieved, rather than being progressive, reflecting the geometric pattern of temperature change controlled by the processes of heat transfer. At higher pressures than those where ice I is the stable phase, other forms of ice exist such as ice II, ice III, ice IV, and so forth. These forms are not found under any conditions relevant to the handling and processing of foods and need not be discussed further.

In considering equilibria in vapor–liquid systems, note that the vapor pressure of pure liquid water increases from 610 Pa at 0°C to 101,323 Pa at 100°C. It is also possible to measure a vapor pressure of water above undercooled liquid water at temperatures below 0°C, under conditions where the equilibrium form of HOH is ice. These pressures are always higher than the equilibrium vapor pressure of water above ice at the same temperature (Table 2.3). The significance of these observations to food science, in particular with respect to the use of relative vapor pressure as an indicator of "water availability" will be discussed later in this chapter. Since water is an important component of food, we need to develop some system(s) to describe the amount, state, and condition of the water in the food. However, before settling upon a suitable descriptor, first we must consider systems more complex than pure water to understand the influence of the molecular environment on the properties exhibited by water at both the molecular and the bulk level.

2.8 WATER IN THE PRESENCE OF SOLUTES

In all food systems, both water and solutes are present. It is therefore necessary to discuss the effects of solutes on the nature and behavior of a collection of water molecules including its solvent properties.

2.8.1 Ice in the Presence of Solutes

The presence of solutes influences both the amount (through thermodynamic effects) and the propagation patterns (through kinetic effects) of ice in an aqueous system. As the concentration

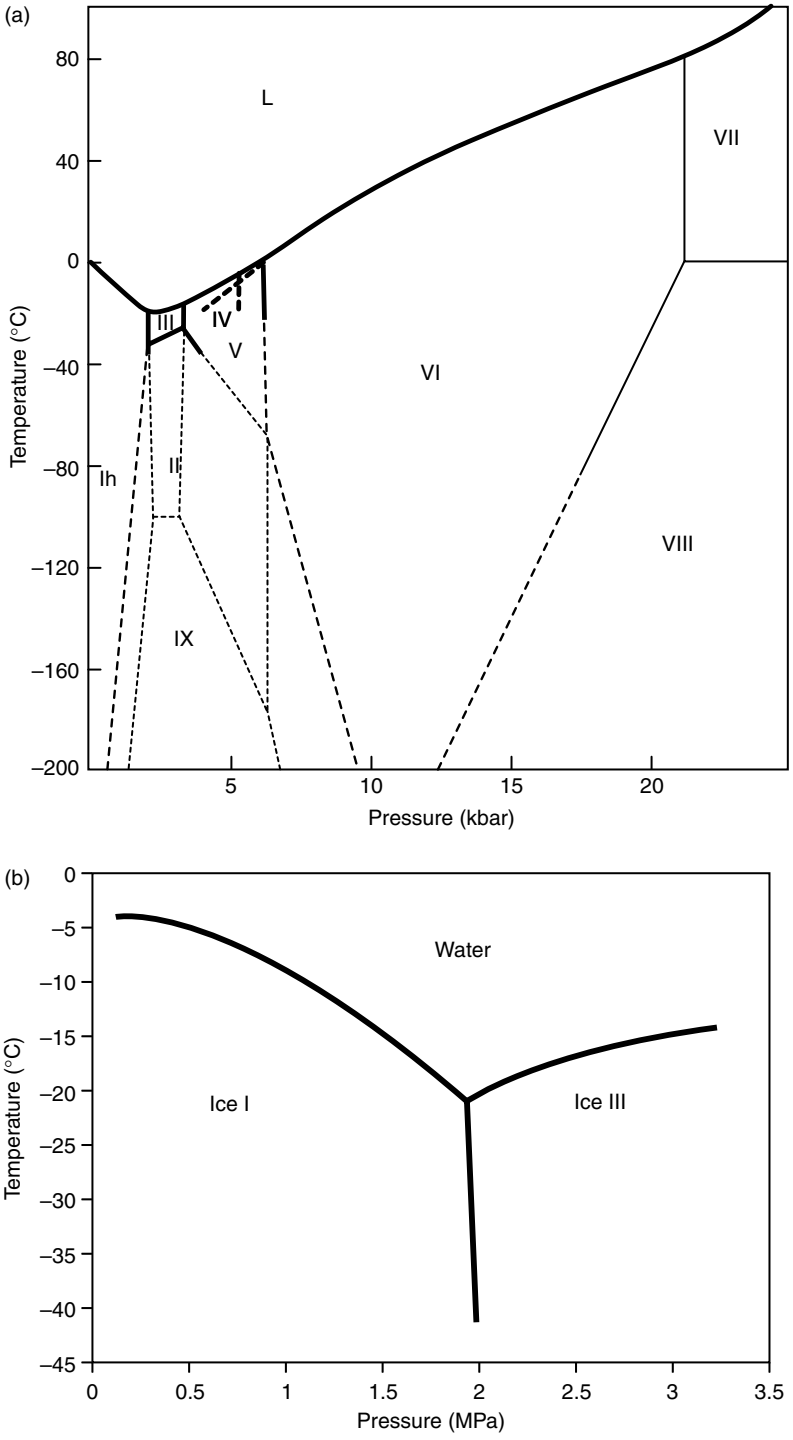

FIGURE 2.9 The pressure–temperature phase diagram for (a) pure water, (b) details of the behavior of liquid water, ice I, and III.

TABLE 2.3
Vapor Pressures and Vapor Pressure Ratios of Water and Ice

Temperature (°C)	$(p^o)_w$ Water (kPa)	$(p^o)_i$ Ice (kPa)	$((p^o)_i/(p^o)_w)$
100	101.325		
90	70.123		
80	47.379		
70	31.181		
60	19.936		
50	12.346		
40	7.382		
30	4.245		
20	2.338		
10	1.228		
0	0.611	0.611	1.00
−5	0.421[a]	0.402	0.954
−10	0.287[a]	0.260	0.905
−15	0.191[a]	0.165	0.863
−20	0.125[a,b]	0.103	0.824
−25	0.0807[a,b]	0.063	0.780
−30	0.0509[a,b]	0.038	0.746
−40	0.0189[a,b]	0.013	0.687
−50	0.0064[a,b]	0.039	0.609

[a] Supercooled liquid.
[b] Calculated data.

Source: Lide, D.R. (Ed.) (1993/1994) *Handbook of Chemistry and Physics*, 74 edn., CRC Press: Boca Raton, FL and Mason, B.J. (1957) *The Physics of Clouds*. Clarendon Press: Oxford, p. 445.

of a particular solute increases, the amount of ice formed at any temperature decreases. This is a manifestation of freezing point depression and colligative effects. Figure 2.10, a simple phase diagram for a binary aqueous system, shows how the freezing point of a binary aqueous solution changes with concentration. Phase and state diagrams will be discussed in more detail later.

The amount and kind of solutes present influence not only the quantity, but also the size, structure, location, and orientation of ice crystals resulting from any particular cooling protocol. Consider, for example, the effects of solute on ice structure. In pioneering studies, Luyet and coworkers [19–21] studied the appearance of ice crystals formed under a range of different cooling conditions in the presence of various solutes including sucrose, glycerol, gelatin, albumin, and myosin. They devised a classification system based on morphology, elements of symmetry, and the cooling velocity required for development of various types of visible ice structures. Their four major classifications of visible ice structures are hexagonal forms, irregular dendrites, coarse spherulites, and evanescent spherulites.

The hexagonal form, which is most highly ordered, is found exclusively in foods, provided that extremely rapid freezing is avoided, and the solute is of a type and concentration that does not interfere unduly with the mobility (ease of spatial reorganization) of water molecules. Gelatin, at high concentrations will, for example, result in more disordered forms of ice crystal. In these early studies, Luyet and coworkers found clear evidence for the existence of a glassy (amorphous) unfrozen phase surrounding the ice crystals at low temperatures and linked the existence of this phase to phenomena such as "collapse" in freeze drying. Around this same time, Rey [22,23] was also performing pioneering studies of the properties of the phases involved in the freeze-drying process and provided similar insights. Though the full significance of these studies was not immediately

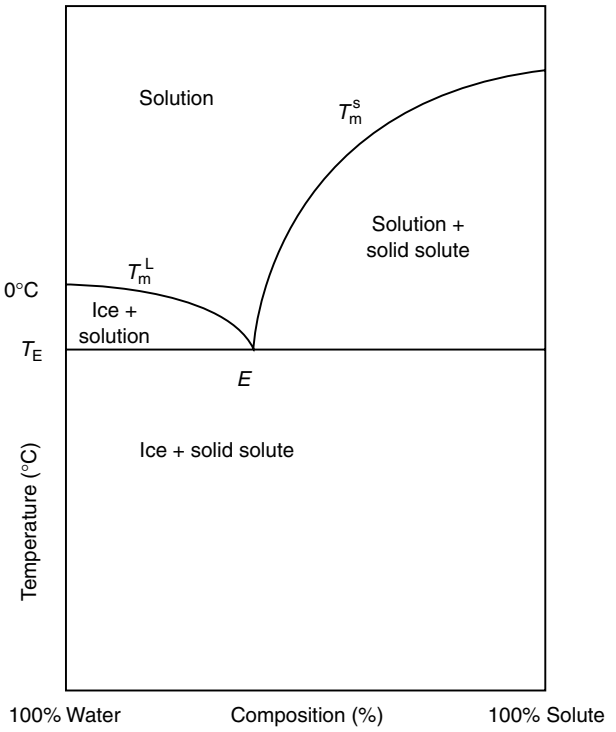

FIGURE 2.10 Schematic binary phase diagram for a simple aqueous system.

realized, they were early precursors to the development of concepts of the role of the glassy state in governing the kinetic properties of frozen systems. These important concepts will be discussed in more detail later.

2.8.2 Water–Solute Interactions in Aqueous Solutions

2.8.2.1 Macroscopic Level

Before dealing with a description of water–solute interactions at a molecular level, it is appropriate to introduce some general observations on the behavior of water. The presence of water has a significant impact on the properties of foods, with properties changing with changes in water content. Terms such as water binding, hydration, water holding capacity have been coined to help describe the influences of water on system properties [24,25]. Often based upon macroscopic observation, these historic terms may prove to be unfortunate when considered in the light of an understanding of the underlying molecular processes that they presumably reflect. Nevertheless, it is important to introduce these descriptive concepts, as they have played an important role in the evolution of our understanding of the properties, and influences, of water in foods.

In the past, "water binding" and "hydration" were often used to describe the general tendency for water to associate with hydrophilic substances, including cellular materials. When used is this context, these terms pertain to the macroscopic level. Although more specialized terms such as "water binding potential" are defined in quantitative terms they still apply only at the macroscopic level. The degree and tenacity of water binding or hydration depend on a number of factors including the nature of the nonaqueous constituent, salt composition, pH, and temperature.

"Water holding capacity" is a term that is frequently employed to describe the ability of a matrix of molecules, usually macromolecules present at low concentration, to physically entrap large amounts

of water in a manner that inhibits exudation under the application of an external, often gravitational, force. Familiar food matrices that entrap water in this way include gels of pectin and starch, and cells of tissues, both plant and animal.

Physically entrapped water does not readily flow from tissue foods, even when they are cut or minced. Nevertheless, this water behaves during processing with properties close to those of pure water. It is easily removed during drying, easily converted into ice during freezing, and is readily available as a solvent. Thus, though its bulk flow is severely restricted, the movement of individual molecules is essentially similar to that of water molecules in a dilute salt solution.

Most of the water in tissues and gels can be categorized as physically entrapped, and impairment of this entrapment capability (water holding capacity) of foods has a profound effect on food quality. Examples of quality defects associated with impairment of water holding capacity are syneresis of gels, thaw exudation from previously frozen foods, and inferior performance of animal tissue in sausage resulting from the decline in muscle pH that accompanies normal physiological events postmortem. In all cases, the quality defect stems from the physical relocation of water molecules in space, but does not necessarily reflect any significant change in the interactive properties of these molecules.

2.8.2.2 Molecular Level: General

The intimate mixing of solutes and water results in alteration of the properties of both constituents as compared to their properties when not mixed. These changes result from molecular interactions, and therefore depend upon the nature of the solute at the molecular level. Ions, or charged groups, interact with water primarily through electrostatic forces. These may enhance, or may interfere with, the normal geometric orientations of water molecules. Predominantly hydrophilic solutes interact strongly with water and cause changes in the structural associations and mobility of adjacent water, and at the same time water changes the reactivity, and sometimes also structure, of the hydrophilic solutes. In contrast, the hydrophobic groups of added solutes interact only weakly with adjacent water, seeming to prefer a nonaqueous environment. However, this weak interaction can have profound structural consequences. The bonding forces existing between water and various kinds of solutes are summarized in Table 2.4.

2.8.2.3 Molecular Level: "Bound Water"

A terminology that is in common use, "bound water" is not an easily defined term and does not refer to a homogeneous entity. It does not necessarily refer even to water truly in some form of bonding association with solute. A unified, coherent descriptive terminology for bound water is difficult,

TABLE 2.4
Classifications of Types of Water–Solute Interactions

Type	Example	Strength	Comments
Water–water	Hydrogen bond	5–25 kJ/mol	
Dipole–ion	Water-free ion	40–600 kJ	Depends on ion size and charge
	Water-charged substituent on organic molecule		Influenced by pH and ionic strength
Dipole–dipole	Water–protein NH	5–25 kJ/mol	
	Water–protein CO	5–25 kJ/mol	
	Water-side chain OH	5–25 kJ/mol	
Hydrophobic hydration	Water + R → R(hyd)	Low	Cumulative sum larger
Hydrophobic interaction	2R(hyd) → R_2(hyd) + H_2O	Low	Cumulative sum larger

as numerous, often conflicting definitions illustrate, and there is no consensus about which one, if any, is the best. The term is controversial, frequently misused, and often poorly understood, and many scientists have suggested that the use of the term be discontinued. Although such a step would indeed be desirable in the interests of more precise communication, the term bound water is so common in the literature that it must be discussed and its severe limitations appreciated.

The following partial list of definitions that have been proposed for bound water illustrates why use of the term has created such confusion [24,25]:

1. Bound water is the equilibrium water content of a sample at some appropriate (and arbitrary) temperature and low humidity.
2. Bound water is that water which does not contribute significantly to permittivity at high frequencies and therefore has its rotational mobility restricted by the substance with which it is associated.
3. Bound water is that which remains unfrozen at some arbitrary low temperature, usually −40°C or lower.
4. Bound water is that which is unavailable as a solvent for additional solutes.
5. Bound water is that which produces line broadening in experiments involving proton nuclear magnetic resonance.
6. Bound water is that which moves with the macromolecule in experiments involving sedimentation rates, viscosity, or diffusion.
7. Bound water is that which exists in the vicinity of solutes and other nonaqueous substances, and has apparent properties differing significantly from those of "bulk" water in the same system.

All of these definitions have some validity under the appropriate conditions, but few will produce the same value when they are separately applied to the same, given system. Also, in some cases, the value obtained for bound water using a particular technique and definition will depend on the total water content of the system even when this content is already in excess of the amount of the bound water determined.

From a conceptual point of view it can be useful to think of bound water as somehow imperfectly describing the "water that exists in the vicinity of solutes and other nonaqueous constituents, and that as a result of its location exhibits apparent properties that are significantly altered from those of 'bulk water' in the same system." Bound water can be thought of as in some way having "hindered mobility" as compared to bulk water, not as being "immobilized." In a typical food of high water content, this type of water comprises only a minute part of the total water present, corresponding approximately to the first layer of water molecules adjacent in space to hydrophilic groups. Bear in mind, however, that this is not a static population of water molecules.

This subject of bound or hindered water will be discussed further in the section dealing with molecular mobilities in frozen systems.

2.8.2.4 Interactions of Water with Ions and Ionic Groups

Individual ions and also the ionic groups of organic molecules appear to hinder or influence the mobility of water molecules to a greater degree than do any other types of solutes. The strength of electrostatic water–ion bonds is greater than that of water–water hydrogen bonds, but still much less than that of covalent bonds.

The accepted normal structure of pure water (based on a hydrogen-bonded, generally tetrahedral arrangement) may be disrupted by the addition of dissociable solutes. Water and simple inorganic ions undergo dipole–ion interactions. The example in Figure 2.11 illustrates hydration of the NaCl ion pair. Only the first-layer water molecules in the plane of the paper, oriented by the radial electrical fields associated with the ions, are depicted. In a dilute solution of the ions in water, a second layer of

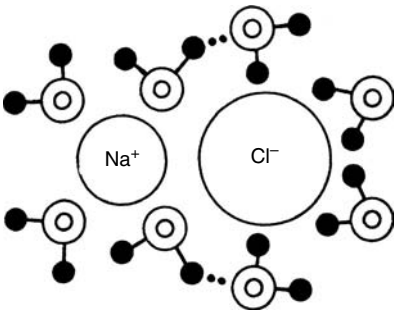

FIGURE 2.11 Likely arrangement of water molecules adjacent to sodium chloride ion pair. Only water molecules in the plane of the paper are represented.

water molecules beyond this first layer is believed to exist in a structurally perturbed state, because of the conflicting structural influences of first-layer water surrounding the charged ions and the more distant, tetrahedrally oriented "bulk-phase" water that is remote from the influence of the radial electrical fields surrounding the ions. In concentrated salt solutions, where individual ion electrical fields would be expected to overlap, bulk-phase water would not exist, and water structure would be dominated by the ions.

There is abundant evidence indicating that some ions in dilute aqueous solution, have a "net structure breaking" effect (solution more fluid than pure water) whereas others have a "net structure forming" effect (solution less fluid than pure water). This is not to suggest that this "structure" is that existing in pure water. The term "net structure" refers to all kinds of structures, either the normal organization of water, or new types of water organization. Clearly, from the standpoint of "normal" water structure, all ions are disruptive, since normal water structure does not possess radial symmetry [26].

The ability of a given ion to alter net structure is related closely to its polarizing power (charge divided by radius) or simply the strength of its electric field. Small and/or multivalent ions (such as Li^+, Na^+, H_3O^+, Ca^{2+}, Ba^{2+}, Mg^{2+}, Al^{3+}, F^-, and OH^-) have strong electric fields and are net structure promoters. The structure imposed by these ions more than compensates from any loss in normal water structure. These ions strongly interact with four to six first-layer water molecules, causing them to be less mobile, and to pack more densely than HOH molecules in pure water. Ions that are large and monovalent, such as K^+, Rb^+, Cs^+, NH_4^+, Cl^-, Br^-, I^-, NO_3^-, BrO_3^-, IO_3^-, and ClO_4^- have rather weak electric fields and are net structure breakers although the effect is very slight with K^+. These ions disrupt the normal structure of water and fail to impose a compensating amount of new structure.

Ions, of course, have important effects in addition to their influence on water structure. Through their varying abilities to hydrate (compete for water), influence the permittivity of the aqueous medium, and govern the thickness of the electrical double layer around colloids, ions profoundly influence the "degree of hospitality" extended to other solutes present in the aqueous medium, and also to substances suspended in the medium. Early recognition of this was the Hofmeister or lyotropic series, which ranked ions in order of their effectiveness in salting-in or salting-out proteins, or their effectiveness in influencing various other properties such as colloid stability. It is encouraging to note that the empirically derived Hofmeister series correlates well with a series based on the expected structural influences of the various ions [27,28].

2.8.2.5 Interaction of Water with Neutral Groups Capable of Hydrogen Bonding (Hydrophilic Solutes)

Interactions between water and nonionic, hydrophilic solutes are weaker than water–ion interactions and about the same strength as those of water–water hydrogen bonds. Depending on the strength of the

water–solute hydrogen bonds, first-layer water (i.e., water immediately adjacent to the hydrophilic species), may or may not exhibit reduced mobility and other altered properties as compared to bulk-phase water.

Solutes capable of hydrogen bonding might at first glance be expected to enhance, or at least to not disrupt the normal structures of pure water. This simplistic expectation ignores the importance of spatial orientation and spatial location to the existence of a viable hydrogen-bonded network. In some instances it is found that the distribution and orientation of the hydrogen-bonding sites of the solute are geometrically incompatible with those existing in pure water. Such solutes frequently have a disruptive influence on the normal three-dimensional, tetrahedrally oriented structure of pure water. Urea is a good example of a small hydrogen-bonding solute that, for geometric reasons may have a marked disruptive effect on the normal structure of water. Conversely, some molecules may have potential hydrogen-bonding hydrophilic groups at orientations and spacings compatible with the hydrogen-bonding structures of water. The simple carbohydrates provide an example. It has been noted that they possess equatorial hydroxyl groups that have similar spatial relationships to those of water molecules in a cluster (see Figure 2.12). Such a degree of compatibility might even enhance the total level of hydrogen bonding. It should be noted that, since the oxygen atom spacings of water and of the individual molecules are temperature dependent, it is not claimed that there is an exact correspondence under all situations, rather it is claimed that there is a close correspondence, and thus potentially a facilitated interaction.

It is important to understand that the total number of hydrogen bonds per mole of water might not be significantly altered by the addition of a hydrogen-bonding solute that disrupts the normal structure of water. This is possible since disrupted water–water hydrogen bonds may be replaced by

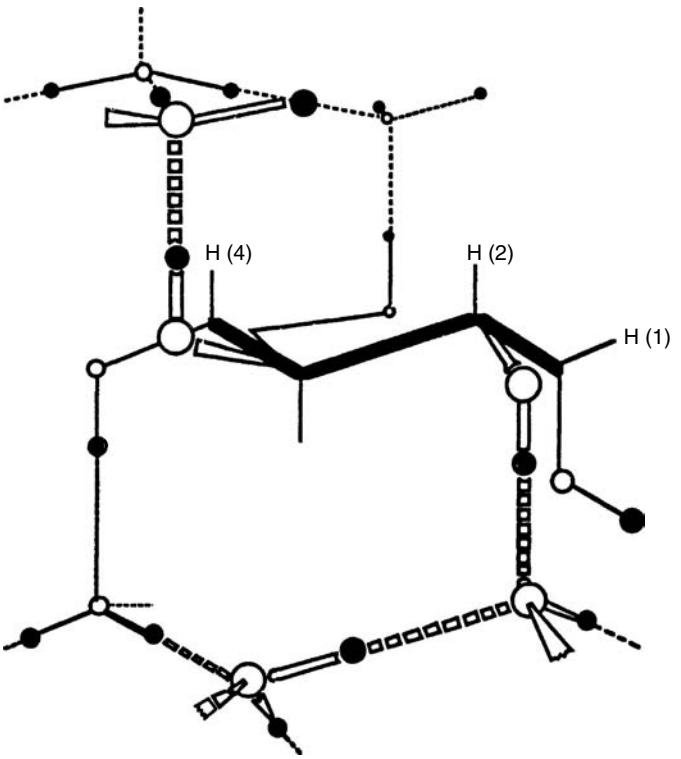

FIGURE 2.12 Possible association of D-glucose with tetrahedrally arranged water molecules. The side view of the pyranose ring is represented by a heavy line. Oxygen and hydrogen atoms of water molecules are represented by open and filled circles, respectively. The hydroxymethyl protons are not shown. (From Suggett, A. (1976) *J. Solution Chem.* **5**: 33–46.)

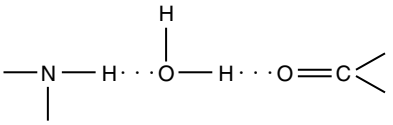

FIGURE 2.13 Hydrogen bonding (dotted lines) of water molecules to two kinds of functional groups commonly occurring in proteins.

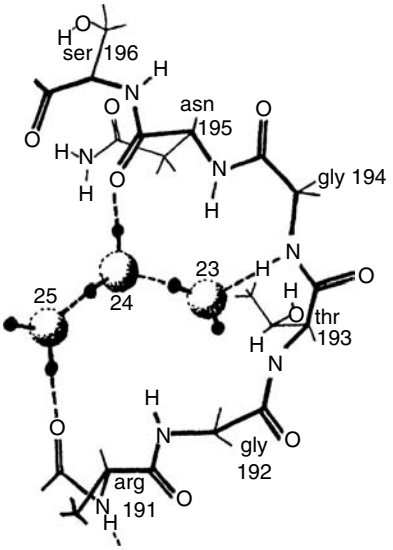

FIGURE 2.14 Example of a three molecule water bridge in papain: 23, 24, and 25 are the water molecules of the bridge. (From Berendsen, H.J.C. (1975) In *Water, a Comprehensive Treatise* (F. Franks, Ed.), Plenum Press: New York, pp. 293–349.)

water–solute hydrogen bonds. Solutes that behave in this manner have little effect on "net structure" as previously defined.

Hydrogen bonding of water can occur with various potentially eligible groups (e.g., hydroxyl, amino, carbonyl, amide, imino groups, etc.). This sometimes results in water bridges, where one water molecule interacts with two eligible hydrogen-bonding sites on one or more solutes. Schematic depiction of hydrogen bonding (dotted lines) of water to two kinds of functional groups found in proteins is shown in Figure 2.13. A more elaborate example involving a three HOH bridge between backbone peptide units is shown in Figure 2.14.

As has been observed for some sugars [29], hydrophilic groups in many crystalline macromolecules are separated by distances very similar to the nearest neighbor oxygen spacing in pure water. Should this spacing prevail in the hydrated macromolecule, this would tend to encourage cooperative hydrogen bonding involving both first- and second-layer water by enhancing the stability (lifetime) of the cluster.

2.8.2.6 Interaction of Water with Nonpolar Substances

The mixing of water and hydrophobic substances such as hydrocarbons, rare gases, and the apolar groups of fatty acids, amino acids, and proteins is, not surprisingly, a thermodynamically unfavorable event ($\Delta G > 0$). However, the free energy of this process is positive not because ΔH is positive, which is typically the case for solutes with a low solubility, but rather because $T\Delta S$ is negative [30].

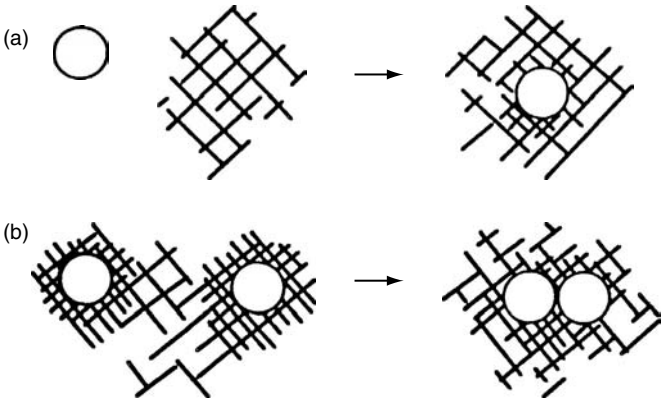

FIGURE 2.15 Schematic depiction of (a) hydrophobic hydration and (b) hydrophobic association. Open circles are hydrophobic groups. Hatched areas are water. (Adapted from Franks, F. (1975) In *Water, a Comprehensive Treatise* (F. Franks, Ed.), Plenum Press: New York, pp. 1–94.)

This reduction in entropy, considered an indicator of increased "order," is thought to occur because of special structures in water that form in the vicinity of these incompatible apolar entities. This process has been termed "hydrophobic hydration" (Table 2.4 and Figure 2.15a).

Because hydrophobic hydration is thermodynamically unfavorable, it follows that the system adjusts in an attempt to minimize the association of water with the apolar entities that are present. Thus, if two separated apolar groups are present, their incompatibility with the aqueous environment serves to encourage their association, thereby lessening the water–apolar interfacial area, a process that is thermodynamically favorable ($\Delta G < 0$). This process, a partial reversal of hydrophobic hydration, is referred to as "hydrophobic interaction" [31] and, in its simplest form, can be represented as

$$\text{R (hydrated)} + \text{R (hydrated)} \rightarrow \text{R}_2\text{ (hydrated)} + \text{H}_2\text{O}$$

where R is an apolar group (Table 2.4 and Figure 2.15b).

Because water and apolar groups exist in an antagonistic relationship, water structure adjusts to minimize contact with apolar groups. The type of water structure that was believed to exist in the layer next to apolar groups is depicted in Figure 2.16. Two aspects of this antagonistic relationship are worthy of further discussion: formation of clathrate hydrates and association of water with hydrophobic groups in proteins.

2.8.2.6.1 Clathrate Hydrates

A clathrate hydrate is an ice-like inclusion compound wherein water, the host substance, forms a hydrogen-bonded cage-like structure that physically entraps a small apolar molecule known as the guest molecule. These compounds are of interest because they represent the most extreme structure forming response of water to an apolar substance, and because microstructures of similar type may occur naturally in biological matter. Clathrate hydrates can be crystalline. Clathrate crystals can easily be grown to visible size, and some are stable at temperatures above 0°C, provided the pressure is sufficient [32]. The guest molecules of clathrate hydrates are characteristically low molecular weight compounds with sizes and shapes compatible with the dimensions of host water cages comprised of 20–74 water molecules. Typical guests include low molecular weight hydrocarbons and halogenated hydrocarbons; rare gases; short chain primary, secondary, and tertiary amines; and alkyl ammonium, sulfonium, and phosphonium salts. Direct interaction between water and guest is slight, usually involving nothing more than weak van der Waals forces; indeed often the guest molecule is free to

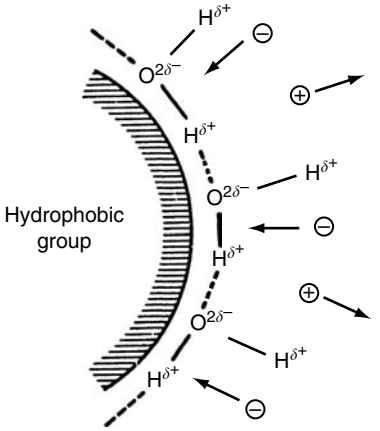

FIGURE 2.16 Proposed water orientation at a hydrophobic surface. (Adapted from Lewin, S. (1974) *Displacement of Water and its Control of Biochemical Reactions*. Academic Press: London.)

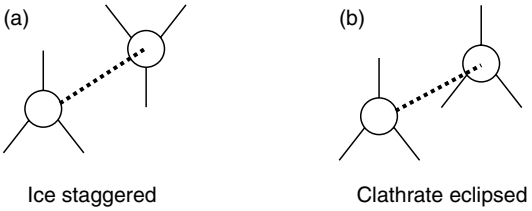

FIGURE 2.17 Relative orientation of hydrogen-bonded water molecules: (a) staggered conformation (ice) and (b) eclipsed conformation (clathrate).

rotate within the cavity. Clathrate hydrates are the extraordinary result of water's attempt to minimize contact with hydrophobic groups. While at first sight the water structure in a clathrate hydrate is very different from the structure in ice, this structure arises from a subtle change in the geometry of the hydrogen bond. In ice, water molecules, tetrahedrally coordinated to their neighbors, have their hydrogen bonds in the staggered conformation if one looks along the direction of an oxygen–oxygen link while in a clathrate hydrate the geometry of the tetrahedral coordination of the water molecules is in the eclipsed form (Figure 2.17). This rotation of 60° in the bond orientation results in structures in which three of the four hydrogen bonds of a water molecule can help form the curved surface (like a geodesic surface) of a cage, while the fourth hydrogen bond projects out normal to this surface. Thus, there are no hydrogen bonds projecting into the internal cavity, and hence no unfavorable interaction with any apolar group within the cavity. As noted, a small, apolar molecule in the cavity may freely rotate. It is also important to note that, if the free energies of the ice structure and that of the clathrate cage structure (any guest molecules in the cages being absent) are computed, the ice structure is more stable than that of the empty clathrate by only a small amount. Thus, the presence of a suitable guest, stabilizing the cavity through steric interactions, can result in a crystalline structure of much higher stability than ice [33,34].

There is evidence that hydrogen-bonded structures similar to the crystalline clathrate hydrates, but that are less spatially extensive (i.e., hydrogen-bonded multimers with eclipsed orientation), may exist naturally in biological matter [35–37], and should this be the case, these localized structures would be of far greater importance in food science than the crystalline hydrates, since they would be likely to influence the conformation, reactivity, and stability of molecules such as proteins. For example, it has been suggested that partial clathrate structures may exist around exposed hydrophobic

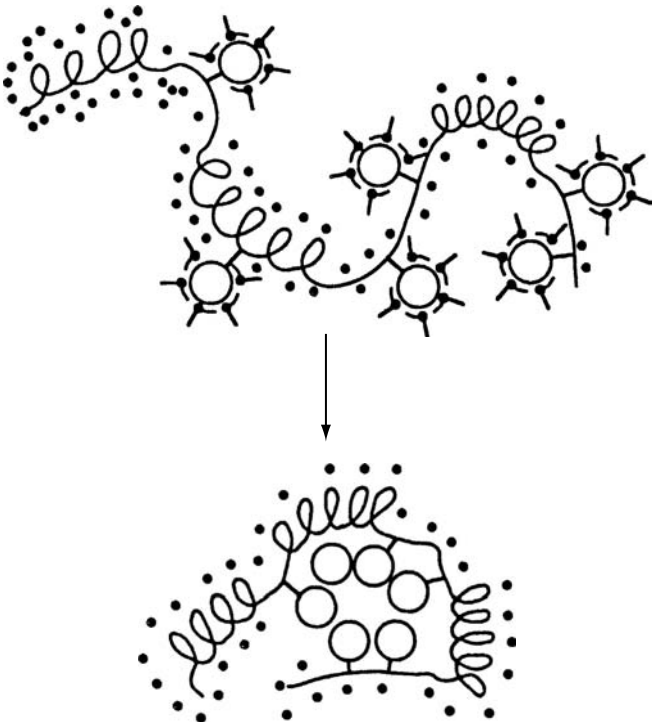

FIGURE 2.18 Schematic illustration of a globular protein undergoing hydrophobic interaction. Open circles are hydrophobic groups. L-shaped entities are water molecules oriented in accordance with proximity to a hydrophobic surface and dots represent water molecules associated with polar groups.

groups of proteins [38]. Figures 2.16 and 2.18 illustrate this concept. It is also possible that clathrate-like structures of water have a role in the anesthetic action of rare gases such as xenon. For further information on clathrate hydrates, the reader is referred to Davidson [32].

Molecular dynamic simulations of aqueous systems with included nonpolar species provide additional evidence for the possible reorientation of the water–water hydrogen bond into a "clathrate-type" orientation as a response to the presence of the nonpolar entity. While in detail, the results of molecular modeling do not show structures with hydrogen-bonding geometries akin to the clathrate-type orientations, the shift in average direction of bonds is consistent with the more simplistic pictorial model. In models incorporating hydrophobic solutes, there is a tendency for hydrogen bonds to be tangential to molecular surfaces [7].

2.8.2.6.2 Interaction of Water with Complex Molecular Structures

Although determination of the arrangement of water molecules near organic molecules is experimentally difficult, this is an active field of research, and useful data have been obtained. The hydrated pyranose sugar ring is shown in Figure 2.12 and a computer simulated cross section of myoglobin [39] is shown in Figure 2.19. Assuming a separation distance of 2.8 Å between hydration sites, and full occupancy of those sites, about 360 HOH molecules would be in the primary hydration shell of myoglobin.

Given the coexistence of polar, hydrophilic, and hydrophobic regions within a large molecule, unavoidable interactions and interferences are inevitable. In proteins, for example, unavoidable association of water with certain hydrophobic groups has an important influence on protein functionality [11,30,38]. The extent of these unavoidable contacts is potentially quite large because

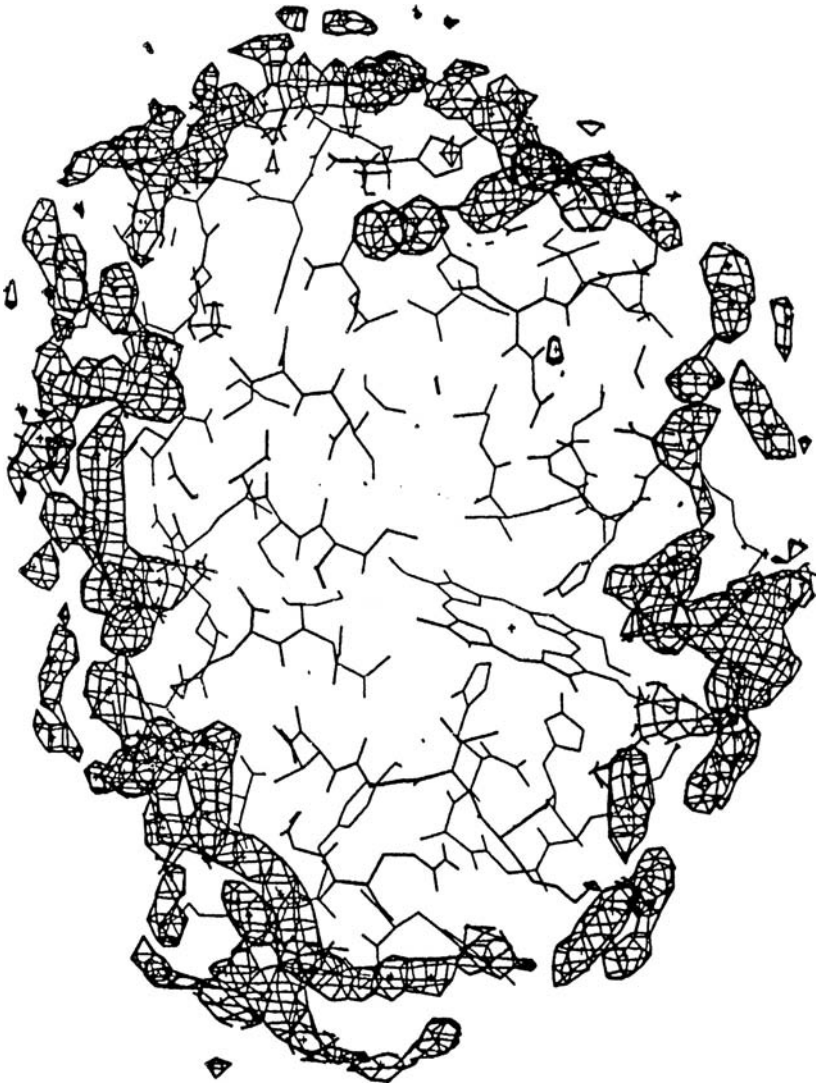

FIGURE 2.19 Cross section of a hydrated myoglobin molecule as determined by a molecular dynamics simulation. Mesh cages represent high probability sites of first layer water molecules. The stick figure represents the protein time-averaged structure. (From Lounnas, V. and B.M. Pettitt (1994) *Proteins: Struc. Func. Genet.* **18**: 133–147.)

apolar side chains exist on about 40% of the amino acids in typical oligomeric food proteins. These nonpolar groups include the methyl group of alanine, the benzyl group of phenylalanine, the isopropyl group of valine, the mercaptomethyl group of cysteine, and the secondary butyl and isobutyl groups of the leucines. The apolar groups of other compounds such as alcohols, fatty acids, and free amino acids also can participate in hydrophobic interactions, but the consequences of these interactions are less important than those involving proteins.

Because the exposure of protein apolar groups to water is thermodynamically unfavorable, the association of hydrophobic groups or hydrophobic interaction is facilitated. This is the process depicted schematically in Figure 2.18. The hydrophobic interaction is believed to be a major driving force for protein folding, causing many hydrophobic residues to assume locations buried in the protein interior. Nevertheless, despite such hydrophobic interactions, it is estimated that nonpolar

groups in globular proteins still typically occupy about 40–50% of the surface area. As a consequence of these surface-located hydrophobic groups, hydrophobic interactions are also regarded as being of primary importance in maintaining the tertiary structure (subunit associations, etc.) of most proteins [40,41]. It is therefore of considerable importance to the structural complexities of proteins that a reduction in temperature causes hydrophobic interactions to become weaker, and hydrogen bonds to become stronger.

Recent applications of molecular modeling to the solvation effects of solutes tend to confirm that the hydrogen-bonding associations of water are important, and indicate that the primary effects of solutes is to modulate the hydrogen-bonding associations that occur within the pure solvent, in particular, causing changes that mirror the changes that are induced in the pure solvent by changes in temperature and pressure, and which are reflected in the equation of state of the solvent water [42].

The foregoing outline of the properties of water, and of aqueous solutions, provides a good foundation for understanding the many roles of water in food systems, and also the influence of the amount and the characteristics of water on the chemistry and microbiology of the food. In the ensuing discussion we will examine the utility of different approaches to understanding the detailed role of water in determining food properties and food stability.

2.9 WATER ACTIVITY AND RELATIVE VAPOR PRESSURE

2.9.1 Introduction

It has long been recognized that a relationship, though imperfect, exists between the water content of food and its perishability, with origins dating back to prehistory. Concentration and dehydration processes are conducted primarily for the purpose of decreasing the water content of a food, simultaneously increasing the concentration of solutes and thereby decreasing perishability.

However, it has also been observed that various types of food with the same water content differ significantly in perishability. Thus, it is evident that water content alone is not a reliable indicator of perishability. This situation is attributable, in part, to differences in the intensity with which water is associated with nonaqueous constituents—one might expect that water engaged in strong associations would be less likely to be able to support degradative activities such as growth of microorganisms and hydrolytic chemical reactions, than would weakly associated water. The term "water activity" (a_w) was developed to reflect the intensity with which water associates with various nonaqueous constituents.

Experience shows that food stability, safety, and other properties can be predicted far more reliably from a_w than from water content. Even so, a_w is not a totally reliable predictor. The reasons for this will be explained in a later section. Despite this lack of perfection, a_w correlates sufficiently well with rates of microbial growth and rates of many degradative reactions to make it a useful indicator of potential product stability and microbial safety. The fact that a_w is specified in some U.S. federal regulations dealing with good manufacturing practices for food attests to its usefulness and credibility [43], and also dictates that this topic be fully explored.

2.9.2 Definition and Measurement

As described in most physical chemistry textbooks, Lewis and Randall rigorously derived the notion of substance "activity" from the laws of thermodynamics, and Scott [44,45] pioneered its application to foods. It is sufficient here to state that,

$$a_w = (f/f^o)_T \tag{2.1}$$

where f is the fugacity of the solvent (fugacity being the escaping tendency of a solvent from solution) and f^o is the fugacity of the pure solvent in some defined standard state. The subscript T refers to the measurement being at constant temperature. At low pressures (e.g., ambient) the difference between f/f^o and p/p^o is less than 1%, so defining a_w in terms of p/p^o is clearly justifiable. Thus,

$$a_w = (p/p^o)_T \tag{2.2}$$

It is important to be aware that this equality is based on the assumption of thermodynamic equilibrium. Since with foods this assumption is generally violated, Equation 2.2 must be considered approximate, and the proper expression is

$$a_w \approx (p/p^o)_T \tag{2.3}$$

In food science, because p/p^o is a readily measured term, which sometimes does not equate to a_w, it is more appropriate to use the term $(p/p^o)_T$ rather than a_w. This practice will be followed here. Relative vapor pressure (RVP) is the name for $(p/p^o)_T$ and these terms will be used interchangeably. Despite the scientific soundness of using RVP rather than a_w, in that RVP does not imply equilibrium, the reader should be aware that the term a_w is in widespread use, appears in other chapters of this book, and is not improper provided the user understands its true meaning and the constraints implied by its use.

Failure of the a_w–RVP approach to be a perfect estimator of food stability occurs for two basic reasons, both violation of the assumptions underlying Equation 2.2 and solute-specific effects. Violation of the assumptions of Equation 2.2 can, but fortunately usually does not, detract unduly from the usefulness of RVP as a technological tool. An exception occurs if dry products are prepared by absorption of water rather than desorption (hysteresis effect). This will be discussed later. Violation of the assumptions of Equation 2.2 does, however, invalidate the use of RVP as a tool for mechanistic interpretation in instances where the theoretical models are based on the validity of these assumptions. This is often true of models of moisture sorption isotherms, where great care should be exercised in applying the apparent conclusions.

In a few instances that can be of great importance, solute-specific effects can cause RVP to be a poor indicator of food stability and safety. This can occur even when the assumptions underlying Equation 2.2 are fully met. In such situations, foods with the same RVP but different solute compositions will exhibit different stabilities and other properties. This is a very important point that must never be overlooked by anyone relying on RVP as a tool for judging the safety and stability of food. Figure 2.20 serves to reinforce this point. These data clearly indicate that the minimum $(p/p^o)_T$ for growth of *Staphylococcus aureus* is dependent upon solute type [46].

Relative vapor pressure is related to percent equilibrium relative humidity (%ERH) of the product environment as follows:

$$\text{RVP} = (p/p^o)_T = \%\text{ERH}/100 \tag{2.4}$$

Two aspects of this relationship are noteworthy. First, RVP is an intrinsic property of the sample, whereas %ERH is a property of the atmosphere established in steady state with the sample. Note that the existence of a steady state does not necessarily assure existence of equilibrium. Second, the equality described in Equation 2.4 exists only if equilibrium has been established between the product and its environment. Establishment of equilibrium is a time-consuming process even with very small samples (<1 g) and almost impossible for large samples, especially at temperatures below 20°C.

Since ERH implies equilibrium, it might therefore be more appropriate to use a modified form of this relationship, which more correctly states that the measured RVP is related to the steady-state

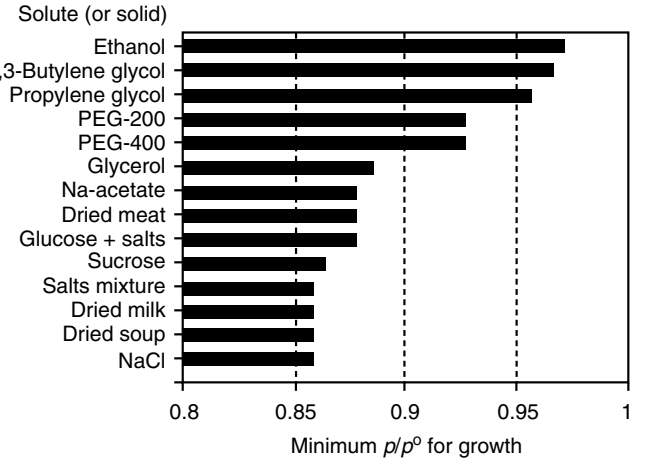

FIGURE 2.20 Minimum RVP for growth of *Staphyloccus aureus* as influenced by solute used to control the RVP. Temperature is close to optimal for growth. PEG is polyethylene glycol. (From Chirife, J. (1994) *J. Food Eng.* **22**: 409–419.)

relative humidity (SSRH) of the product environment:

$$\text{RVP} = (p/p^{\text{o}})_{\text{T}} \approx \%\text{SSRH}/100 \tag{2.5}$$

The RVP of a small sample can be determined by placing it in a closed chamber for a time sufficient to achieve apparent equilibrium (constant weight) and then measuring either pressure or relative humidity in the chamber [47–50]. Various types of instruments are available for measuring pressure (manometers) and relative humidity (electric hygrometers, dew point instruments) [51]. Knowledge of the freezing point depression can also be used to determine RVP, though this relates exactly only to the temperature at the freezing point. On the basis of many collaborative studies, the precision of a_{w} determinations is around ± 0.005 [48].

If one desires to adjust a small sample to a specific RVP, this can be done by placing it in a closed chamber at constant temperature, maintaining sample atmosphere at a constant and known relative humidity by means of an appropriate saturated salt solution or other equivalent method, and storing until constant sample weight is achieved.

2.9.3 Temperature Dependence

Relative vapor pressure is temperature dependent, and the Clausius–Clapeyron equation in modified form provides a means for estimating this temperature dependence. This equation, though based on a_{w}, can often be applied to RVP and takes the form

$$\frac{\text{d} \ln a_{\text{w}}}{\text{d}(1/T)} = \frac{-\Delta H}{R} \tag{2.6}$$

where T is absolute temperature, R is the gas constant, and $-\Delta H$ is the isosteric heat of sorption at the water content of the sample. By rearrangement, this equation can be made to conform to the generalized equation for a straight line. It is then evident that a plot of $\ln a_{\text{w}}$ vs. $1/T$ (at constant water content) should be linear, and if the same holds true for $\ln(p/p^{\text{o}})_{\text{T}}$ vs. $1/T$, then the equation can be used to estimate effective sorption heats for the purposes of comparison. These relationships assume that equilibrium has been achieved, which is often not the case.

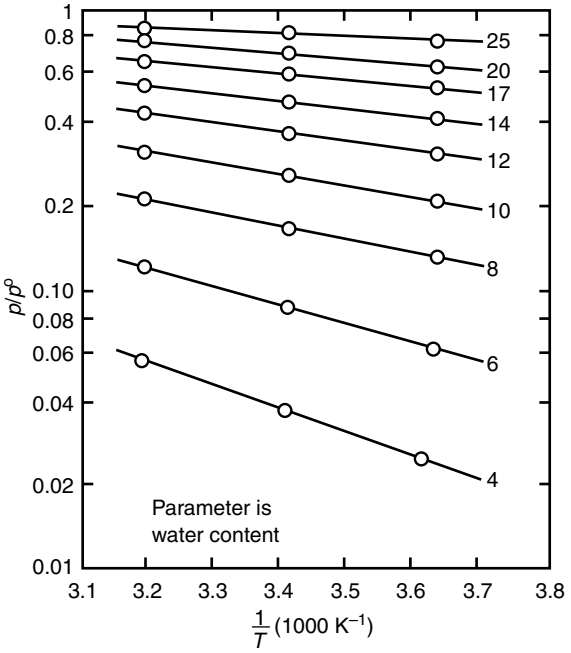

FIGURE 2.21 Relationship between RVP and temperature for native starch of different water contents. Water content values displayed after each line are expressed as g HOH/g dry starch. (From van den Berg, C. and H.A. Leniger (1978) In *Miscellaneous Papers*. Wageningen Agricultural University.)

Linear plots of $\ln(p/p^o)_T$ vs. $1/T$ for native starch at various moisture contents are shown in Figure 2.21. It is apparent that the degree of temperature dependence is a function of moisture content. At a starting $(p/p^o)_T$ of 0.5, the temperature coefficient is 0.0034 K^{-1}over the temperature range 275–313 K (2–40°C). On the basis of the work of several investigators [48,52], temperature coefficients for $(p/p^o)_T$ (temperature range 5–50°C at a starting $(p/p^o)_T$ of 0.5) range from 0.003 to 0.02 K^{-1} for high carbohydrate or high protein foods. Thus, depending on the product, a 10 K change in temperature can cause a 0.03–0.2 change in $(p/p^o)_T$. This behavior can be important for a packaged food because it will undergo a change in RVP with a change in temperature, causing the temperature dependence of its stability to be greater than that of the same product unpackaged.

Plots of $(p/p^o)_T$ vs. $1/T$ are not always linear over broad temperature ranges. For example, they generally exhibit sharp breaks at the onset of ice formation. Before interpreting data at subfreezing temperatures, it is appropriate to consider the definition of RVP as it applies to subfreezing temperatures. As pointed out earlier, undercooled water can exist, as metastable, at temperatures below 0°C. Hence a question arises as to whether the denominator term p^o, the vapor pressure of the pure solvent, should be equated to the vapor pressure of undercooled water, or to the vapor pressure of ice. While pure ice is the equilibrium form of pure water at these temperatures, for useful comparisons to systems above the freezing point, it emerges that the more appropriate choice for standard state is the vapor pressure of undercooled water (1) because the values of RVP at subfreezing temperatures can then, and only then, be directly compared with those at above-freezing temperatures and (2) because making the choice of the vapor pressure of ice as defining p^o would result, for samples containing ice, in a situation whereby the RVP would be unity at all subfreezing temperatures. This second point results because, as is evident from standard thermodynamic relationships, the partial pressure of water of any frozen food is equal to the vapor pressure of ice at the same temperature.

Because the vapor pressure of undercooled water has been measured down to −15°C, and estimated by extrapolation to −30°C (Table 2.3) and the vapor pressure of ice has been measured

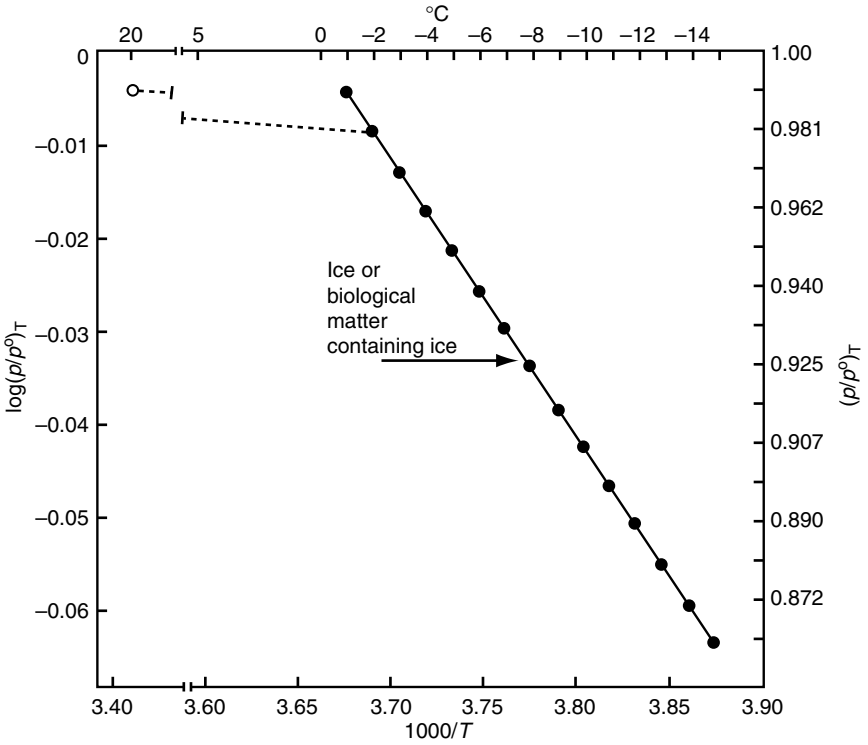

FIGURE 2.22 Relationship between RVP and temperature for aqueous systems above and below freezing. (Modified from Fennema, O. (1978) In *Dry Biological Systems* (J.H. Crowe and J.H. Clegg, Eds.), Academic Press: New York, pp. 297–322.)

to much lower temperatures, it is simple to calculate RVP values for frozen foods based on the undercooled water standard state,

$$a_w = \left[\frac{p_{ff}}{p^o(\text{UCW})}\right]_T = \left[\frac{p_{ice}}{p^o(\text{UCW})}\right]_T \tag{2.7}$$

where p_{ff} is the partial pressure of water in partially frozen food, p^o(UCW) is the vapor pressure of pure undercooled water, and p_{ice} is the vapor pressure of pure ice, all at the same temperature T.

Presented in Table 2.3 are RVP values calculated from the vapor pressures of ice and undercooled water. These values are identical to those of frozen foods at these same temperatures. Figure 2.22 is a plot of $\log(p/p^o)_T$ vs. $1/T$ for a typical aqueous solution, illustrating that (1) the relationship is linear at subfreezing temperatures, (2) the influence of temperature on RVP is typically far greater at subfreezing temperatures than at above-freezing temperatures, and (3) a sharp break occurs in the plot at the freezing point of the sample. Similar behavior is to be expected of biological systems.

Two important distinctions should be noted when comparing RVP values at above- and below-freezing temperatures. First, at above-freezing temperatures, RVP is a function of sample composition and temperature, with the former factor predominating. At subfreezing temperatures, RVP becomes independent of sample composition, and depends solely on temperature since in the presence of an ice phase, RVP values are not influenced by the kind or ratio of solutes present [53]. As a consequence, any subfreezing event that is influenced by the kind of solute present (e.g., diffusion-controlled processes, catalyzed reactions, and reactions affected by the presence or absence of cryo-protective agents, antimicrobial agents, and/or chemicals that alter pH and oxidation–reduction

potential) *cannot* be accurately forecasted based on the RVP value. Consequently, RVP values at subfreezing temperatures are far less valuable indicators of physical and chemical events than are RVP values at above-freezing temperatures. It follows that knowledge of RVP at a subfreezing temperature cannot be used to predict RVP at an above-freezing temperature. Note also that using freezing point depression to estimate a_w or RVP is actually a determination of the break point in the curve.

Second, as the temperature is changed sufficiently to form or to melt ice, the meaning of RVP, in terms of food stability, also changes. For example, in a product at $-15°C$ ($(p/p^o)_T = 0.86$) microorganisms will not grow, and chemical reactions will occur slowly. However, at $+20°C$ and $(p/p^o)_T = 0.86$, some chemical reactions will occur rapidly, and some microorganisms will grow at moderate rates.

This lack of utility of RVP as an indicator of product stability at subfreezing temperatures served as one of the drivers in the development of the molecular mobility approach to understanding food stability relationships, which we shall now discuss. Discussion of moisture sorption isotherms that depict the relationship between moisture content and sample RVP and relate these to the stability of foods is better held until after a discussion of molecular mobility, since the concepts developed in the molecular mobility approach can help clarify some of the relationships between moisture sorption isotherms and product stability.

2.10 MOLECULAR MOBILITY AND FOOD STABILITY

2.10.1 Introduction

Even though the RVP approach has served the food industry well, this should not preclude consideration of other approaches that can supplement or partially replace RVP as a tool for predicting and controlling food stability and processability. Compelling evidence has accumulated to indicate that molecular mobility (Mm: translational or rotational motion) is an attribute of foods that deserves careful attention because it is related causally to many important diffusion-limited properties of food.

In the molecular mobility approach, attention is paid to the mobilities of the constituent molecules. Both rotational and translational mobilities are considered relevant. This consideration of mobilities implies that careful attention should be given to the diffusional aspects of many reactions, and in particular, the importance of diffusion-limited reactions to the quality in many foods.

2.10.2 The Early History

As indicated earlier, Luyet and associates in the United States [19,20] and Rey and associates in France [22,23] were the first to draw attention to the relevance of Mm (glassy states, recrystallization, collapse temperatures during freeze drying) to the properties of biological materials. Many of the basic concepts pertaining to Mm in nonequilibrium systems consisting of synthetic amorphous polymers were formulated by Ferry and associates [54,55] and White and Cakebread [56,57] described the important role of glassy and supersaturated states in various sugar containing foods, and suggested that the existence of these states had an important influence on the stability and processability of many foods. Duckworth et al. [58] demonstrated the relevance of Mm to rates of nonenzymic browning and ascorbic acid oxidation, thereby providing more evidence that the relationship between Mm and food stability is one of considerable importance.

2.10.3 The Next Stage

From this starting point, things have moved rapidly, such that now Mm is accepted as one of the key determinants of food stability. The beginning of the modern approach to Mm emerged from pioneering studies by Franks [59] and Slade and Levine [60–65], who demonstrated that Ferry's concepts could be applied, in modified form, to the understanding of food stability. The important

advance was the postulation that aqueous sugar glasses and other materials in the glassy state in food systems could be conceived of as having properties similar to those of the amorphous polymers characterized by Ferry et al., and that relationships similar to those developed by Ferry could be applied to rate behavior in these "aqueous food glasses." In particular, Levine and Slade proposed the application of the Williams–Landel–Ferry (WLF) equation to food systems. The WLF equation takes the form

$$\log \frac{\eta}{\eta_g} = \frac{-C_1(T - T_g)}{C_2 + (T - T_g)} \tag{2.8}$$

where η is the viscosity at product temperature T (K), η_g is the viscosity at product temperature T_g (K) (usually the glass transition temperature) and C_1 (dimensionless), and C_2 (K) are constants. η can be replaced by 1/Mm, the molecular mobility, or any other diffusion-limited relaxation process. This equation describes the dependence of system viscosity, and other diffusion-enabled processes, on the amorphous state behavior of a polymer. In polymer systems, universal values have been established for C_1 and C_2. It is a topic of dispute as to whether these values can be usefully applied to systems of aqueous food glasses. While Levine and Slade coined the phrase "food polymer science approach" to describe these interrelationships, it is perhaps more helpful to focus on the underlying concept of molecular mobility, as we have chosen to do in this chapter.

2.10.4 Factors That Influence Reaction Rates in Solution

Before discussing the concepts of molecular mobilities as determinants of reaction rates in diffusion-limited systems, it is important to note that at ambient temperatures, chemical reactions in aqueous solution are often not diffusion limited. At conditions of constant temperature and pressure, three primary factors govern the rate of a chemical reaction, a diffusion factor, D, describing the probability of an encounter, a frequency of collision factor, A, defining the number of collisions per unit time following encounter, and a chemical activation energy factor, E_a, defining the energy barrier to be surmounted in a collision between properly oriented reactants. The latter two terms occur in the Arrhenius relationship describing the temperature dependence of the reaction rate constant. For a reaction to be diffusion limited, neither A nor E_a can be rate limiting; in other words, properly oriented reactants must collide with great frequency, and with a sufficiently low activation energy to ensure that collisions have a high probability of resulting in reaction. Therefore, diffusion-limited reactions typically have low activation energies (8–25 kJ/mol). Most "fast reactions" (small E_a, large A) are diffusion limited. Examples of diffusion-limited reactions are proton transfer reactions, acid–base reactions, many enzyme catalyzed reactions, protein folding, polymer chain growth, radical recombination reactions, and oxygenation/deoxygenation of hemoglobin and myoglobin. A rate constant of 10^{10} to 10^{11} M^{-1} $s^{-1}$is regarded as presumptive evidence of a diffusion-limited reaction. The diffusion-limited rate is the maximum rate possible for a reaction in solution (conventional reaction mechanisms, which are normal, are assumed).

The viscosity and temperature dependence of the diffusion constant is pertinent. The second-order diffusion-limited rate constant for uncharged spherical particles is given by the Smoluchowski's equation

$$k_{dif} = \frac{4\pi N_A}{1000}(D_1 + D_2)r \tag{2.9}$$

where N_A is Avogadro's number, D_1 and D_2 are diffusion coefficients for particles 1 and 2, and r is the distance of closest approach of particles 1 and 2, represented by the sum of their radii.

And, from the Stokes–Einstein equation:

$$D = kT/\pi\beta\eta r_s \tag{2.10}$$

where k is the Boltzmann constant, T is the absolute temperature, β is a numerical constant, η is the viscosity, and r_s is the hydrodynamic radius of the diffusing species.

Since viscosity increases rapidly as temperature is reduced in the WLF region, this dependence of D, and hence k_{dif} on viscosity is of particular interest.

It appears likely that the rates of some reactions in high moisture foods under ambient conditions are diffusion limited, while others are not. Those rates that are diffusion limited would be expected to conform with WLF kinetics as temperature is lowered, or as moisture content is decreased.

2.10.5 The Role of Molecular Mobility in Food Stability

The major concept regarding the relationship between molecular mobility and stability of foods is very simple. As a food is cooled, molecular mobilities decrease. This is a normal consequence of lowered temperature. The different molecular species of the food will, of course, each have their own characteristic mobilities. Two scenarios are possible. In the simpler scenario, as temperature is lowered, at some point the mobility of the larger molecules becomes so constrained that their diffusion becomes highly restricted and processes depending on their mobility will slow down markedly. At some lower temperature, intermediate size molecules also experience restricted motion, and the properties of the system, and its reactions, exhibit increased temperature dependence in the temperature zone where restricted motion occurs.

In the more complex scenario, as temperature is lowered, a new solid phase begins to separate. This is most relevant when the solid phase is ice (i.e., freezing). As ice separates out, concentration of solutes in the unfrozen aqueous phase increases. Molecular mobility is not solely a function of the temperature, it is also a function of the concentration, since at higher concentrations collisions and entanglements become more likely. Hence, in these systems, as temperature is lowered, molecular mobility is reduced both through the effect of temperature and also through the effect of increasing concentration. The combination of these factors leads to a reduction in mobility with decreasing temperature, which is much more pronounced than that that occurs when temperature lowering is the only driving force. As before, molecular size is a factor, with large molecules exhibiting severely restricted mobilities at higher temperatures than do smaller molecules. The patterns of behavior of frozen systems have been studied in great detail over the past 30+ years and are discussed further in terms of molecular mobilities later in this section.

Evidence suggests that Mm is causatively related to diffusion-limited properties of foods that contain, besides water, substantial amounts of amorphous, primarily hydrophilic molecules, ranging in size from monomers to polymers. The key constituents with respect to Mm are water and the dominant solute or solutes. Foods of this type include starch containing foods, boiled confections, protein-based foods, intermediate moisture foods and dried, frozen, or freeze dried foods.

When a food is in a condition where Mm is greatly reduced, diffusion-limited properties become quite stable, changing very slowly, or not at all with time. Note that while most processes of physical change are diffusion limited, not all processes of chemical change are so limited. Sometimes chemical reactivities are the dominant factor in food stability. Nevertheless, diffusion-limited processes often play an important role in food stability.

As we now discuss the Mm approach to food stability in more detail, one should consider this approach as a powerful complement to, rather than a replacement for, RVP as a tool to predict the stability of food systems containing water as a major component.

2.10.6 The State Diagram

2.10.6.1 Introduction

Since food systems rarely exist in equilibrium, traditional phase diagrams are of limited use for understanding the phase behaviors of foods. It is better to utilize an extended form of diagram, often termed a state diagram, which provides information on nonequilibrium, perhaps metastable "states," in addition to information on equilibrium phases. The term "state" refers to the nonequilibrium manifestation of what would, at equilibrium, be labeled a phase. Its use is encouraged, to distinguish clearly between equilibrium or nonequilibrium observations. State diagrams are in essence "supplemented" phase diagrams.

A simplified temperature-composition state diagram for a binary system is shown in Figure 2.23. Compare this to the phase diagram of Figure 2.10. In these diagrams, solid lines are assumed to be thermodynamically defined, while dashed lines indicate the locus of a property or parameter that is kinetically defined, or metastable. In general, these loci are plotted as the limit lines, defining the putative final reality of the property. It is assumed, in using these diagrams, that pressure is constant, and that the time dependence of metastable states is of little or no significance in the systems of

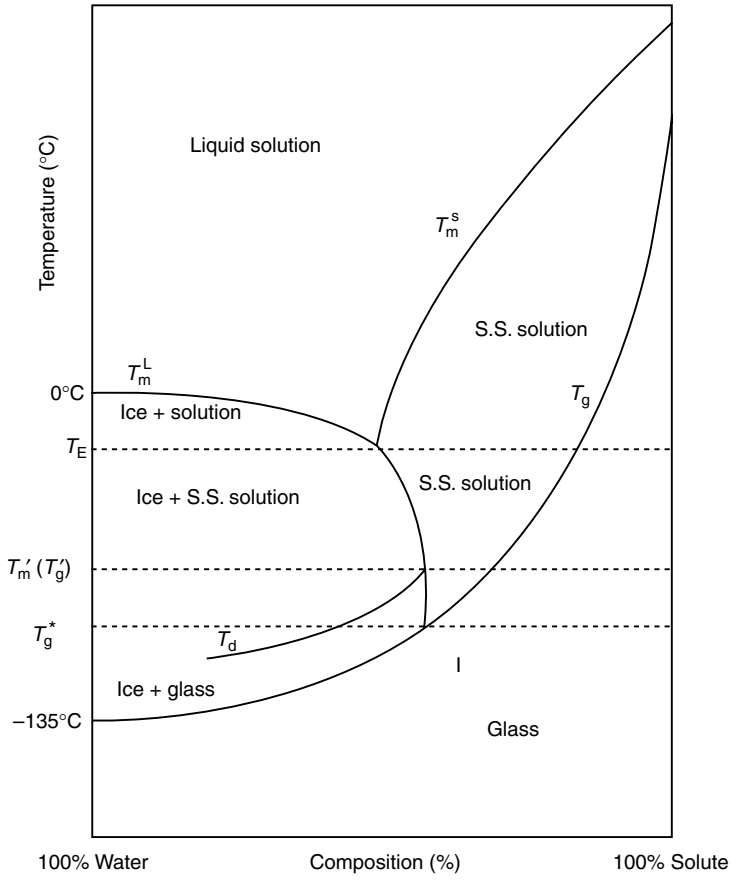

FIGURE 2.23 Annotated temperature composition state diagram for a binary aqueous system. The assumptions are of maximal freeze concentration, no solute crystallization, constant pressure, and no time dependence. T_m^L is the melting point curve, T_E is the eutectic point, T_m^s is the solubility curve, T_g is the glass transition curve, T_d is the glass devitrification curve, T'_m (T'_g) is the onset of melting, and T_g^* is the solute specific glass transition temperature of the maximally freeze concentrated solution.

interest. While all state diagrams for simple binary systems will have the same form, real, complex foods cannot be easily represented by a binary state diagram. However, providing the only material to crystallize is water, a binary state diagram can provide an adequate approximation of the state behavior of a complex food, and can display the glass transition curve with sufficient accuracy to be of value. To use such a diagram, one considers the totality of all nonaqueous components of the aqueous phase as though they were a single solute. This is acceptable providing no component of the nonaqueous solute mix separates out (crystallizes, precipitates, or forms a separate new liquid phase). Since in most frozen foods ice is the sole component to separate from the aqueous phase, a pseudobinary diagram can easily be obtained by plotting T_m^L as a function of concentration. It should be realized, however, that in a complex food, different regions of the food, or different component molecules, may exist in phases distinct from those of other regions or those containing other component molecules, and thus may require description by multiple binary state diagrams. It can be challenging to identify which is the dominant component or dominant region, controlling the critical properties, in such a system. For example, in some systems containing a mixture of polymers, phase separations occur, creating domains that may contain differing dominant polymer species. In such a complex system, identifying the most relevant glass transition, or mobility restriction, is difficult. The critical reactant may be in one, or several, of the many phases present.

2.10.6.2 Interpreting a State Diagram

It is now appropriate to discuss some of the constraints when interpreting state diagrams. The region of the diagram that represents the true phase diagram, indicated by solid lines, depicts the true equilibrium situation. Both the ice melting point line T_m^L and the saturation line T_m^s, and their intersection at point E, the eutectic point, describe true equilibrium situations. Line T_m^L is located by conducting cooling and warming cycles, with data collected from the warming experiments. Beyond E, the continuation of line T_m^L describes a new, and more complex, reality. First, it exists only if the solute has failed to crystallize (failure is common). In the absence of solute crystallization, the portion of the diagram to the higher concentration side of T_m^L represents a supersaturated (SS) solution. Thus, E to T_g^* represents a nonequilibrium state. The extension of the T_m^L line from E to T_g^* is usually taken to represent metastable equilibrium and represents the highest concentrations of solute in solution (supersaturated) that can be achieved by crystallization of ice at any temperature. It is possible to have, at any given temperature, less ice in the system, and hence a lower solute concentration, depending on the exact crystallization kinetics during cooling to that point. The more rapid the cooling, and the lower the temperature, the more likely incomplete ice crystallization becomes.

At some temperature a condition is reached where no further ice will separate on cooling. In the ideal diagram, this is represented by the intersection of line T_m^L with line T_g at T_g^*, with solute concentration C_g^*. Line T_g represents the temperature of the glass transition for a *homogeneous* amorphous matrix as a function of matrix composition. Note that in order to determine the entire line T_g from pure HOH to pure solute, cooling conditions must be applied in systems representing the entire range of concentration such that *neither* solute nor solvent can crystallize, as a result forming a series of homogeneous glasses of known concentration at appropriately low temperatures. Achieving this can present a challenge, particularly at the higher water concentrations, where very rapid cooling might be necessary to prevent any ice crystallization. Curve T_g for an amorphous aqueous system extends from $-135°C$ for pure water to whatever is the appropriate T_g for the pure solute.

In equilibrium systems, in which ice crystallization is taking place, the eutectic point E defines the concentration, C_E, that represents the critical concentration of the equilibrium system at which there is a transformation from ice crystallization alone to simultaneous ice and solute crystallization. Only at this unique solution phase concentration can ice and solute cocrystallize, and they do so at a constant ratio equivalent to the ratio of water to solute in the solution phase at concentration C_E. At higher initial water concentrations, solute concentration C_E is arrived at by ice crystallization and at higher initial solute concentrations by solute crystallizing.

Cryobiologists, who have an interest in the properties of dilute aqueous glasses, have studied aqueous glasses extensively [66–68]. Of particular interest to us is the observation that, on warming a homogeneous, dilute glass from a very low temperature, a glass transition is observed at T_g. On further warming, at some temperature T_d, devitrification occurs, with the formation of some ice, an exothermic process, and a concomitant increase in the solute concentration of the residual glassy phase to approach a maximum possible concentration $(C_g)_T$ defined by line T_g at temperature T_d. This result suggests that, at T_d, solute molecular mobility has increased sufficiently to allow for some spatial molecular rearrangement, and the formation of pure water domains in the form of ice. The resultant increased concentration within the residual solution phase domains results in decreased solute mobility, such that these domains remain effectively in the glassy state, with T_g appropriate to their increased solute concentration. The exact location of T_d will depend upon the experimental timescale. For longer timescales, T_d will be at a lower temperature. Note that, since ice crystallization is exothermic, devitrification will be a self-accelerating process, and therefore should be readily observed.

Consider now what happens as a system whose overall concentration is more dilute than the eutectic concentration, C_E, is cooled less rapidly than is required to form the homogeneous glass. For this exercise, we will assume that initial ice nucleation occurs readily (not always so in practice) such that there is no significant undercooling. As cooling progresses, the initial T_m^L for the starting concentration is reached and ice formation commences. On further cooling, more ice forms, and the resulting composition of the unfrozen phase tracks T_m^L. Eventually, point E is reached, and if equilibrium is maintained, solute and ice will cocrystallize at temperature T_E in constant proportion (defined by the proportion at C_E) until the whole system becomes solid. With further cooling, the temperature will again decline, but with no additional change in phase concentration (a vertical descent from E). However, nucleation and growth of solute crystals can be difficult. Supersaturation is common. Should supersaturation occur, continued cooling on reaching point E produces more ice, but no simultaneous solute crystallization, and therefore the composition of the unfrozen phase continues to increase beyond C_E, tracking along line T_m^L from E to T_g^*, at which point the unfrozen phase enters the glassy state. This concentration can be denoted as $(C_m^L)_T$. At T_g^*, $(C_m^L)_T$ is C_g^*. As was previously noted, on concentration increase and also on temperature decrease, solution viscosity increases. Hence, the mobility of solute molecules within the solution phase, particularly large solute molecules, decreases, and the segregation process required to form regions of pure water in the form of ice takes more time. The continuation of line T_m^L from E, as drawn, defines the *maximal* concentration $(C_m^L)_T$ possible for the unfrozen phase at each temperature. Should the rate of ice crystallization be restricted (e.g., by rapid freezing), the concentration of solute in the unfrozen phase will be less than $(C_m^L)_T$ at any given sub-T_E temperature. Eventually during continued cooling, this unfrozen phase will attain a temperature and concentration that coincides with some point on the line T_g, representing the glass transition of a more dilute glass than the maximally freeze concentrated T_g^* glass.

2.10.6.3 The Interplay of Equilibrium and Kinetics

Fixing the exact location of this intersection of the line T_m^L with line T_g has been a subject of considerable controversy. Levine and Slade identified, from DSC curves, a temperature they termed T_g', which they assumed to be the temperature of the glass transition of the maximally freeze-concentrated matrix. From their data, they attempted to calculate the concentration (W_g', the concentration of water, or C_g', the concentration of solute) at this point [69], but their initial calculations proved to be in error [70–72]. Later studies, determining T_g in higher concentration quenched systems, or using a revised method to estimate the ice content, were required to arrive at the estimates of W_g^* or C_g^*, respectively the water content of the glass and the concentration of the glass, in Table 2.5. Other workers, including Roos and Karel [73] and Simatos and Blond [74], have challenged Levine and Slade's characterization of the point they labeled T_g' as representing a glass transition. Evidence was

TABLE 2.5
C_g^* Estimates for Selected Carbohydrates

	C_g^* (wt%)		
Carbohydrate	**Levine and Slade**	**Other Workers**	T_m' **(K)**
Glycerol	54	80	208
Ribose	67	81	226
Glucose	70.9	80	230
Fructose	51	83	231
Galactose	56	83	232
Sucrose	64	81	241
Maltose	80	81	244
Maltotriose		81	250

Source: Slade, L. and H. Levine (1995) In *Food Preservation by Moisture Control* (G.V. Barbosa-Canovas and J. Welti-Chanos, Eds.), Technomic Press: Lancaster, PA, pp. 33–132.

presented suggesting that the true glass transition was seen at a lower temperature. It was suggested that the T_g' of the Levine and Slade terminology was really the initiation of melting, and it was proposed that the symbol T_m' be used to identify this point. This chapter follows this terminology, with T_m' representing the point initially labeled T_g' by Levine and Slade. Since Levine and Slade proposed that T_g' was the significant temperature to be used in the WLF equation when estimating reaction rates in frozen systems, this was not a trivial dispute. It has since been resolved by realizing that, indeed, this important temperature probably represents the point at which, on warming, the melting process for ice emerges from the kinetic constraints of reduced solute mobility, and follows line T_m^L defining the metastable system. It may therefore be considered as the final point of the limit T_d curve, representing the changeover from mobility constraints on ice crystallization to mobility constraints on ice melting. Line T_d represents the highest temperature at which an effective kinetic constraint on ice crystallization in a nucleated system at sub-T_m temperatures is found to exist. Combining concepts, the symbol T_m' could be considered to represent the "mobility temperature" at which the constraints due to reduced solute mobility are overcome during warming. It represents the temperature where diffusion of solute in the maximally freeze-concentrated system can occur at a reasonable rate. As will be discussed later, this temperature is an important parameter when estimating stability and reaction rates in frozen systems maintained at subfreezing temperatures above T_m'. Since T_m' clearly represents the point at which solute mobility first becomes sufficient to observe measurable change, it is an appropriate reference temperature to use in a WLF equation estimating mobility increase (and its consequences). In the WLF equation, the reference temperature is assumed to represent a repeatable mobility threshold for a variety of systems. Clearly, using T_m' to represent the temperature at which the system has its reference mobility uses the initiation of solute diffusion sufficient to enable ice melting as the criterion. This provides support for the proposal by Levine and Slade that T_m' was the appropriate temperature to use in the WLF equation when attempting to predict frozen product stability. Note that the concentration of the limit unfrozen system at T_m' will be very close to C_g^*, since until solute mobility is sufficient to allow for ice melting, and dilution of the unfrozen matrix, there should be no change in the concentration of the unfrozen matrix. It should be remembered that this discussion refers to the ideal of the limit metastable systems. In reality, temperatures and concentrations will be determined in a range around T_m' and C_g^*. The term T_g^* is used in this chapter to represent the temperature of the glass transition of the maximally freeze-concentrated glass, in preference to T_g', to avoid unnecessary confusion, given the multiple definitions that have been assigned to T_g' in the literature.

2.10.6.4 Extending the Concept to Complex Food Systems

An approach with some merit is to identify the dominant food solute within a system, then deduce the properties of the complex food from the binary state diagram for this solute. An important useful example is the use of a sucrose–water state diagram to predict the properties and behavior of cookies during baking and storage [75]. If in other situations more than one primary solute is present, a state diagram for each solute should be considered. It should be borne in mind that the state diagram is constructed from observations of the temperatures of phase and/or glass and related transitions (such as devitrification) as a function of the moisture content of the system. In single solute (or fixed solute ratio) systems that can form ice, T'_m and T^*_g are the same for all starting compositions (though T_d and T_g are composition dependent), and the changing liquidus temperature (T^L_m) can be tracked by following, as discussed, the change in amount of ice (and hence C^L_m, the concentration of the liquid phase in contact with ice) at each temperature. However, in binary systems with water contents lower than that of the maximally freeze-concentrated matrix (and hence unable to form ice), separate determinations of all the transition temperatures are required for each moisture content. At low moisture content, identification of T_g is usually feasible because solute seldom crystallizes. However, determination of the saturation line, T^s_m, is often difficult because of the reluctance of solutes to crystallize at or to their saturation concentration. In complex systems, where no dominant solute (DS) can be identified, such as in dry or semidry complex foods, determining the T^s_m curves is not yet possible. It is, however, as discussed above, a relatively simple task to determine T^L_m and hence it is possible to determine a state diagram for a complex frozen food. Figure 2.24 indicates how the state diagram changes for different solutes.

One final comment should be made. While, at temperatures above T_E, T^L_m, and T^s_m are indeed lines, T_g and T_d are descriptors of kinetic barriers, and better considered as bands. The exact event temperature is dependent upon the "characteristic frequency" or inherent response time of measurement, as one might expect for a kinetic process [76,77].

Examining the state diagram for solute concentrations greater than the maximal freeze concentration, the T_g curve is seen to rise with increasing steepness toward T^s_g, the T_g of the solute. Described differently, even a small amount of water present in the solute greatly influences T_g. This phenomenon, known as plasticization, is a property of all glasses to which are added amounts of significantly smaller molecules than the molecules whose mobility defines the glass transformation. A widely accepted explanation for plasticization involves consideration of free volume, the space between the major molecules of the glass. Should this free volume increase, it is clear that molecular movement would become easier, corresponding to a lowered glass transition temperature. Small molecules can enter the interstices between larger molecules, thus increasing the free volume, and consequently lowering T_g. Water, as a very small molecule, is an effective plasticizer. Other molecules, such as ethanol and glycerol, can also provide plasticization, assuming that they can enter the phase occupied by the molecules that constitute the amorphous phase. Should the small molecule not be miscible with the larger molecule on the molecular level, then plasticization as described here cannot occur, though a lubrication effect between separate "microphase domains" might still occur. Such lubrication would influence mechanical properties, but the thermal properties of the system would still reflect the T_g of the domains, and the kinetics would be expected to conform to the T_g of the domains also.

2.10.6.5 Identifying the Assumptions

The applicability of this molecular mobility approach to food stability is dependent upon several key concepts and assumptions. The first, and most important premise, is that *many (if not most) foods contain amorphous components, and exist in either a state of metastable equilibrium or in a nonequilibrium, kinetically labile state.* This is true of many complex foods because most of them contain amorphous solid, and supersaturated liquid regions. Biopolymers are typically at least partly

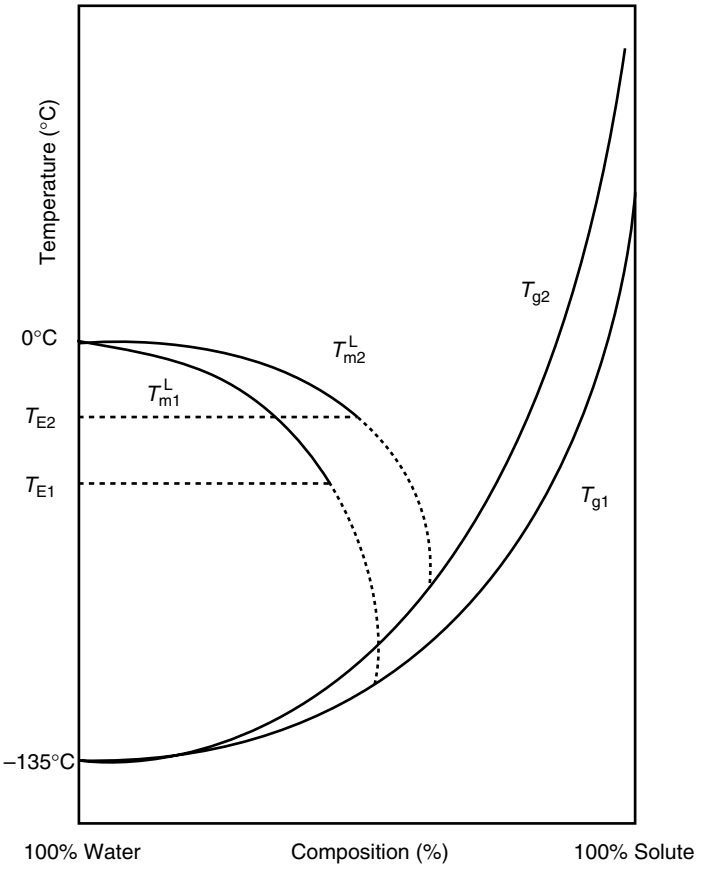

FIGURE 2.24 State diagrams for binary systems showing the influence of solute type on the position of T_m^L and on T_g. The extreme left of T_g is fixed at the vitrification temperature of pure water (−135°C). The assumptions stated in Figure 2.23 apply here.

amorphous. Many small molecules are difficult to crystallize from solution, and thus exist in an amorphous state when in excess of saturation. This amorphous state may be kinetically constrained, and therefore metastable, or may be slowly changing with time, and therefore in nonequilibrium. Essentially, the lower (T_g) boundary line in a state diagram defines the limiting conditions for the metastable amorphous phase, and the region of $C > C_E$ above T_g and below T_m^s represents a nonequilibrium amorphous state with the upper boundary of this condition being defined by the saturation solubility line (T_m^s) above which exists the simple solution. Note that the part of T_m^L to the left of point E ($C < C_E$) (Figure 2.23) similarly defines the upper limit of the nonequilibrium amorphous state for compositions where ice is not present owing to rapid cooling, or other constraints. Since it is more difficult to prevent ice crystallization than it is to prevent solute crystallization in foods, the amorphous state for compositions to the left of point E is not readily attained, except for (1) the region of initial undercooling prior to the initial nucleation of ice and (2) the region with C^L less than, but close to C_m^L as defined by the liquidus representing an unfrozen phase that can be termed a nonmaximally freeze-concentrated matrix. It is a major goal of food scientists and technologists to maximize the number of desirable food attributes that depend on metastable equilibrium states, and to find conditions providing acceptable stability for those desirable attributes that depend on the maintenance of nonequilibrium states.

The next key point is to reiterate that *the rates of most physical processes, and also of many chemical processes, are governed by molecular mobility*, in that they require some form of molecular

motion to be accomplished. Since, as we have discussed, most foods exist in metastable or nonequilibrium states, kinetic approaches are often most relevant to the understanding, prediction, and control of their properties. Molecular mobility provides an appropriate kinetic approach, as it is causally related to the rates of diffusion-limited processes in foods. The use of the WLF equation, to provide estimates of Mm at temperatures above that of the glass transition, T_g, but below T_m^L has been established as a standard procedure over the last decades. State diagrams usefully define regions of temperature and composition that permit metastable or nonequilibrium conditions to exist for useful periods of time. In frozen systems, a particular controversy has addressed the issue of which T_g to employ in the WLF equation. As has been noted, while Levine and Slade recommended the use of T'_m (T'_g) in their terminology, it is clear that this does not take into account the dilution of the unfrozen phase due to melting at the higher temperature. Nor does it acknowledge that the true glass transition temperature of the maximally freeze-concentrated matrix is T_g^*. As has been suggested by several workers [74,78,79], it would appear to be more correct to use T_g, the temperature of the glass transition for this more dilute phase. However, given that the parameters of the WLF equation do not have universal values, it emerges that the use of either convention is equally effective in real systems [79]. Given that establishing the true value of T_g is a major challenge, it is indeed fortunate that, as indicated earlier, use of T'_m in the WLF equation provides sufficient accuracy.

2.10.7 Limitations of the Concept

While the Mm approach is useful for predicting many kinds of physical change, its utility is not universal. Examples of where it is unsatisfactory include chemical reactions whose rates are little influenced by diffusion, effects achieved through the action of specific chemicals, and situations where the estimated Mm reflects the properties of a polymeric component, while the process of concern involves smaller molecules whose mobility is little hindered by the loss in mobility of the primary matrix. Also, in the growth of vegetative cells of microorganisms, the mobility of water, and consequently $(p/p^o)_T$ serves as a better predictor.

Returning to the discussion of reaction kinetics, in the last 20 years, there has been an active discussion as to whether the WLF equation or the Arrhenius equation provides the better description of the temperature dependence of reaction kinetics in aqueous food systems, particularly at temperatures between T_g and T_m^L or T_m^s. Consider systems that can form ice. In this region, in taking the molecular mobility approach, there are two factors that might be expected to influence mobility, temperature, and concentration. As temperature is lowered, concentration increases. At first the influence on mobility is primarily that of temperature, but as the temperature continues to drop, the increasing concentration becomes a factor of increasing importance as more ice forms. Figure 2.25 illustrates the effect of temperature and the effect of concentration separately upon viscosity and mobility. The combined effect is shown in Figures 2.26 and 2.27. Both the Arrhenius equation and the WLF equation properly describe the effects of temperature on kinetics only if concentration is constant. The effect of concentration on kinetics enters as another term in the analysis. For a first order reaction, concentration does not influence the *fractional rate* of reaction (i.e., $t_{1/2}$ is independent of concentration), but for all higher orders of reaction, the relative rate of reaction is concentration dependent. For many reactions in frozen systems, a pseudo first order description is adequate, but this does not guarantee that, especially in the freeze-concentrated zone, the effect of concentration can be ignored when estimating extent of reaction. As previously noted, empirical evidence shows that an equation of the WLF form can provide adequate estimates for rate and extent of reaction as a function of temperature and time, using either T'_m, T_g^*, or the T_g of the homogeneous glass of composition C_T^L (where T is the storage temperature of interest) as the reference temperature. Given the limited range of temperatures in the region between T_g and T_m^L in frozen systems, it is not surprising that the Arrhenius equation also produces a satisfactory fit to the raw data.

Note that another factor that is little discussed is the "equimolal" nature of the unfrozen phase in frozen systems. The presence of ice defines the osmolality of the unfrozen phase, assuming that

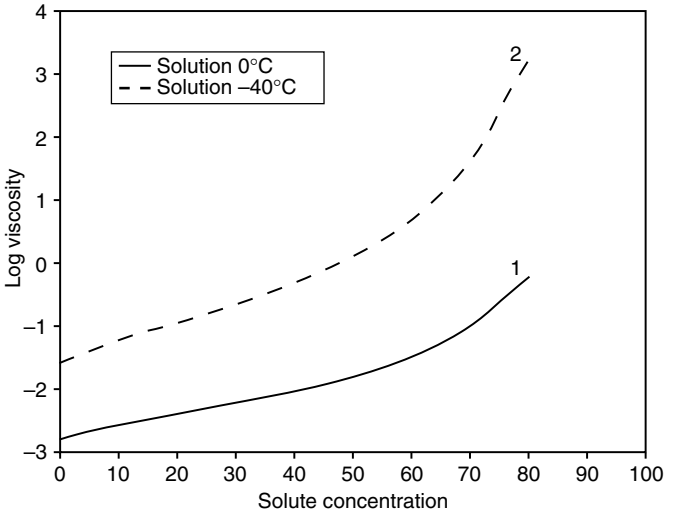

FIGURE 2.25 Comparison of the effect of concentration on the viscosity of aqueous solutions at two different temperatures: (1) 0°C and (2) −40°C.

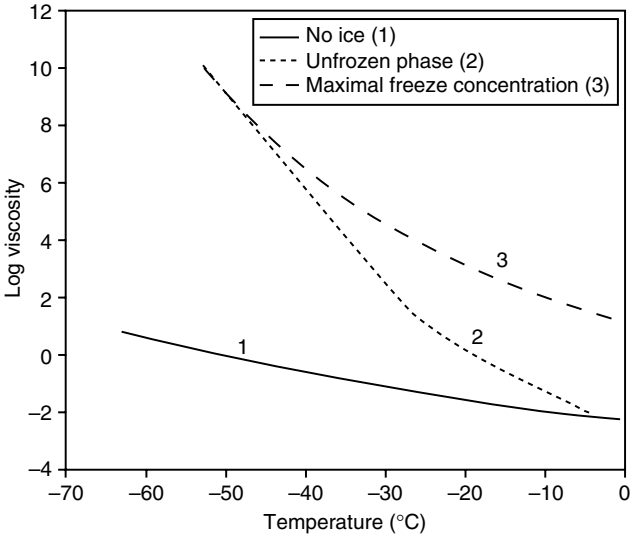

FIGURE 2.26 Predicted viscosities in aqueous systems as a function of temperature: (1) no ice formation on cooling; (2) ice separation such that solution phase concentration tracks line T_m^L; (3) system concentration is C_g^*.

T_m^L defines the concentration. Should the composition (and hence mole ratios) of solutes change as a consequence of reactions, in contrast to an unfrozen system, the amount of ice, and hence the individual concentrations, will adjust to maintain the defined osmolality of the unfrozen phase. Hence, the evolution of reactant and product concentrations could depend upon the stoichiometry of the reaction in a way different from that of an unfrozen system.

In a system of concentration in excess of T_g^*, where ice crystallization is not possible, above T_m^s, in the fluid system, Arrhenius kinetics hold. It is not uncommon for an Arrhenius plot incorporating temperatures that span T_m^s to exhibit a change in slope around T_m^s. Between T_m^s and T_g the system can be described as rubbery. Particularly note that there is a rapid decrease in mobility as the temperature is lowered, and this is reflected by a rapid change in reaction rates. In this region, while it is difficult

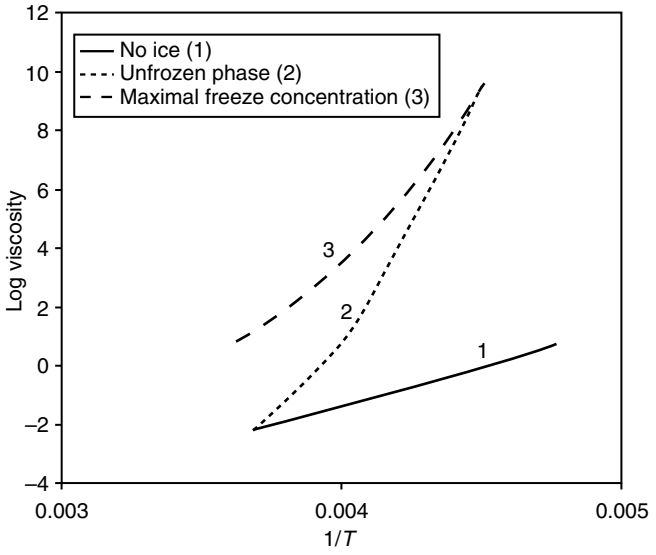

FIGURE 2.27 Reciprocal temperature plots of the data of Figure 2.26.

to come up with a uniform approach, it has been noted that the rates of many physical events conform more closely to an equation of the form of the WLF equation than to the Arrhenius equation. For chemical reactions, the dependence on molecular mobility is very dependent on reaction type, and neither WLF nor Arrhenius kinetics describes all reactions in this zone. Note that this discussion does not apply to frozen foods (concentrations less than C_g^*), as it fails to account for the influence of increasing concentration of the unfrozen phase, as ice content increases, on the properties of the unfrozen matrix, illustrated in Figures 2.26 and 2.27.

2.10.8 Practical Applications

2.10.8.1 Developing the State Diagram

Having discussed in some detail the applicability of the state diagram, and the WLF equation, in understanding product stability, it is appropriate to discuss in more detail the challenges involved in determining the state diagram and also in the application of the WLF equation. The state diagram is constructed by, instrumentally, identifying temperatures of "change" for systems at a wide range of concentrations. Techniques such as DSC, DMTA have proved useful, but require special instrumentation, and are demanding to interpret. In each case, an instrument response is plotted as a function of temperature, and the temperatures at which breaks in the trends of the response occur are plotted. While, as Levine and Slade initially demonstrated, it is possible to obtain an estimate of T'_m for many systems by determining the DSC melting curve for frozen solutions of overall concentration of 20% solute, 80% water, the determination of the concentration of the maximally freeze-concentrated phase from such data is challenging, as is the precise determination of T'_m. Considering first the challenge of determining T'_m, it is better to study initial solutions of a range of concentrations, as in this way the influence of instrumental artifacts and also slow crystallization can be minimized. Temperature cycling also provides a useful tool, as cycling above and below T_g^* and also around T'_m assists in approaching the formation of maximal ice during the cooling cycles. Obtaining a consistent value for T'_m from a range of initial solution concentrations allows a level of confidence to be attached to the value. The estimation of C_g^* is subject to greater difficulty. The approach initially used by Levine and Slade was to estimate the amount of ice present in the system after formation of the maximally freeze-concentrated glass. Unfortunately, their initial method for estimating the ice

content had a serious flaw. Using solutions of initial concentration 20% in solute, the ice content was determined from the area of the peak corresponding to ice melting in a warming thermogram. To do this, Levine and Slade assumed the melting enthalpy of ice to be that of ice at 0°C. Unfortunately, the melting enthalpy of ice is temperature dependent, decreasing as temperature is lowered. Hence this method leads to an underestimation of the quantity of ice, and therefore a value for C_g^* that is too low. Other workers have suggested means of better estimating the ice content, allowing for the temperature dependent enthalpy of fusion, and have also suggested that methods that employ several initial solution concentrations are more robust, since, as in the estimation of T'_m, agreement among results obtained from samples of a range of initial concentration generate greater confidence in the reliability of the estimate [72,80–82]. As with T'_m, application of a temperature cycling protocol prior to the final warming scan used for the estimation of the ice content leads to a closer approach of the system to that containing the maximally freeze-concentrated glass, and therefore a better estimate of C_g^*. Determining T_g for a glass of the composition of the initial solution is a much greater challenge than determining T'_m. As discussed previously even with very rapid cooling it is difficult, except at initial concentrations close to C_g^*, to prevent all ice crystallization. Hence it is often necessary to estimate, rather than measure, T_g for a particular concentration of solute. Various equations exist for this purpose. The oldest and simplest of these is that of Gordon and Taylor, which for a binary system is

$$T_g = \frac{w_1 T_{g1} + k w_2 T_{g2}}{w_1 + k w_2} \tag{2.11}$$

where w_1 is the weight fraction of species 1, w_2 is the weight fraction of species 2, T_{g1} is the glass transition temperature for pure species 1, T_{g2} is the glass transition temperature for pure species 2, and k is a constant.

The initial development of the molecular mobility approach to food stability, by Franks, Levine, and Slade, focused primarily on understanding the behavior of predominantly carbohydrate systems. Many important concepts have been derived by looking at the behavior of carbohydrates, which are major food components. Empirically, for frozen systems, T'_m was found to depend significantly on the molecular weight of the solute. As molecular weight increases, T'_m increases. There is a smaller effect of molecular characteristics for sugars of the same molecular weight. A plot of T'_m vs. molecular weight for sugars, glycosides, and polyols (Figure 2.28) shows T'_m to increase

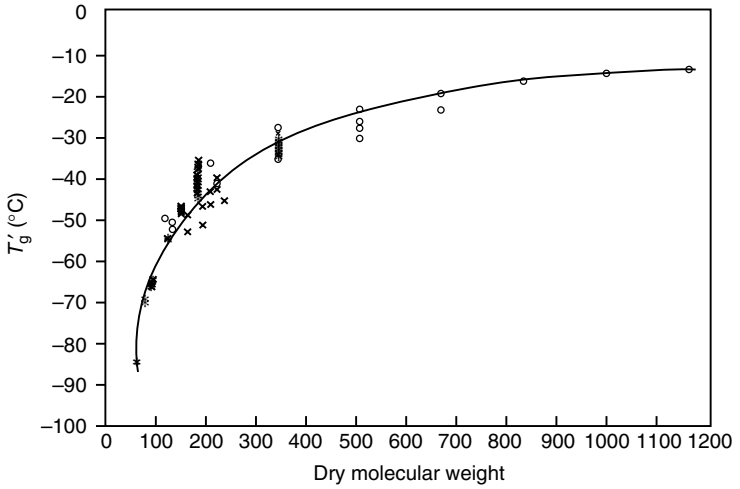

FIGURE 2.28 Typical results from Levine and Slade for T'_g (T'_m) as influenced by solute molecular weight: of solutions of sugar (o), glycoside (×), polyol (∗).

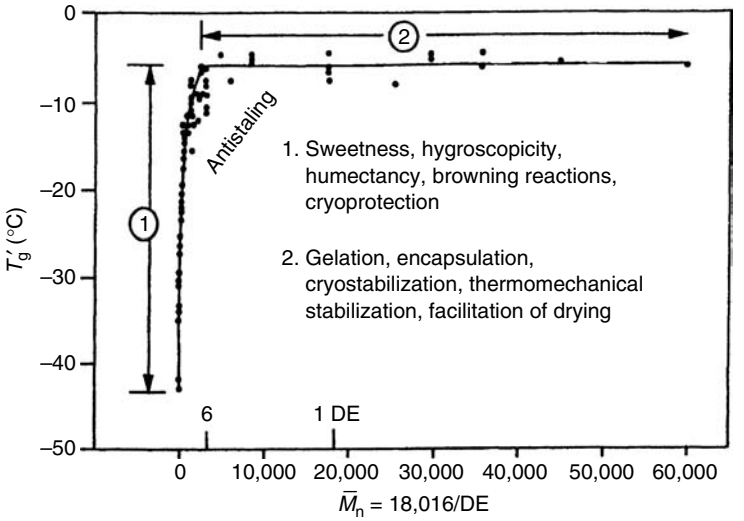

FIGURE 2.29 Typical results from Levine and Slade on the influence of dextrose equivalent (DE) and number average molecular weight of commercial starch hydrolysis products on T'_g.

proportionately with increase in solute molecular weight. This is to be expected, as translational mobility of molecules decreases with increasing size, so that a large molecule requires a higher temperature for movement than does a small one. At molecular weights above 3000 T'_m appears to become independent of molecular weight (Figure 2.29). Some data collected by Levine and Slade for sugars are reported in Table 2.6. Data are also reported for the dry sugars. Extreme care is required in collecting these data, since even slight traces of moisture can significantly lower T_g through plasticization. Assuming acceptable dryness, the T_g of the dry sugars is also found to depend upon molecular weight, as well as the nature of the individual sugar.

The concentration of the maximally freeze-concentrated matrix, C^*_g depends to some extent upon molecular size, but exact measurement can be, as has been indicated, a challenging problem. Assuming molecular mobility to be an important factor, differences in T'_m, and more particularly C^*_g, for molecules of the same molecular weight could result in very different effects on product stability. This presumably explains in part the differing efficacies of glucose vs. fructose and lactose vs. trehalose as stabilizing sugars.

2.10.8.2 The Freezing Process, Frozen Foods

Freezing preservation is recognized as one of the best methods for the long-term preservation of foods. A primary factor in providing the long-term stability is the low temperature, since, as has been emphasized earlier, reaction rates tend to decrease as temperatures are reduced. The formation of ice in frozen foods is somewhat of a two-edged sword. There are two important adverse consequences of ice formation in cellular foods and food gels. First the nonaqueous components become concentrated in the unfrozen phase and second there is a volume increase of around 9% associated with the transformation from liquid water to ice.

During freezing, water transforms to ice of high purity. Hence, solutes in the aqueous phase coexist with a decreasing amount of solvent water. This process is akin to regular dehydration, except that the temperature is lower, and that the separated water remains locally, but in the form of ice, rather than being physically removed from the local environment. The composition of the unfrozen phase at any temperature approaches that defined by the appropriate state diagrams.

As the freeze-concentration process progresses, the unfrozen phase changes significantly in its properties such as pH, titrable acidity, ionic strength, and so forth. Should solutes crystallize,

TABLE 2.6
Glass Transition Values and Associated Properties of Pure Carbohydrates

Carbohydrate	MW	Properties Dry			Properties Aqueous
		T_m (K)	T_g (K)	T_m/T_g	T'_m (K)
Glycerol	92.1	291	180	1.62	208
Xylose	150.1	426	282–287	1.49	225
Ribose	150.1	360	260–263	137	226
Glucose	180.2	431	304–312	1.39	230
Fructose	180.2	397	280–290	1.39	231
Galactose	180.2	443	303–305	1.45	232
Sorbitol	182.2	384	269–271	1.45	229
Sucrose	342.3	465	325–343	1.40	241
Maltose	342.3	402	316–368	1.19	243
Trehalose	342.3	476	350–352	1.35	243
Lactose	342.3	487	374	1.37	245
Maltotriose	504.5	407	349	1.17	250
Maltopentose	828.9		398–438		257
Maltohexose	990.9		407–448		259
Maltoheptose	1153.0		412		260

Source: Levine, H. and L. Slade (1988) In *Food Structure—Its Creation and Evaluation* (J.M.V. Blanshard and J.R. Mitchell, Eds.), Butterworths: London, pp. 149–180 and Slade, L. and H. Levine (1995) *Adv. Food Nutr. Res.* **38**: 103–269.

solute ratios will change, and pH can shift markedly. Also, dissolved gases may be expelled. At the higher, freeze-induced concentrations, macromolecules, forced into proximity, may aggregate. As has previously been mentioned, even though the effect of temperature per se is to reduce reaction rates, overall reaction rates, especially at high subfreezing temperatures, may increase or decline less than expected as a result of the higher concentrations of reactant resulting from freeze concentration. This can occur even though the total amount of reactant in a particular sample remains unchanged from the initial amount. Under such complex conditions, it is not surprising that reaction rates at subfreezing temperatures do not always conform to either Arrhenius or WLF kinetics. At low subfreezing temperatures, the higher concentrations resulting from freeze concentration, and the nearness to T'_m usually lead to reduced reaction rates, and enhanced storage life.

It is instructive to follow the freezing process in frozen foods in more detail with the aid of appropriate state diagrams. Consider first the slow freezing of a complex food. Slow freezing allows for close conformance to solid–liquid equilibrium and a close approach to maximal freeze concentration. Starting at A in Figure 2.30, removal of sensible heat moves the product to B, the initial equilibrium freezing point of the sample. Because nucleation is a difficult process, further removal of heat results in undercooling, rather than freezing, until point C is reached, where nucleation begins. Crystal growth immediately follows nucleation, releasing the latent heat of crystallization and causing the temperature to rise to D. Further removal of heat causes additional ice formation and the concentration of the unfrozen phase tracks along line T_m^L from D to E, at T_E. In a complex food, T_E represents T_{Emax} for the solute with the highest eutectic point (i.e., the lowest solubility). Solutes in complex frozen foods rarely crystallize at or below their eutectic points. An occasional exception is the crystallization of lactose in some frozen desserts, which leads to the textural defect known as "sandiness."

Assuming eutectics do not form, further ice formation leads to the metastable supersaturation of many solutes, with the composition following the line from E to the point F, the recommended

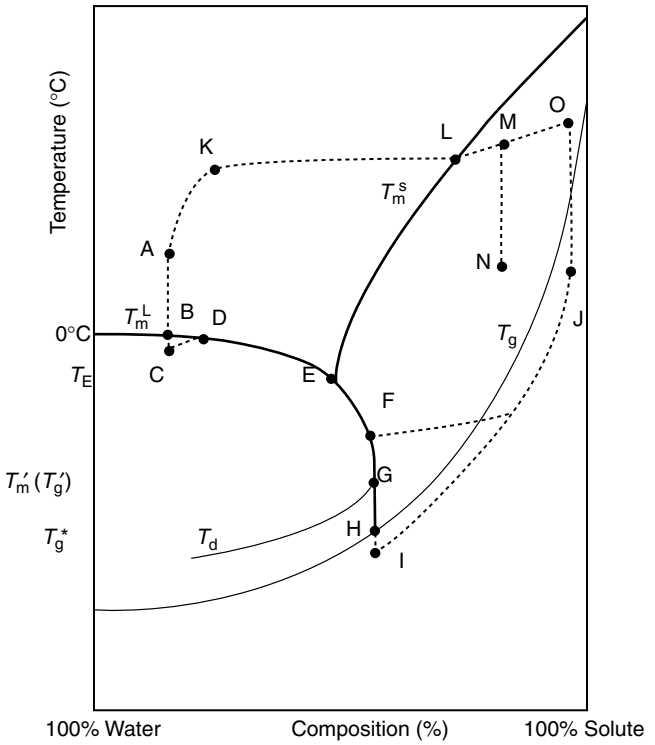

FIGURE 2.30 State diagram of a binary system showing possible paths for freezing (unstable sequence ABCDEF; stable sequence ABCDEFGHI), drying (unstable sequence AKLMN; stable sequence AKLMOJ), and freeze drying (unstable sequence ABCDEFJ; stable sequence ABCDEFGHIJ). The temperature scale is schematic to facilitate data entry.

storage temperature. For most foods, F is above T_m', indicating that molecular mobilities will still be quite large, and that the food's diffusion-limited physical and chemical properties will still be highly temperature dependent. Empirically, it has been found that rates of change are proportional to the temperature difference $(T - T_m')$ within about 20°C of T_m'.

If cooling continues beyond F, additional ice formation and freeze concentration occur, until the concentration reaches that at T_m' (point G). Further cooling does not lead to any additional ice formation, and at temperature T_g^* (point H) the supersaturated unfrozen phase converts to the glassy state, in which are embedded to ice crystals formed during the cooling process. T_g^* is a quasi-invariant T_g, being that of the maximally freeze-concentrated unfrozen matrix. T_g^* depends on solute ratios in the sample, but not initial solute concentrations. Maximal freeze concentration seldom occurs on the initial cooling cycle. Hence not only does the observed T_m' depend on solute ratios, but also to some extent on initial water content of the sample, as attainment of maximal freeze concentration is influenced by a range of kinetic factors. Appropriate temperature cycling around T_m' usually leads to a closer approach to C_g^* and hence the lowest measured T_m'.

It is important to note that the failure of ice to crystallize is not a consequence of reduced mobility of the water. These water molecules are observed to be still mobile and they freely exchange. The limiting process is the failure of solute molecules to translate or rotate in the applicable timescale, thus preventing the addition of further water molecules to the existing ice. In this situation (rapid freezing) water molecules are still exchanging on and off the ice.

As T_m' represents the temperature below which removal of ice from the matrix (on cooling) or dissolution of ice into the matrix (on warming) first becomes feasible in the timescale of our measurements, it defines a temperature at which Mm is greatly reduced during cooling and

diffusion-limited properties are found to exhibit excellent stability. Some T'_m values for various materials are shown in Tables 2.6 through 2.9. The question arises as to what happens when higher cooling rates are employed. Figure 2.31 illustrates the effect of increased cooling rate. Initially, after some undercooling, the unfrozen phase would be expected to track T_m^L. As the temperature declines, and the concentration of the unfrozen phase increases, Mm of the solutes decreases. The time required to produce clusters of pure water, at the same time rejecting solute from the volume to be occupied by the water, may exceed the time available. Hence less ice forms than is required by the T_m^L line, and the concentration of the unfrozen liquid phase, C_T^L at temperature T is less than would be predicted by the T_m^L line. Since the latent heat that would be associated with formation of this "missing" ice is not released, with continued removal of heat, the rate of reduction of temperature

TABLE 2.7
T'_m and DE for Selected Commercial Starch Hydrolysis Products (SHP)

SHP	Manufacturer	Source	DE	T'_m (K)
Staley 300	Staley[a]	Corn	35	249
Maltrin M250	GPC[b]	Dent corn	25	255
Maltrin M150	GPC	Dent corn	15	259
Paselli SA-10	Avebe[c]	Potato	10	263
Star Dri 5	Staley	Dent corn	5	265
Crystal gum	National[d]	Tapioca	5	267
Stadex 9	Staley	Dent corn	3.4	268
AB 7436	Anheuser-Busch	Waxy maize	0.5	269

[a] A.E. Staley manufacturing.
[b] Grain Processing Corporation.
[c] Avebe America.
[d] National Starch Corporation.

Source: Levine, H. and L. Slade (1988) In *Food Structure—Its Creation and Evaluation* (J.M.V. Blanshard and J.R. Mitchell, Eds.), Butterworths: London, pp. 149–180.

TABLE 2.8
T'_m for Selected Proteins

Protein	T'_m (K)
Bovine serum albumin	260
Lysozyme	256
α-Lactalbumin	262
α-Casein	260
Sodium caseinate	263
Gelatin 300 bloom	263
Gelatin 250 bloom	262
Gelatin 175 bloom	261
Gelatin 50 bloom	260

Source: Levine, H. and L. Slade (1990) In *Thermal Analysis of Foods* (V.R. Harwalkar and C.-Y. Ma, Eds.), Elsevier Applied Science: London, pp. 221–305.

TABLE 2.9
Estimates of T'_m for Selected Foods

	T'_m (K)			T'_m (K)	
Food	**Levine and Slade[a]**	**Other Workers**	**Food**	**Levine and Slade[a]**	**Other Workers**
Dairy			*Vegetable*		
Cottage cheese	252		Broccoli	246	252[d]
Cheddar cheese	249		Cauliflower	248	253[d]
Cream	250		Potato	257–262	
Ice cream	232–246		Spinach	256	239[d]
Skim milk	246	241[b]	Sweet corn	259–265	
Whole milk	251		Tomato	232	
Fresh fruit			*Meat and fish*		
Apple	231	245[d]	Beef muscle		261[c], 260[d]
Banana	238		Pork muscle		257[d]
Blueberry	232		Chicken		251[d]
Peach	237	244[d]	Turkey		253[d]
Strawberry	232–239		Cod muscle		262[c], 256[d]
Fruit juice			Catfish		256[d]
Apple	233	243[d]	Pollock		261[d]
Lemon	230		Salmon		256[d]
Orange	236	243[d]	Shrimp		241[d]
Pear	233				
Pineapple	232	241[d]			

[a] Levine, H. and L. Slade (1990) In *Thermal Analysis of Foods* (V.R. Harwalkar, and C.-Y. Ma, Eds.), Elsevier Applied Science: London, pp. 221–305 and Levine, H. and L. Slade (1989) *Comments Agric. Food Chem.* **1**: 315–396.
[b] Jouppila, K. and Y.H. Roos (1994) *J. Dairy Sci*. **77**: 2907–2915.
[c] Brake, N. and O. Fennema, unpublished.
[d] Hsu, J. and D. Reid, unpublished.

increases, further reducing Mm, and resulting in a greater and greater deviation of C_T^L from that defined by the T_m^L line. The deviations of C_T^L from the predictions of the T_m^L line increase with rate of cooling and with reduction in temperature.

2.10.8.3 Drying Processes

The state diagram of Figure 2.30 can also be used to illustrate the progress of many other processes involving changes in the state or amount of water in a system. Using it, the differences between air drying and vacuum freeze drying can be better appreciated.

First consider air dehydration at constant temperature. Starting from A, air drying will elevate temperature and remove moisture, until soon the product attains properties described by point K (the wet bulb temperature of the air). Further moisture removal causes the product to arrive at, and pass through, point L, on the solubility curve. At this point, saturation for the DS is reached. Crystallization does not immediately occur, and the product becomes supersaturated in DS, and any other solute with saturation temperature above DS. Each of these supersaturated solutions can be considered as an amorphous liquid phase. With continued removal of water the system can pass through point M, corresponding to the dry bulb temperature of the air, and on further to point O. Cooling the system at point M leads to N, which is above the T_g curve, and cooling from point O leads to J, which is below the T_g curve. This suggests that drying should be continued beyond the dry bulb air temperature (M) since should drying be terminated at M the product, at N, being above

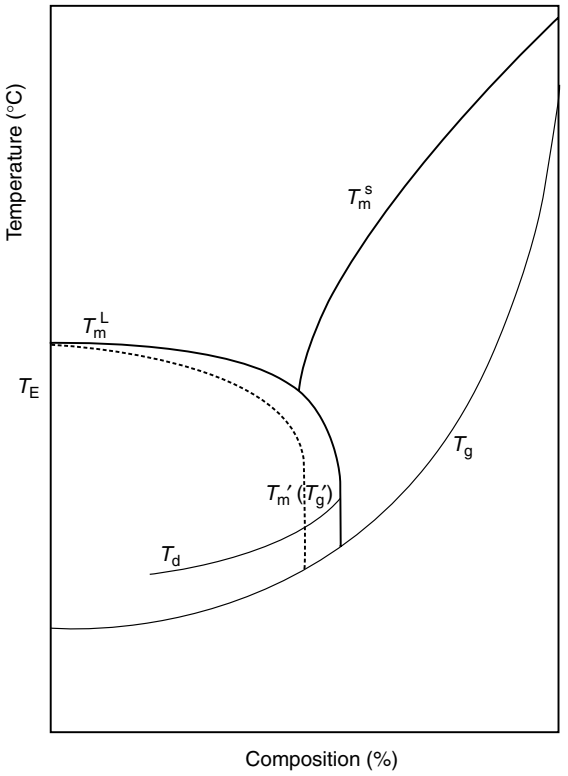

FIGURE 2.31 The effect of more rapid cooling on the composition and state of the unfrozen phase.

T_g will have relatively high Mm and consequent poor stability of diffusion-limited properties, which are strongly temperature dependent (WLF kinetics). Terminating drying at O, leads, at J to a product below T_g with a much reduced Mm, stable diffusion-limited properties, with only weak temperature dependence.

Product paths for vacuum freeze drying are also illustrated in the figure. The first stage of freeze drying coincides fairly closely to the path for slow freezing, ABCDEF. Should the product temperature not be allowed to go below temperature F during sublimation (primary freeze drying), path FJ would be typical. The initial stages of FJ involve ice sublimation. At some point with concentration around C_g^* ice sublimation will be complete and a desorption phase is entered. Since the sample is above the T_g curve, collapse is possible, particularly in products that were initially fluid, though the possibility exists to some extent for food tissues. Collapse is possible because no ice is present to provide structural support, and the product T is above T_g, and possesses sufficient Mm to preclude rigidity. Collapse results in a product of less than optimum quality. There is decreased product porosity, resulting both in slower drying and poorer rehydration characteristics. To prevent collapse the path ABCDEFGHIJ must be followed, where the portion HI represents cooling below T_g^*.

Provided maximal ice crystallization (maximal freeze concentration) has occurred, the critical temperature for structural collapse, T_c, the highest temperature at which collapse can be avoided during the primary stage of freeze drying, will lie somewhere between T_m' and T_g^*. The exact temperature will depend upon the rate of the drying process and hence the time period during which collapse would be feasible. The slower the process, the lower will be T_c. Should ice crystallization not be maximal, the highest temperature at which collapse can be avoided will approach T_d.

If the composition of the product to be freeze dried can be adjusted, it is desirable to raise T_m' as much as possible. This can be achieved by adding high molecular weight polymers, which enable

higher freeze-drying temperatures to be used. Increasing C_g^* (which increases the amount of ice formed) also enhances structural rigidity and minimizes the potential extent of collapse.

2.11 MOISTURE SORPTION ISOTHERMS

The molecular mobility approach is not the only approach to understanding food stability as a function of water content. Given the ability to determine both water content and RVP, it is instructive to consider the information that can be derived by examining the apparent dependence of water content upon RVP. This approach predates the molecular mobility approach by many years.

2.11.1 Definitions and Zones

A plot of water content (expressed as a mass of water per unit mass of dry material) of a food vs. $(p/p^o)_T$ is known as a moisture sorption isotherm (MSI). Information derived from MSIs are useful (1) for studying and controlling concentration and dehydration processes, because the ease or difficulty of removing water is related to RVP, (2) for formulating food mixtures so as to avoid moisture transfer among the ingredients, (3) to determine the moisture barrier properties needed in a packaging material required to protect any particular system, (4) to determine what moisture content will curtail growth of microorganisms of interest within a system, and (5) to predict the chemical and physical stability of foods as a function of changes in their water content.

Shown in Figure 2.32 is a schematic MSI for a high moisture food plotted to include the full range of moisture content from normal to dry. This kind of plot is not very useful because the data of greatest interest—those in the low moisture region—are not depicted in sufficient detail. Omission of the high moisture region and expansion of the low moisture region, as is normal practice, yields an MSI that is much more useful (Figure 2.33).

Moisture sorption isotherms exhibit a variety of shapes, many of which are amenable to at least qualitative interpretation. As an example, the sorption isotherms associated with several substances that have MSIs of markedly different shapes are shown in Figure 2.34. These are resorption (or adsorption) isotherms prepared by adding water to previously dried samples. Desorption isotherms are also common. The correspondence of adsorption and desorption isotherms will be discussed in Section 2.11.3. Isotherms with a sigmoidal shape are characteristic of most foods. However,

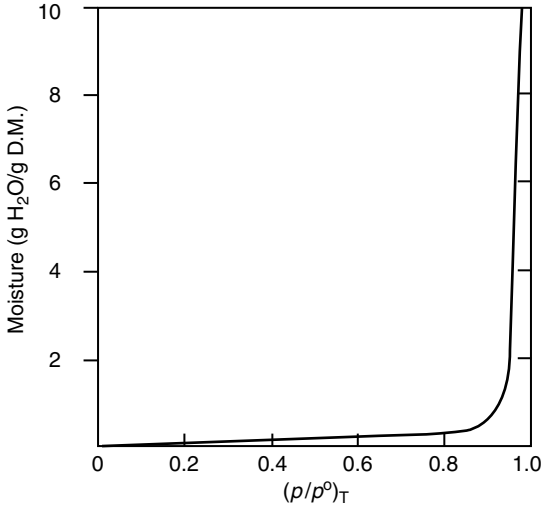

FIGURE 2.32 Schematic MSI encompassing a broad range of moisture contents.

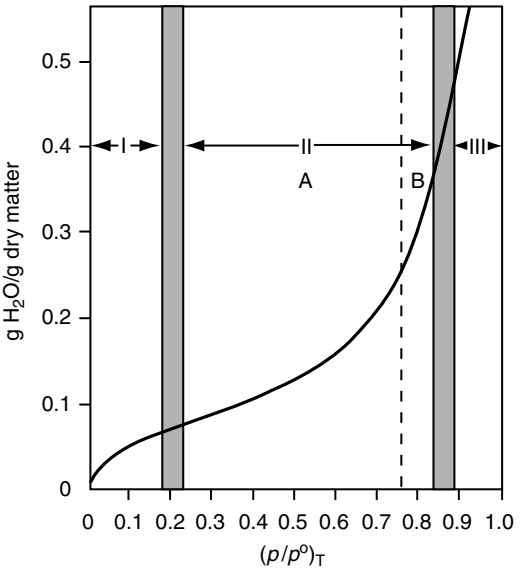

FIGURE 2.33 Generalized MSI for the low moisture segment of a food (20°C).

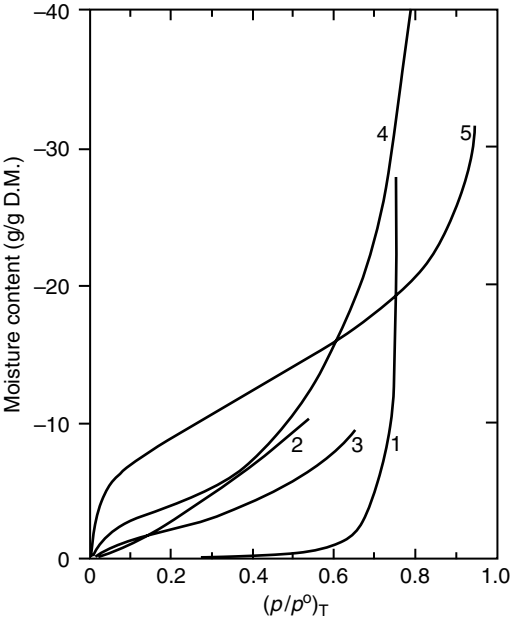

FIGURE 2.34 Resorption isotherms for various foods and biological substances. Temperature 20°C, except for number 1, which is 40°C. (1) confection (major component powdered sucrose), (2) spray dried chicory extract, (3) roasted Columbian coffee, (4) pig pancreas extract powder, and (5) native rice starch. (From van den Berg, C. and S. Bruin (1981) In *Water Activity: Influences on Food Quality* (L.B. Rockland and G.F. Stewart, Eds.), Academic Press: New York, pp. 1–61.)

foods (such as fruits, confections, and coffee extract) that contain large amounts of sugar and other small soluble molecules, and are not rich in sparingly soluble hydrophilic polymeric materials, may exhibit a J-type isotherm shown as curve 1 in Figure 2.34. The shapes and positions of the isotherms are determined by several factors including sample composition (including molecular

weight distribution and hydrophilic/hydrophobic characteristics of solutes), physical structure of the sample (e.g., crystalline or amorphous), sample pretreatments, temperature, and methodology.

Many attempts have been made to model MSIs, but success in achieving good conformance of a model to the full range of actual data for an MSI has been difficult. The oldest and best-known model is that of Brunauer, Emmett, and Teller (BET), derived for nonpolar gas sorption [83], but applied to aqueous systems with some redefinition of key terms. One of the better models is that developed by Guggenheim [84], Anderson [85], and De Boer [86], which is referred to as the GAB model. In food systems, it must be borne in mind that both models, though helpful, provide essentially empirical fits. The underlying models have parameters that are descriptive of much simpler systems. As an aid to interpreting moisture isotherms it is sometimes appropriate to divide them conceptually into zones as indicated in Figure 2.33. As water is added (resorption), the sample composition moves gradually from zone I (dry) to zone III (high moisture) and the properties of water associated with each zone differ significantly. These characteristic properties are described next and are summarized in Table 2.10. It should be realized that, even within a zone, water is freely exchanging and so the average properties of water within a zone depend upon the exact extent of population of the potential sites within the zone. The properties of water within different zones, however, are sufficiently different such that, on the commencement of populating a higher zone, even given easy exchange of water between zones, clear populations with different average properties corresponding to the separate zones can be seen.

Water present in amounts up to the zone I boundary limit of the isotherm can be considered most strongly sorbed and least mobile. This water is probably associated with accessible polar sites by water–ion or water–dipole interactions. It remains unfrozen at $-40°C$, it does not act as a solvent, and it is not present in sufficient amount to have a plasticizing effect on the solid. It behaves simply as a part of the solid.

The high-moisture end of zone I (boundary of zones I and II) corresponds to the "BET monolayer" moisture content of the food. Thus, the BET monolayer value can be thought of as corresponding approximately to the amount of water needed to form a monolayer over only the readily accessible, highly polar groups of the dry matter. In the case of starch, this amounts to one HOH per anhydroglucose unit. Zone I water is an amount corresponding to just a tiny fraction of the total water content in a high moisture food material. This amount of water clearly is less than the potential "sorption sites" represented by all of the polar or other active groups of the solute molecules. Additional water added in an amount not exceeding the limit set by the zone II boundary can be considered to populate those first-layer sites that are still available. This second water population, which probably associates with neighboring water molecules in this first layer and solute molecules primarily by hydrogen bonding, is slightly less mobile than bulk water and most of it remains unfrozen at $-40°C$. Moisture added in the vicinity of the low moisture end of zone II exerts a significant plasticizing action on solutes, lowers their glass transition temperatures, and causes incipient swelling of the solid matrix. Exchange of all water molecules is enhanced, but two populations become evident in relaxation spectroscopy experiments. This action, coupled with the beginning of the solution process, leads to acceleration in the rate of most reactions due to increasing interaction and accessibility. The amount of water that fully occupies zones I and II usually constitutes $<5\%$ of the water in a high moisture food material. Note that individual zones are defined only for water contents below that of their upper zone boundaries, since at this water concentration a new population begins to emerge. This initiates exchange processes that allow, at higher water contents, water molecules to exchange between separate populations. It is also a consequence of the influence of a more swollen, higher water content environment on access to potential interactive sites that were sterically or otherwise restricted in the early stages of sorption from being completely dry. Though now exchangeable, identifiable fractions of the water can be considered to share the characteristics of either zone I or zone II. Quantification of zone populations is a challenge, with perhaps the best estimates coming from relaxational spectroscopy. Lillford et al. [87] showed that relaxation spectroscopy in foods exhibited a complex decay curve that could be interpreted in

TABLE 2.10
Protein Hydration Levels

	Increasing Water Content in System					
	Constitutional Water[a]		Hydration Shell (≤3 Å from Surface)		Bulk-Phase Water	
Property					**Free[b]**	**Entrapped[c]**
Relative vapor pressure (p/p^o)	<0.02 p/p^o	0.02–0.2 p/p^o	0.2–0.75 p/p^o	0.75–0.85 p/p^o	>0.85 p/p^o	>0.85 p/p^o
Isotherm "zone"[d]	Extreme left, zone I	Zone I	Zone IIA	Zone IIB	Zone III	Zone III
Mol H_2O/mol dry protein	<8	8–56	56–200	200–300	>300	>300
g H_2O/g dry protein (h)	<0.01	0.01–0.07	0.07–0.25	0.25–0.58	>0.58	>0.58
Weight percent based on lysozyme (%)	1	1–6.5	6.5–20	20–27.5	>27.5	>27.5
Water characteristics: structure	Critical part of native protein structure	Water interacts primarily with charged groups (~2HOH/group). At 0.07 h transition in surface water organization; appearance of clusters associated with completion of charged group hydration	Water interacts primarily with polar surface groups (~1 HOH/polar site). Water clusters center on charged polar sites. Clusters fluctuate in size and arrangement. At 0.15 h long range connectivity of surface water is achieved	At 0.25 h water starts to condense on to weakly interacting unfilled protein surface patches. At 0.38 h "monolayer" of water covers the entire surface of the protein. Distinct water phase begins to appear, location of glass–rubber transition		
Water characteristics: thermodynamic transfer properties[e]						
ΔG (kJ/mol)	$>\lvert -6\rvert$	−6	−0.8	Close to bulk		
ΔH (kJ/mol)	$>\lvert -17\rvert$	−70	−2.1	Close to bulk		

Residence time (approximate mobility)	10^{-2}–10^{-8} s	$<10^{-8}$ s	$<10^{-9}$ s	10^{-9}–10^{-11} s	10^{-11}–10^{-12} s	10^{-11}–10^{-12} s
Freezability	Unfreezable	Unfreezable	Unfreezable	Unfreezable	Normal	Normal
Solvent power	None	None	Slight	Moderate	Normal	Normal
Protein characteristics: structure	Folded state, stable	Amorphous regions begin to be plasticized by water	Further plasticization of amorphous regions			
Protein characteristics: mobility (reflected in enzyme activity)	Enzyme activity negligible	Enzyme activity negligible	Proton exchange increases from 1/1000 at 0.04 h to full solution rater at 0.15 h. Some enzymes develop activity between 0.1 and 0.15 h	At 0.38 h lysozyme activity is 0.1 than in dilute solution	Maximum activity	Maximum activity

[a] Water molecules that occupy specific locations in the interior of the solute macromolecule.
[b] Macroscopic flow physically unconstrained by a macromolecular matrix.
[c] Macroscopic flow physically constrained by a macromolecular matrix.
[d] See Figure 2.33.
[e] Partial molar values for transfer of water from bulk phase to hydration shell.

Note: Constitutional water is assumed to be present in the dry protein at the onset of the hydration process. Water is first absorbed at sites of ionized carboxylic and amino side chains, with about 40 mol water/mol lysozyme associating in this manner. Further water absorption results in gradual hydration of less attractive sites, mainly amide carbonyl groups of the protein backbone. At 0.38 h monolayer coverage is achieved through water associating with those surface sites that are still less attractive. At this stage in hydration of the protein, there is, on average, 1 HOH/20 $Å^2$ of protein surface. At water content above 0.58 h the protein is considered fully hydrated.

Source: Data, largely on lysozyme, from Franks, F. (1988) In *Characteristics of Proteins* (F. Franks, Ed.), Humana Press: Clifton, NJ, pp. 127–154; Lounnas, V. and B.M. Pettitt (1994) *Proteins: Struc. Func. Genet.* **18**: 133–147; Rupley, J.A. and G. Careri (1991) *Adv. Protein Chem.* **41**: 37–172; Otting, G., et al. (1991) *Science* **254**: 974–980; and Lounnas, V. and B.M. Pettitt (1994) *Proteins: Struct. Func. Genet.* **18**: 148–160.

terms of water populations and exchange between populations. Hills and coworkers [88–91] further expanded upon this approach to quantify and characterize the changing water populations in different environments in foods, and in model systems, in particular starch-based systems. Schmidt [4] provides a detailed discussion of such studies. The results show greater complexity than the simple three-zone model, but confirm that this model provides a simple framework upon which to build an understanding.

As water content increases further, in the vicinity of the junction of zones II and III, the amount of water is sufficient to complete a true monolayer hydration shell for individual macromolecules such as globular proteins, and is also sufficient to lower the glass transition temperature of the hydrated macromolecules so that sample temperature and T_g are equal. A third separately detectable population enters the picture. Further addition of water (zone III) causes a glass–rubber transition in samples containing glassy regions, as evidenced by a very large decrease in viscosity, consequent upon a large increase in molecular mobility, and accompanied by commensurate increases in the rates of many reactions. Only at and beyond this water content at which the third population begins to appear can added water be frozen. Also, zone III water is available as a solvent and readily supports the growth of microorganisms. At water contents in excess of the lower zone III boundary, the additional water behaves as bulk-phase water (Table 2.10). Its addition to the system does not alter the properties of existing solutes, though as before all water molecules are freely exchanging. The zones are defined more as the populations of water molecules involved in particular classes of interaction with the solute. The relaxation spectroscopy studies show that as the water content increases, the various exchangeable populations may change in size. The water fraction at which a new population just begins to appear does not necessarily define the maximum size of the prior population at higher total water content.

In gels or cellular systems, bulk-phase water is physically entrapped so that macroscopic flow is impeded. However, in all other aspects this water has properties similar to those of water in a dilute salt solution. This is reasonable, since a typical water molecule, while occupying zone III, is "insulated" from the effects of solute molecules by several layers of zones I and II water molecules. The bulk-phase water population of zone III, either entrapped or free, usually constitutes more than 95% of the total water in a high moisture food, a fact that is not evident from Figure 2.33.

The important effects that such differences in water properties have on the stability of foods are discussed in a later section. At this point, suffice it to say that the most mobile water fraction existing in any food sample frequently governs stability.

2.11.2 Temperature Dependence

As mentioned earlier, RVP is temperature dependent, thus MSIs must also exhibit temperature dependence. An example of such temperature dependence involving potato slices is shown in Figure 2.35. At any given moisture content, food $(p/p^o)_T$ increases with increasing temperature, frequently in conformity with the Clausius–Clapeyron equation, though this conformity does not itself indicate true equilibrium.

2.11.3 Hysteresis

The foregoing discussion has indicated that MSIs may be obtained using either adsorption or desorption protocols. However, an additional complication to our discussion of MSIs is that a MSI prepared by the addition of water (resorption) to a dry sample will not necessarily be superimposable on an isotherm prepared by desorption. This lack of superimposability is referred to as "hysteresis" and a schematic example is shown in Figure 2.36. Typically, at any given $(p/p^o)_T$, the water content of the sample will be greater during desorption than during resorption. It has been found that MSIs of polymers, glasses of low molecular weight compounds, and many foods exhibit such sorption hysteresis [52,92].

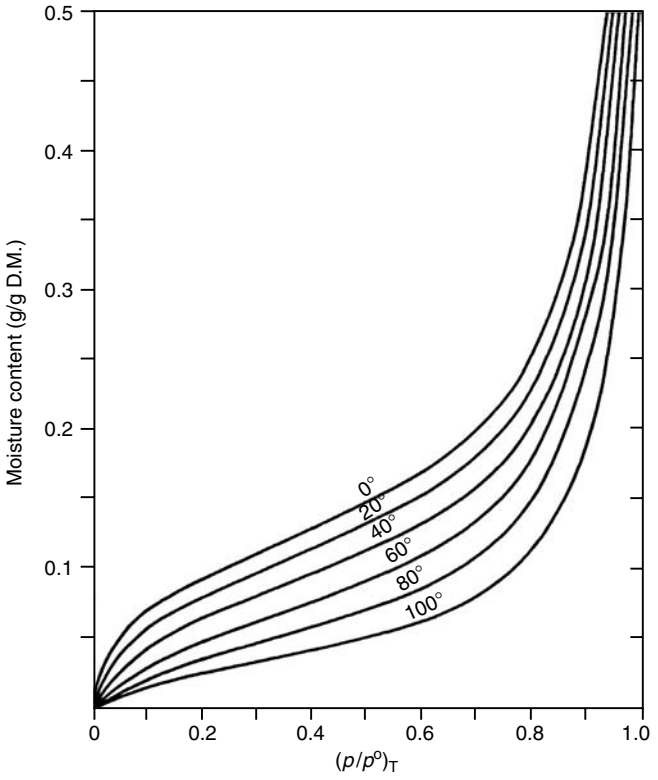

FIGURE 2.35 Moisture desorption isotherms for potatoes at various temperatures. (Redrawn from Gorling, P. (1958) In *Fundamental Aspects of the Dehydration of Foodstuffs*. Society of Chemical Industry: London, pp. 42–53.)

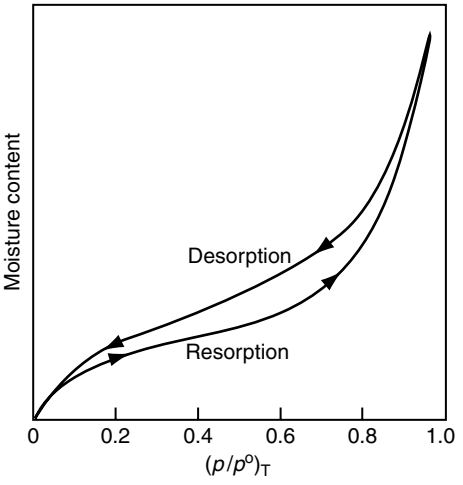

FIGURE 2.36 Hysteresis of a MSI.

The magnitude of hysteresis, the shape of the curves, and the inception and termination points of the hysteresis loop can vary considerably depending on factors such as nature of the food, the physical changes it undergoes when water is removed or added, temperature, the rate of desorption, and the degree of water removal during desorption [92]. The effect of temperature is pronounced:

hysteresis is often not detectable at high temperatures (~80°C) and generally becomes increasingly evident as the temperature is lowered.

Several largely qualitative theories have been advanced to explain sorption hysteresis [52,92]. These theories involve factors such as swelling phenomena, metastable local domains, chemisorption, phase transitions, capillary phenomena, and the fact that nonequilibrium states become increasingly persistent as the temperature is lowered. A definitive explanation (or explanations) of sorption hysteresis has yet to be formulated.

Sorption hysteresis is more than a laboratory curiosity. Labuza et al. [93] have conclusively demonstrated that lipid oxidation in strained meat from chicken and pork at $(p/p^o)_T$ values in the range 0.75–0.84 proceeds much more rapidly if the samples are adjusted to the desired $(p/p^o)_T$ value by desorption rather than resorption. The desorption samples, as already noted, contain more water at a given $(p/p^o)_T$ than the resorption samples. This would cause the high moisture sample to have a lower viscosity, which in turn would cause greater catalyst mobility, greater exposure of catalytic sites because of the swollen matrix, and somewhat greater oxygen diffusivity than in the lower moisture (resorption) sample. In another study, Labuza et al. [94] found that the $(p/p^o)_T$ needed to stop the growth of several microorganisms is significantly lower if the product is prepared by desorption rather than resorption. The existence of hysteresis is yet further compelling evidence that, as commonly determined, sorption isotherms define steady-state systems (assuming that sufficient time has been allowed for the system to attain steady state) rather than true equilibrium systems.

By now it should be very clear that MSIs are highly product specific, that the MSI for a given product can be changed significantly by the manner in which the product is prepared, and that these points are of practical importance. Further discussion on the measurement and utility of MSIs can be found in References 48 and 95–98 and a compilation of typical MSIs is to be found in Reference 99.

2.11.4 Hydration Sequence of a Protein

It is instructive to consider further water absorption by a dry food component and the location and properties of water at each state of the process. Lyoszyme is chosen for this exercise because proteins are of major importance in foods and because they contain all of the major types of functional group important to hydration. Even "dry" lysozyme contains some constitutional water, which is an integral part of the structure. This amounts to around 8 mol water/g dry protein. On exposure to increasing levels of RVP, water is first adsorbed at the sites of ionized, carboxylic acid, and amino side chains. This requires about 40 mol water/mol dry lysozyme and corresponds approximately to the water content at the BET monolayer, the junction of zones I and IIA, at a RVP around 0.2. Further increase in RVP, to around 0.25 (end of zone IIA) leads to sorption at less active sites such as amide carbonyls, and continued sorption to RVP 0.75 (end of zone IIB) results in full surface coverage with water content 0.38. At this point (the junction of zones IIB and III), all available surface sites are considered covered [100]. Beyond this RVP (zone III) the water corresponds to multilayer (bulk) water. Enzyme activity is first seen above the "BET monolayer" coverage, and maximum activity is reached at the full surface coverage point. These observations help illustrate the value of the zonal description of the MSI in categorizing hydration effects. It must be remembered, however, that at any particular water content, all water molecules are freely exchangeable between regions, leading to a continuum of behaviors as water content increases.

2.12 RELATIVE VAPOR PRESSURE AND FOOD STABILITY

Historically, it has often been demonstrated that food stability and $(p/p^o)_T$ are closely related in many situations. The data of Figures 2.20, 2.37 and Table 2.11 provide examples of these relationships. Shown in Table 2.11 are various common microorganisms and the range of RVP permitting their growth [101]. Also shown in this table are common foods categorized according to their RVP.

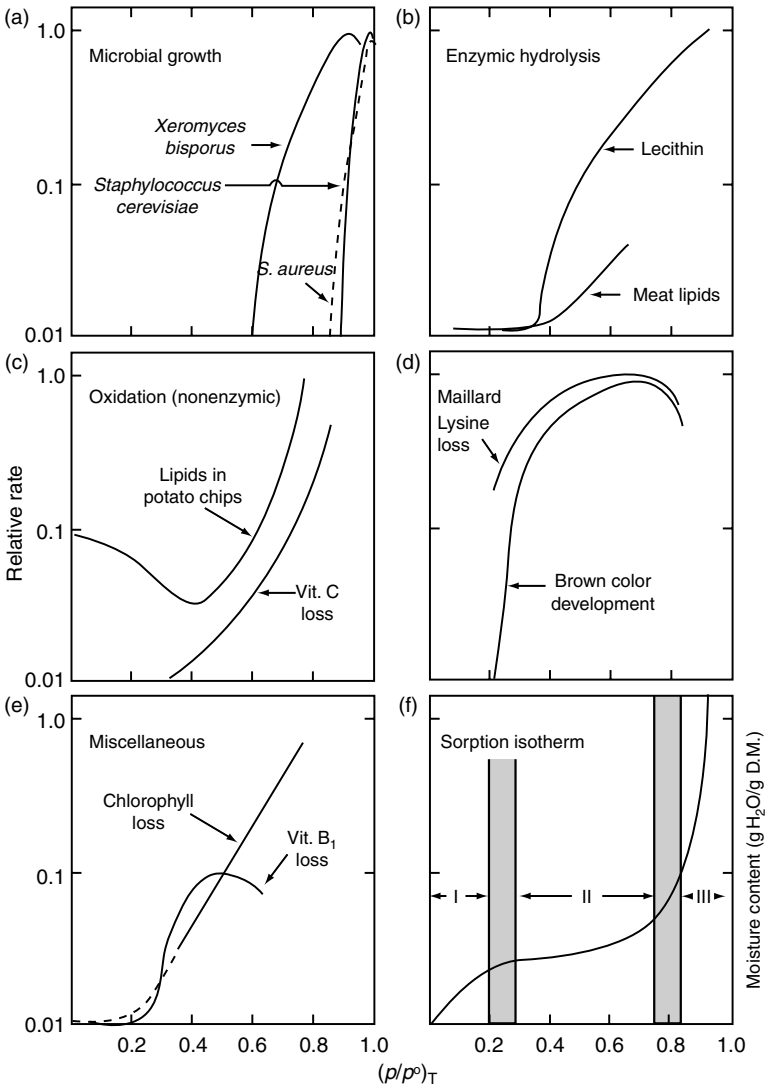

FIGURE 2.37 Relationships among relative water vapor pressure, food stability, and sorption isotherms. (a) Microbial growth vs. $(p/p^{o})_T$, (b) enzymic hydrolysis vs. $(p/p^{o})_T$, (c) oxidation (nonenzymic) vs. $(p/p^{o})_T$, (d) Maillard browning vs. $(p/p^{o})_T$, (e) miscellaneous reaction rates vs. $(p/p^{o})_T$, and (f) water content vs. $(p/p^{o})_T$. All ordinates are "relative rate" except for F. Data from various sources.

Data in Figure 2.37 are typical relationships between reaction rate and $(p/p^{o})_T$ in the temperature range 25–45°C. For comparative purposes a typical isotherm is also shown in Figure 2.37f. It is important to remember that the exact reaction rates and the positions and shapes of the curves in Figure 2.37 can be altered by sample composition, physical state and structure of the sample, composition of the atmosphere (especially oxygen), temperature, and by hysteresis effects. The reader is also cautioned that this empirical relationship is between a thermodynamic parameter and a kinetic parameter, and that there is no intrinsic theoretical reason why such parameters should correlate, since thermodynamics deals with equilibrium positions, and kinetics deals with rates. Thermodynamics is predictable and kinetics is empirical.

The unusual relationship between the rate of lipid oxidation and $(p/p^{o})_T$ at very low values of $(p/p^{o})_T$ deserves comment (Figure 2.37). Starting at the extreme left of the isotherm, added

TABLE 2.11
Potential for Growth of Microorganisms in Food at Different Relative Vapor Pressures

Range of p/p^o	Microorganisms Generally Inhibited by Lowest p/p^o of the Range	Foods Generally within this Range of p/p^o
1.00–0.95	*Pseudomonas, Escherischia Proteus, Shigella, Klebsiella, Bacillus, Clostridium perfringens,* some yeasts	Highly perishable (fresh) foods, canned fruits, vegetables, meat, fish, and milk; cooked sausages and breads; foods containing up to 7% (w/w) sodium chloride or 40% sucrose
0.95–0.91	*Salmonella*, *Vibrio parahaemolyticus*, *C. Botulinum*, *Serratia*, *Lactobacillus*, some molds, yeasts (*Rhodotorula*, *Pichia*)	Some cheeses (Cheddar, Swiss, Muenster, Provolone), cured meats (ham), some fruit juice concentrates, foods containing up to 12% (w/w) sodium chloride or 55% sucrose
0.91–0.87	Many yeasts (*Candida, Torulopsis, Hansenula, Micrococcus*)	Fermented sausages (salami), sponge cakes, dry cheeses, margarine, foods containing up to 15% (w/w) sodium chloride or saturated (65%) sucrose
0.87–0.80	Most molds (mycotoxigenic penicillia), *Staphylococcus aureus*, most *Saccharomyces* (*bailii*) spp., *Debaryomyces*	Most fruit juice concentrates, sweetened condensed milk, chocolate syrup, maple and fruit syrups; flour, rice, pulses of 15–17% moisture content; fruit cake; country style ham, fondants
0.80–0.75	Most halophilic bacteria, mycotoxigenic aspergilli	Jam, marmalade, marzipan, glace fruits, some marshmallows
0.75–0.65	Xerophilic molds (*Aspergillus chevalieri, A. candidus, Wallemia sebi*) *Saccharomyces bisporus*	Rolled oats of 10% moisture content; grained nougats, fudge, marshmallows, jelly, molasses, raw cane sugar, some dried fruits, nuts
0.65–0.60	Osmophilic yeasts (*Saccharomyces rouxii*), few molds (*Aspergillus echinulatus, Monascus bisporus*)	Dried fruits of 15–20% moisture content, toffees and caramels, honey
0.60–0.50	No microbial proliferation	Pasta of 12% moisture content, spices of 10% moisture content
0.50–0.40	No microbial proliferation	Whole egg powder of 5% moisture content
0.40–0.30	No microbial proliferation	Cookies, crackers, bread crusts, and so forth of 3–5% moisture content
0.30–0.20	No microbial proliferation	Whole milk powder of 2–3% moisture content; dried vegetables of 5% moisture content; corn flakes of 5% moisture content, country style cookies, crackers

Source: Beuchat, L.R. (1981) *Cereal Foods World* **26**: 345–349.

water decreases the rate of oxidation until a water content equivalent to the BET monolayer value is attained. Clearly, overdrying of samples subject to oxidation will result in less than optimal stability. Karel and Yong [102] have offered the following interpretative suggestions regarding this behavior. The first water added to a very dry sample is believed to bind hydroperoxides, interfering with their decomposition, and thereby hindering the progress of oxidation. In addition, this water hydrates metal ions that catalyze oxidation, apparently reducing their effectiveness.

Addition of water beyond the boundary of zones I and II (Figure 2.37) results in increased rates of oxidation. Karel and Yong suggested that water added in this region of the isotherm accelerates

oxidation by increasing the solubility of oxygen and by allowing macromolecules to swell, thereby exposing more catalytic sites. At still greater $(p/p^o)_T$ values ($>\sim 0.80$), the added water may retard rates of oxidation, and the suggested explanation is that dilution of catalysts reduces their effectiveness.

It should be noted that the curves for the Maillard reaction, vitamin B_1 degradation, and microbial growth all exhibit rate maxima at intermediate to high $(p/p^o)_T$ values (Figure 2.37). Two possibilities have been advanced to account for the decline in reaction rate that sometimes accompanies increases in RVP in foods having moderate to high moisture contents:

1. For those reactions in which water is a product, an increase in water content can result in product inhibition.
2. When the water content of the sample is such that the solubility, accessibility (surfaces of macromolecules), and mobility of rate-enhancing constituents are no longer rate limiting, further addition of water serves only to dilute rate-enhancing constituents and decrease the reaction rate.

Since the BET monolayer value of a food frequently provides a good first estimate of the water content providing maximum stability of a dry product, knowledge of this value is of considerable practical importance. Determining the BET monolayer value for a specific food can be done with moderate ease if data for the low-moisture end of the MSI are available. One can then use the BET equation developed by Brunauer et al. [83] to compute the monolayer value:

$$\frac{a_w}{m(1-a_w)} = \frac{1}{m_1 c} + \frac{c-1}{m_1 c} a_w \tag{2.12}$$

where a_w is water activity, m is moisture content (g H_2O/g dry matter), m_1 is the BET monolayer value and c is a constant. In practice $(p/p^o)_T$ values are used in Equation 2.12 rather than a_w values.

From this equation it is apparent that a plot of $a_w/m\,(1-a_w)$ vs. a_w, known as a BET plot, should yield a straight line. An example, for native potato starch with a_w replaced by $(p/p^o)_T$ is shown in Figure 2.38. The linear relationship, as is generally acknowledged, begins to deteriorate at $(p/p^o)_T$ values greater than about 0.35.

The BET monolayer value can be calculated as follows:

$$\text{Monolayer value} = m_1 = 1/((y \text{ intercept}) + (\text{slope}))$$

From Figure 2.38, the y intercept is 0.6. Calculation of the slope yields a value of 10.7. Thus:

$$m_1 = 1/(0.6 + 10.7) = 0.088 \text{ g } H_2O/\text{g dry matter}$$

In this particular example, the BET monolayer value corresponds to a $(p/p^o)_T$ of 0.2. The GAB equation yields a similar monolayer value.

In addition to chemical reactions and microbial growth, $(p/p^o)_T$ also influences the texture of dry and semidry foods. For example, suitably low RVPs are necessary if crispness of crackers, popped corn, and potato chips is to be retained; if caking of granulated sugar, dry milk, and instant coffee is to be avoided; and if stickiness of hard candy is to be prevented. The maximum $(p/p^o)_T$ that can be tolerated in dry materials without incurring loss of desirable properties ranges from 0.35 to 0.5, depending on the product [103]. Furthermore, suitably high $(p/p^o)_T$ values of soft-textured foods are needed to avoid undesirable hardness.

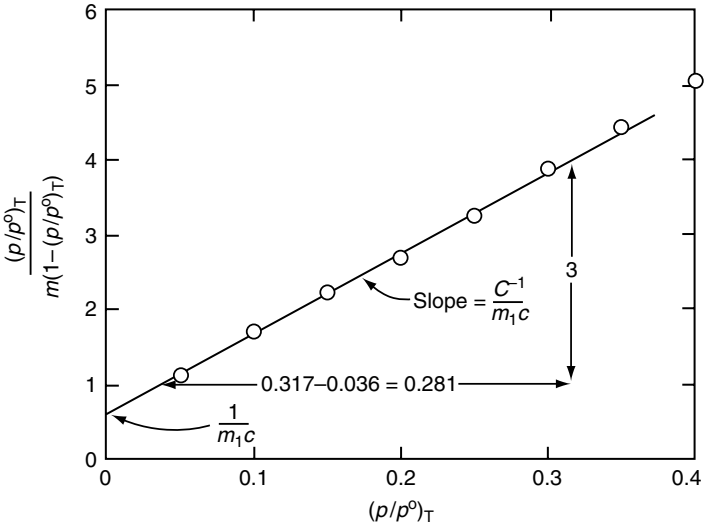

FIGURE 2.38 BET plot for native potato starch (resorption data, 20°C). (Data from van den Berg, C. (1981) *Vapour Sorption Equilibria and Other Water–Starch Interactions: A Physico-Chemical Approach*. Wageningen Agricultural University: Wageningen, The Netherlands.)

2.13 COMPARISONS

2.13.1 The Interrelationships Between the RVP, Mm, and MSI Approaches to Understanding the Role of Water in Foods

The equilibrium freezing temperature of a system provides a measure of its a_w, since at the freezing point the a_w of the system is identical to that of pure water ice at that same temperature. Bearing this in mind, we can construct an annotated state diagram (Figure 2.39) to map out the interrelationships between the RVP, Mm, and MSI approaches to understanding the roles of water in foods. The Mm approach has already been extensively discussed using appropriate state diagrams. In Figure 2.39, the area where RVP is most utilized is the top left. Considering systems of RVP = 0.8. These lie to the left of the line representing the composition of a system with a T_m^L of −22°C, the temperature where the RVP of ice is 0.8. The region of primary applicability of RVP to microbial stability is represented by the hatched box. This is far removed from the T_d and T_g lines, indicating that Mm of both solutes and solvent is sufficient to allow rapid rearrangement and adjustment to a long-term steady-state condition at a constant temperature. At lower RVP, corresponding to systems with hypothetical equilibrium freezing temperatures below −30°C, the corresponding RVP is less than 0.75. In such systems, solute mobilities are reduced, and attaining long-term steady state is more challenging. At RVP below 0.6 the hypothetical T_m^L would be around −52°C. Such systems are difficult to equilibrate, and measurement of a meaningful steady-state RVP is difficult, if not impossible.

In MSI, we tend to utilize both sorption and desorption. Consider first sorption. Plots from the right side of the state diagram represent sorption on to a dry product, with the right axis representing the dry product. The condition of the dry product defines whether line T_g or line T_m^s is appropriate to describe the state boundary as moisture content increases. Frequently partial crystallization has occurred within the dry product, such that portions of the product are appropriately considered in terms of each of these lines defining a change in physical state. Entry to the more mobile, fluid states occurs with initially low mobilities, and the processes of change may be slow. Water enters the product first at the surfaces, resulting in mobility gradients; as with a higher moisture content, surface mobility

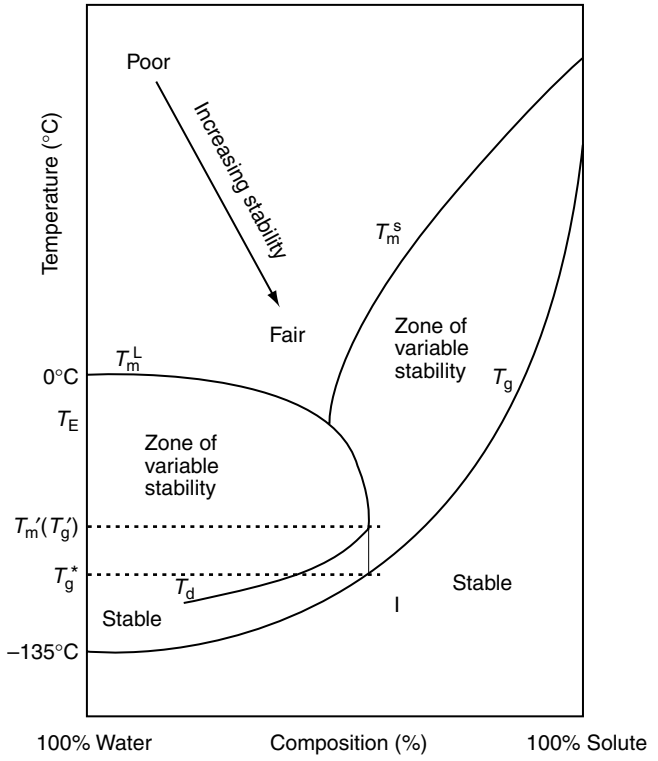

FIGURE 2.39 State diagram of a binary system showing potential stabilities in different zones.

is enhanced (and surface T_g is reduced). For desorption, the composition of samples is moving from left to right on the diagram, and a more fluid system is losing mobility as desorption progresses. Hence, rapid desorption will tend to lead to less solute crystallization than will slow desorption.

2.14 CONCLUSION

Each of the approaches to product stability described has best applicability under certain, constrained conditions. It is appropriate, therefore, to utilize all approaches in order to better appreciate the role of water in foods, and the potential mechanisms and routes through which water, and water content, can influence product stability. Both Schmidt [4] and Sherwin and Labuza [104] in recent articles have provided useful discussion of the relative importance of each approach under a range of different conditions. Water plays a critical role in the chemical and physical processes within foods. While an apparently simple molecule, it is clear that the complex nature of the hydrogen bonding networks of water, and between water and solutes, in addition to other influences upon the intermolecular arrangements of water are essential for the functioning of biological systems, and are key to the properties of foods.

REFERENCES

1. Franks, F. (2000) *Water, a Matrix of Life*. Royal Society of Chemistry: London.
2. Fennema, O. (1973) Water and ice. In *Low Temperature Preservation of Foods and Living Matter* (O. Fennema, W.D. Powrie, and E.H. Marth, Eds.), Marcel Dekker: New York, pp. 1–77.
3. Chaplin, M. (2001) Water, its importance to life. *Biochem. Mol. Educat*. **29**: 54–59.

4. Schmidt, S.J. (2004) Water and solids mobility in foods. *Adv. Food Nutr. Res*. **48**: 1–101.
5. Hobbs, P.V. (1974) *Ice Physics*. Clarendon Press: Oxford.
6. Rontgen, W.C. (1882) VIII Uber die constitution des flussigen wassers. *Ann. Phys. Chem.* **281**: 91–97.
7. Ball, P. (2001) *Life's Matrix, a Biography of Water.* University of California Press: Berkeley, CA.
8. Guillot, B. (1991) A molecular-dynamics study of the far infrared spectrum of liquid water. *J. Chem. Phys.* **95**: 1543–1551.
9. Errington, J.R. and P.G. Debenedetti (2001) Relationship between structural order and the anomalies of liquid water. *Nature (London)* **409**: 318–321.
10. Guillot, B. (2002) A reappraisal of what we have learned during 3 decades of computer simulations on water. *J. Mol. Liquids* **101**: 219–260.
11. Bertoluzza, A., C. Fagnano, M.A. Morelli, A. Tinti, and M.R. Tosi (1993) The role of water in biological systems. *J. Mol. Struct.* **297**: 425–437.
12. Luck, W.A.P. (1981) Structures of water in aqueous systems. In *Water Activity: Influences on Food Quality* (L.B. Rockland and G.F. Stewart, Eds.), Academic Press: New York, pp. 407–434.
13. Sceats, M.G. and S.A. Rice (1982) Amorphous solid water and its relationship to liquid water: a random network model for water. In *Water, a Comprehensive Treatise* (F. Franks, Ed.), Plenum Press: New York, pp. 83–214.
14. Stillinger, F.H. (1980) Water revisited. *Science* **209**: 451–457.
15. Brady, G.W. and W.J. Romanov (1960) Structure of water. *J. Chem. Phys.* **32**: 106.
16. Morgan, J. and B.E. Warren (1938) X-ray analysis of the structure of water. *J. Chem. Phys.* **6**: 666–673.
17. Cheftel, J.C., J. Levy, and E. Dumay (2000) Pressure-assisted freezing and thawing: principles and potential applications. *Food Rev. Int.* **16**: 453–483.
18. Cheftel, J.C., M. Thiebaud, and E. Dumay (2002) High pressure–low temperature processing of foods: a review. Advances in high pressure bioscience and biotechnology II, *Proceedings of the International Conference on High Pressure Bioscience and Biotechnology*, Dortmund, Germany, September 16–19, pp. 327–340.
19. Luyet, B. (1960) On various phase transitions occurring in aqueous solutions at low temperature. *Ann. NY Acad. Sci.* **85**: 549–569.
20. Luyet, B.J. (1966) Anatomy of the freezing process in physical systems. In *Cryobiology* (H.T. Meryman, Ed.), Academic Press: New York, pp. 115–138.
21. Rapatz, G. and B. Luyet (1972) Patterns of ice formation and rates of ice growth in gelatin solutions. *Biodynamica* **11**: 117–123.
22. Rey, L.R. (1958) *Etude Physiologique et Physico-Chimique de l'Action des Basses Temperaturessur les Tissues Animaux*. Universite de Paris: Paris, France.
23. Simatos, D. and L. Rey (1965) Freeze-drying of biologic materials. *Fed. Proc.* **24**: 213–215.
24. Berendsen, H.J.C. (1971) The molecular dynamics of water in biological systems. *Proc. First Europ. Biophys. Cong.* **1**: 483–488.
25. Kuntz, I.D. and W. Kauxmann (1974) Hydration of proteins and polypeptides. *Adv. Protein Chem.* **28**: 239–345.
26. Geiger, A. (1981) Molecular dynamics simulation study of the negative hydration effect in aqueous electrolyte solutions. *Berichte der Bunsen-Gesellschaft* **85**: 52–63.
27. Eagland, D. (1975) Nucleic acids, peptides and proteins. In *Water, a Comprehensive Treatise* (F. Franks, Ed.), Plenum: New York, pp. 305–518.
28. Lewin, S. (1974) *Displacement of Water and its Control of Biochemical Reactions*. Academic Press: London.
29. Tait, M.J., A. Suggett, F. Franks, S. Ablett, and P.A. Quickenden (1972) Hydration of monosaccharides. Study by dielectric and nuclear magnetic relaxation. *J. Solution Chem.* **1**: 131–151.
30. Franks, F. (1988) Protein hydration. In *Characteristics of Proteins* (F. Franks, Ed.), Humana Press: Clifton, NJ, pp. 127–154.
31. Franks, F. (1975) The hydrophobic interaction. In *Water, a Comprehensive Treatise* (F. Franks, Ed.), Plenum Press: New York, pp. 1–94.
32. Davidson, D.W. (1973) Clathrate hydrates. In *Water, a Comprehensive Treatise* (F. Franks, Ed.), Plenum Press: New York, pp. 115–234.
33. Koga, K., H. Tanaka, and K. Nakanishi (1994) Stability of polar guest-encaging clathrate hydrates. *J. Chem. Phys.* **101**: 3127–3134.

34. Koga, K., H. Tanaka, and K. Nakanishi (1994) On the stability of clathrate hydrates encaging polar guest molecules: contrast in the hydrogen bonds of methylamine and methanol hydrates. *Mol. Simul.* **12**: 241–252.
35. Gerstein, M. and R.M. Lynden-Bell (1993) Simulation of water around a model protein helix. 1. Two-dimensional projections of solvent structure. *J. Phys. Chem.* **97**: 2982–2990.
36. Uedaira, H. (1995) Properties and structure of water. *Kagaku to Kyoiku* **43**: 494–500.
37. Head-Gordon, T. (1995) Is water structure around hydrophobic groups clathrate-like? *Proc. Natl Acad. Sci. USA* **92**: 8308–8312.
38. Teeter, M.M. (1991) Water–protein interactions: theory and experiment. *Ann. Rev. Biophys. Biophys. Chem.* **20**: 577–560.
39. Lounnas, V. and B.M. Pettitt (1994) A connected cluster of hydration around myoglobin. Correlation between molecular dynamics simulations and experiment. *Proteins: Struc. Func. Genet.* **18**: 133–147.
40. Edelhoch, H. and J.J.C. Osborne (1976) The thermodynamic basis of the stabilty of proteins, nucleic acids and membranes. *Adv. Protein Chem.* **30**: 183–250.
41. Oakenfull, D. and D.E. Fenwick (1977) Thermodynamics and mechanism of the hydrophobic interaction. *Aust. J. Chem.* **30**: 741–752.
42. Ashbaugh, H.S., T.M. Truskett, and P.G. Debenedetti (2002) A simple molecular thermodynamic theory of hydrophobic hydration. *J. Chem. Phys.* **116**: 2907–2921.
43. Johnson, M.R. and R.C. Lin (1987) FDA views on the importance of a_w in good manufacturing practice. In *Water Activity: Theory and Applications to Food* (L.B. Rockland and L.R. Beuchat, Eds.), Marcel Dekker: New York, pp. 287–294.
44. Scott, W.J. (1953) Water relations of *Staphilococcus aureus* at 30°C. *Aust. J. Biol. Sci.* **6**: 549–556.
45. Scott, W.J. (1957) Water relations of food spoilage organisms. *Adv. Food Res.* **7**: 83–127.
46. Chirife, J. (1994) Specific solute effects with special reference to *Staphylococcus aureus*. *J. Food Eng.* **22**: 409–419.
47. Gal, S. (1981) Recent developments in techniques for obtaining complete sorption isotherms. In *Water Activity: Influnce on Food Quality* (L.B. Rockland and G.F. Stewart, Eds.), Academic Press: New York, pp. 89–110.
48. Spiess, W.E.L. and W. Wolf (1987) Critical evaluation of methods to determine moisture sorption isotherms. In *Water Activity: Theory and Application to Foods* (L.B. Rockland and L.R. Beuchat, Eds.), Marcel Dekker: New York, pp. 215–233.
49. van den Berg, C. (1981) *Vapour Sorption Equilibria and Other Water–Starch Interactions: A Physico-Chemical Approach*. Wageningen Agricultural University: Wageningen, The Netherlands.
50. van den Berg, C. and S. Bruin (1981) Water activity and its estimation in food systems: theoretical aspects. In *Water Activity: Influences on Food Quality* (L.B. Rockland and G.F. Stewart, Eds.), Academic Press: New York, pp. 1–61.
51. Reid, D.S., A. Fontana, S. Rahman, S. Sablami, and T. Labuza (2005) Vapor pressure measurements of water. In *Handbook of Food Analytical Chemistry* (R.E. Wrolstad, T.E. Acree, E.A. Decker, M.H. Penner, D.S. Reid, S.J. Schwartz, C.F. Shoemaker, D.M. Smith, and P. Sporns, Eds.), Wiley: New York, pp. Section A2.
52. Kapsalis, J.G. (1987) Influences of hysteresis and temperature on moisture sorption isotherms. In *Water Activity: Theory and Applications to Food* (L.B. Rockland and L.R. Beuchat, Eds.), Marcel Dekker: New York, pp. 173–213.
53. Fennema, O. and L.A. Berny (1974) Equilibrium vapor pressure and water activity of food at subfreezing temperatures. In *Fourth Int. Congress of Food Science and Technology*. Madrid, Spain.
54. Williams, M.L., R.F. Landel, and J.D. Ferry (1955) The temperature dependence of relaxation mechanisms in amorphous polymers and other glass-forming liquids. *J. Am. Chem. Soc.* **77**: 3701–3707.
55. Ferry, J.D. (1980) *Viscoelastic Properties of Polymers*, 3rd edn. John Wiley & Sons: New York.
56. White, G.W. and S.H. Cakebread (1966) The glassy state in certain sugar-containing food products. *J. Food Technol.* **1**: 73–82.
57. White, G.W. and S.H. Cakebread (1969) Importance of the glassy state in certain sugar-containing food products. *Food Sci. Technol. Proc. Int. Congr.*, 1st, pp. 227–235.

58. Duckworth, R.B., J.Y. Allison, and H.A. Clapperton (1976) The aqueous environment for change in intermediate moisture foods. In *Intermediate Moisture Foods* (R. Davies, G.G. Birch, and K.J. Parker, Eds.), Applied Science: London, pp. 89–99.
59. Franks, F. (1995) Aqueous solutions—a new perspective. Amorphous carbohydrates: science and application technology. *J. Solution Chem.* **24**: 1093–1097.
60. Slade, L. and H. Levine (1991) A food polymer science approach to structure–property relationships in aqueous food systems: non-equilibrium behavior of carbohydrate–water systems. *Adv. Exptl Med. Biol.* **302**: 29–101.
61. Slade, L. and H. Levine (1991) Beyond water activity: recent advances based on an alternative approach to the assessment of food quality and safety. *Crit. Rev. Food Sci. Nutr.* **30**: 115–360.
62. Levine, H. and L. Slade (1988) "Collapse" phenomena—a unifying concept for interpreting the behavior of low moisture foods. In *Food Structure—Its Creation and Evaluation* (J.M.V. Blanshard and J.R. Mitchell, Eds.), Butterworths: London, pp. 149–180.
63. Levine, H. and L. Slade (1988) Water as a plasticizer: physico-chemical aspects of low moisture polymeric systems. *Water Sci. Rev.* **3**: 79–185.
64. Slade, L. and H. Levine (1995) Polymer science approach to water relationships in foods. In *Food Preservation by Moisture Control* (G.V. Barbosa-Canovas and J. Welti-Chanos, Eds.), Technomic Press: Lancaster, PA, pp. 33–132.
65. Slade, L. and H. Levine (1995) Glass transitions and water–food structure interactions. *Adv. Food Nutr. Res.* **38**: 103–269.
66. Shalaev, E.Y. and A.N. Kanev (1994) Study of the solid–liquid state diagram of the water–glycine–sucrose system. *Cryobiology* **31**: 374–382.
67. Liu, B., Z. Hua, and H. Ren (1996) The glassy state storage of frozen food. *Zhileng Xuebao* 26–31.
68. Boutron, P., P. Mehl, A. Kauffmann, and P. Angibaud (1986) Glass-forming tendency and stability of the amorphous state in the aqueous solutions of linear polyalcohols with four carbons. I. Binary systems water–polyalcohol. *Cryobiology* **23**: 453–469.
69. Levine, H. and L. Slade (1988) Thermomechanical properties of small-carbohydrate–water glasses and "rubbers": kinetically metastable systems at sub-zero temperatures. *J. Chem. Soc. Faraday Trans. 1: Phys. Chem. Condens. Phases* **84**: 2619–2633.
70. Roos, Y. (1993) Melting and glass transitions of low molecular weight carbohydrates. *Carbohydr. Res.* **238**: 39–48.
71. Hatley, R.H.M. and A. Mant (1993) Determination of the unfrozen water content of maximally freeze concentrated carbohydrate solutions. *Int. J. Macromol.* **15**: 227–232.
72. Reid, D.S., J. Hsu, and W.L. Kerr (1993) Calorimetry. In *The Glassy State in Foods* (J.M.V. Blanshard and P.J. Lillford, Eds.), Nottingham University Press: Loughborough, pp. 123–132.
73. Roos, Y.H. and M. Karel (1993) Effect of glass transitions on dynamic phenomena in sugar containing food systems. In *The Glassy State in Foods* (J.M.V. Blanshard and P.J. Lillford, Eds.), Nottingham University Press: Loughborough, pp. 207–222.
74. Simatos, D. and G. Blond (1991) DSC studies and stability of frozen foods. *Adv. Exptl Med. Biol.* **302**: 139–155.
75. Slade, L., H. Levine, J. Ievolella, and M. Wang (1993) The glassy state phenomenon in applications for the food industry: application of the food polymer science approach to structure–function relationships of sucrose in cookie and cracker systems. *J. Sci. Food Agric.* **63**: 133–176.
76. Angell, C.A. (1997) Entropy and fragility in supercooling liquids. *J. Res. Natl Inst. Stand. Technol.* **102**: 171–185.
77. Angell, C.A. (2001) Water, what we know and what we dont. In *Water Science for Food, Health Agriculture and Environment* (Z. Berk, R.B. Leslie, P.J. Lillford, and S. Mizrahi, Eds.), Technomic: Lancaster, PA, pp. 1–30.
78. Kerr, W.L., M.H. Lim, D.S. Reid, and H. Chen (1993) Chemical reaction kinetics in relation to glass transition temperatures in frozen food polymer solutions. *J. Sci. Food Agric.* **61**: 51–56.
79. Kerr, W.L. and D.S. Reid (1994) Temperature dependence of the viscosity of sugar and maltodextrin solutions in coexistence with ice. *Lebensmittel-Wissenschaft Technologie* **27**: 225–231.
80. Matveev, Y.I. and S. Ablett (2002) Calculation of the C'_g and T'_g intersection point in the state diagram of frozen solutions. *Food Hydrocoll.* **16**: 419–422.

81. Roos, Y. and M. Karel (1991) Nonequilibrium ice formation in carbohydrate solutions. *Cryo-Letters* **12**: 367–376.
82. Roos, Y. and M. Karel (1991) Phase transitions of amorphous sucrose and frozen sucrose solutions. *J. Food Sci.* **56**: 266–267.
83. Brunauer, S., H.P. Emmett, and E. Teller (1938) Adsorption of gases in multimolecular layers. *J. Am. Chem. Soc.* **60**: 309–319.
84. Guggenheim, E.A. (1966) *Applications of Statistical Mechanics*. Clarendon Press: Oxford, pp. 186–206.
85. Anderson, R.B. (1946) Modifications of the Brunauer, Emmett, and Teller equation. *J. Am. Chem. Soc.* **68**: 686–691.
86. De Boer, J.H. (1968) *The Dynamical Character of Adsorption*, 2nd edn. Clarendon Press: Oxford, UK, pp. 200–219.
87. Lillford, P.J., A.H. Clark, and D.V. Jones (1980) *Distribution of Water in Heterogeneous Food and Model Systems.* ACS Symposium Series 127, pp. 177–195.
88. Belton, P.S. and B.P. Hills (1988) The effects of exchange and interfacial reaction in two-phase systems on NMR line shapes and relaxation processes. *Mol. Phys.* **65**: 313–326.
89. Hills, B.P. (1992) The proton exchange cross-relaxation model of water relaxation in biopolymer systems. *Mol. Phys.* **76**: 489–508.
90. Hills, B.P. (1990) Multinuclear relaxation studies of water in carbohydrate and protein systems. *Spectroscopy* (Amsterdam, Netherlands) **8**: 149–171.
91. Hills, B.P. and K.P. Nott (1999) NMR studies of water compartmentation in carrot parenchyma tissue during drying and freezing. *Appl. Magn. Resonance* **17**: 521–535.
92. Karel, M. (1988) Role of water activity. In *Food Properties and Computer-Aided Engineering of Food Processing Systems* (R.P. Singh and A.G. Medina, Eds.), Kluwer Academic: Dordrecht, The Netherlands, pp. 135–155.
93. Labuza, T.P., L. McNally, D. Gallagher, J. Hawkes, and F. Hurtado (1972) Stability of intermediate moisture foods. 1. Lipid oxidation. *J. Food Sci.* **37**: 154–159.
94. Labuza, T.P., S. Cassil, and A.J. Sinskey (1972) Stability of intermediate moisture foods. II. Microbiology. *J. Food Sci.* **37**: 160–162.
95. Leisen, J., H.W. Beckham, and M. Benham (2002) Sorption isotherm measurements by NMR. *Solid State Nucl. Magn. Resonance* **22**: 409–422.
96. Mauer, L.J., D.E. Smith, and T.P. Labuza (2000) Effect of water content, temperature and storage on the glass transition, moisture sorption characteristics and stickiness of β-casein. *Int. J. Food Properties* **3**: 233–248.
97. Schaller-Povolny, L.A., D.E. Smith, and T.P. Labuza (2000) Effect of water content and molecular weight on the moisture isotherms and glass transition properties of inulin. *Int. J. Food Properties* **3**: 173–192.
98. Teoh, H.M., S.J. Schmidt, G.A. Day, and J.F. Faller (2001) Investigation of cornmeal components using dynamic vapor sorption and differential scanning calorimetry. *J. Food Sci*. **66**: 434–440.
99. Iglesias, H.A. and J. Chirife (1982) *Handbook of Food Isotherms: Water Sorption Parameters for Food and Food Components*, Academic Press: New York, p. 347.
100. Rupley, J.A. and G. Careri (1991) Protein hydration and function. *Adv. Protein Chem.* **41**: 37–172.
101. Beuchat, L.R. (1981) Microbial stability as affected by water activity. *Cereal Foods World* **26**: 345–349.
102. Karel, M. and S. Yong (1981) Autoxidation-initiated reactions in foods. In *Water Activity: Influences Food Quality* (L.B. Rockland and G.F. Stewart, Eds.), Academic Press: New York, pp. 511–529.
103. Labuza, T.P. and R. Contreras-Medellin (1981) Prediction of moisture protection requirements for foods. *Cereal Foods World* **26**: 335–344.
104. Sherwin, C.P. and T.P. Labuza (2005) Beyond water activity and glass transition: a broad perspective on the manner by which water can influence reaction rates in foods. In *Water Properties of Food, Pharmaceutical and Biological Materials* (M.P. Buera, J. Welti-Chanos, P.J. Lillford, and H.R. Corti, Eds.), CRC Press: Boca Raton, FL, pp. 343–371.
105. Suggett, A. (1976) Molecular motion and interactions in aqueous carbohydrate solutions. III. A combined nuclear magnetic and dielectric-relaxation strategy. *J. Solution Chem.* **5**: 33–46.

106. Berendsen, H.J.C. (1975) Specific interaction of water with biopolymers. In *Water, a Comprehensive Treatise* (F. Franks, Ed.), Plenum Press: New York, pp. 293–349.
107. van den Berg, C. and H.A. Leniger (1978) The water activity of foods. In *Miscellaneous Papers 15*. Wageningen Agricultural University: Wageningen, The Netherlands, pp. 231–244.
108. Fennema, O. (1978) Enzyme kinetics at low temperature and reduced water activity. In *Dry Biological Systems* (J.H. Crowe and J.H. Clegg, Eds.), Academic Press: New York, pp. 297–322.
109. Gorling, P. (1958) Physical phenomena during the drying of foodstuffs. In *Fundamental Aspects of the Dehydration of Foodstuffs*. Society of Chemical Industry: London, pp. 42–53.
110. Lide, D.R. (ed.) (1993/1994) *Handbook of Chemistry and Physics*, 74 edn. CRC Press: Boca Raton, FL.
111. Mason, B.J. (1957) *The Physics of Clouds*. Clarendon Press: Oxford, p. 445.
112. Levine, H. and L. Slade (1990) Cryostabilization technology. In *Thermal Analysis of Foods* (V.R. Harwalkar and C.-Y. Ma, Eds.), Elsevier Applied Science: London, pp. 221–305.
113. Otting, G., B. Liepinsh, and K. Wuthrich (1991) Protein hydration in aqueous solution. *Science* **254**: 974–980.
114. Lounnas, V. and B.M. Pettitt (1994) Distribution function implied dynamics versus residence times and correlations: solvation shells of myoglobin. *Proteins: Struct. Func. Genet*. **18**: 148–160.
115. Levine, H. and L. Slade (1989) A food polymer science approach to the practice of cryostabilization technology. *Comments Agric. Food Chem.* **1**: 315–396.
116. Jouppila, K. and Y.H. Roos (1994) Glass transitions and crystallization in milkpowders. *J. Dairy Sci*. **77**: 2907–2915.